

(NASA-CR-143863) DEPLOYABLE HEAT PIPE  
RADIATOR Final Report (Grumman Aerospace  
Corp.) 115 p HC \$5.25  
N75-25088  
CSCL 20M  
Unclas  
G3/34 24197

# DEPLOYABLE HEAT PIPE RADIATOR

## FINAL REPORT



# DEPLOYABLE HEAT PIPE RADIATOR

## FINAL REPORT

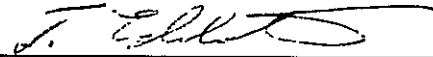
PREPARED FOR

NATIONAL AERONAUTICS AND SPACE ADMINISTRATION  
GEORGE C. MARSHALL SPACE FLIGHT CENTER  
ALABAMA 35812

CONTRACT NO. NAS 8-29905

PREPARED BY

GRUMMAN AEROSPACE CORPORATION  
BETHPAGE, NEW YORK 11714

PREPARED BY:   
F. EDELSTEIN, PROJECT ENGINEER

APPROVED BY:   
R. HASLETT, PROGRAM MANAGER

APRIL 1975

## CONTENTS

<u>Section</u>		<u>Page</u>
1	INTRODUCTION . . . . .	1-1
2	DESIGN . . . . .	2-1
	2.1 Design Requirements . . . . .	2-1
	2.2 System Design . . . . .	2-2
	2.2.1 Heat Pipe Panel . . . . .	2-6
	2.2.2 Flexible Heat Pipe Header . . . . .	2-6
	2.2.3 Heat Exchanger . . . . .	2-11
	2.2.4 Fluid Header . . . . .	2-13
3	SYSTEM PERFORMANCE ANALYSIS . . . . .	3-1
	3.1 Summary . . . . .	3-1
	3.2 Discussion . . . . .	3-1
	3.3 Conclusions . . . . .	3-13
4	COMPONENT TESTS . . . . .	4-1
	4.1 Feeder Heat Pipe Tests . . . . .	4-1
	4.2 Flexible Heat Pipe Header Tests . . . . .	4-9
5	RADIATOR SYSTEM TESTS . . . . .	5-1
6	CONCLUSIONS . . . . .	6-1
7	REFERENCES . . . . .	7-1
	APPENDIXES	
A	Deployable Heat Pipe Radiator - Panel Design Selection . . . . .	A-1
B	Deployable Heat Pipe Radiator Control Requirements . . . . .	B-1
C	Header Heat Pipe Pressure Tests . . . . .	C-1

## ILLUSTRATIONS

Figure		Page
2-1	Radiator Panel Operating Systems . . . . .	2-3
2-2	Deployable Heat Pipe Radiator . . . . .	2-4
2-3	Deployable Heat Pipe Radiator Assembly . . . . .	2-5
2-4	Groove Pipe Extrusion . . . . .	2-7
2-5	Radiator Panel (Painted) Shown Clamped to Fluid Header . . . . .	2-8
2-6	Attachment of Stainless Steel Reservoirs to Aluminum Heat Pipes on Deployable Heat Pipe Radiator . . . . .	2-8
2-7	Header Assembly VCHP Deployable Heat Pipe Radiator . . . . .	2-9
2-8	Gas Trap Region of Deployable Header Heat Pipe. . . . .	2-12
2-9	Heat Exchanger (Clamps to Header Heat Pipe) . . . . .	2-12
2-10	Fluid Header Assembly Deployable Heat Pipe Radiator . . . . .	2-14
2-11	Four by Six Foot Deployable Radiator. . . . .	2-15
3-1	Analytical Performance Summary of Deployable Radiator Systems . .	3-4
3-2	Fluid Outlet Temperature vs Load, $T_{env} = -30^{\circ}\text{F}$ . . . . .	3-5
3-3	Fluid Outlet Temperature vs Load, $T_{env} = -70^{\circ}\text{F}$ . . . . .	3-6
3-4	Fluid Outlet Temperature vs Load, $T_{env} = -110^{\circ}\text{F}$ . . . . .	3-7
3-5	System I Temperatures vs Load . . . . .	3-8
3-6	System A Temperatures vs Load . . . . .	3-9
3-7	System B Temperatures vs Load . . . . .	3-10
3-8	System C Temperatures vs Load . . . . .	3-11
4-1	Feeder Heat Pipe Instrumentation Set-up . . . . .	4-2
4-2	Feeder Heat Pipe Component Test Results . . . . .	4-3
4-3	Feeder Heat Pipe Performance (S/N 02; 03) . . . . .	4-4
4-4	Feeder Heat Pipe Performance (S/N 04; 05) . . . . .	4-5
4-5	Feeder Heat Pipe Performance (S/N 06) . . . . .	4-6
4-6	Feeder VCHP Test Results - Temperature Profile . . . . .	4-7
4-7	Header Heat Pipe Instrumentation Set-up . . . . .	4-10
4-8	Flexible Heat Pipe Header Test Results . . . . .	4-11
4-9	Header Heat Pipe Shown Bent 90 Degrees During Acceptance Test . .	4-11

ILLUSTRATIONS (Cont)

<u>Figure</u>		<u>Page</u>
5-1	Cold Box Testing Arrangement for Systems A, B and I . . . . .	5-2
5-2	Thermocouple Locations: Copper Constantan Type T/C . . . . .	5-3
5-3	Radiator Systems A and I Test Results . . . . .	5-5
5-4	System A Test Results - Panel Temperature Pattern . . . . .	5-6
5-5	Radiator System B Test Results . . . . .	5-7
5-6	System B Test Results - Panel Temperature Pattern . . . . .	5-8

## TABLES

<u>No.</u>		<u>Page</u>
2-1	Heat Pipe Panel Design Details . . . . .	2-7
3-1	Performance of Various Radiator Control Systems . . . . .	3-2
3-2	Thermal Data Input . . . . .	3-2
4-1	Feeder Heat Pipe Bench Test Data S/No. 01 - Bent . . . . .	4-8
4-2	Header Heat Pipe Bench Test Data . . . . .	4-12
5-1	Performance Summary of Radiator Systems . . . . .	5-8

## FOREWORD

This report was prepared by Grumman Aerospace Corporation for the George C. Marshall Space Flight Center of the National Aeronautics and Space Administration. The work was performed under Contract NAS 8-29905. Mr. G. Robinson served as Technical Monitor.

The effort was performed from October 1973 to April 1975 under the direction of Mr. R. Haslett as Program Manager and Mr. F. Edelstein as Project Engineer. The author wishes to express his thanks to J. Alario, T. Canaras and J. Fiorello, who contributed significantly to the thermal design and analysis. Thanks are also extended to E. Leszak, W. Combs, and P. Wagner for help in the manufacturing and test effort.

## GLOSSARY

### Symbols

A	area
C <sub>p</sub>	specific heat
D	diameter
h	heat transfer coefficient
L	length
m	mass flow rate
N	number of active heat pipes
Q	heat load
T	temperature
Δ T	temperature difference
U	overall heat transfer coefficient
ε	heat exchanger effectiveness, = $(T_{in} - T_{out}) / (T_{in} - T_v)$
η	fin efficiency factor
η <sub>x</sub>	fin efficiency factor of fluid header

### Subscripts

e	evaporator
c	condenser
ct	contact area between header and panel HP evaporator
f	panel feeder heat pipe
H	header
HX	heat exchanger
i	inside
in	inlet
LM	log-mean
m	interface between header evaporator and heat exchanger
o	heat exchanger fins
out	outlet
p	polyurethane bond
R	fin root
V	vapor

## SUMMARY

A 1.2 by 1.8 m (4 ft by 6 ft) variable conductance heat pipe radiator has been designed, built and tested which has deployment capability and can passively control Freon-21 fluid loop temperatures under varying loads and environments. The radiator consists of six grooved variable conductance heat pipes attached to a 0.032-in. aluminum panel. Heat is supplied to the radiator via a fluid header or a single fluid flexible heat pipe header. The heat pipe (HP) header is an artery design that has a flexible section capable of bending up to 90 degrees. Radiator loads as high as 850 watts have been successfully tested with the header flexed in a 90 degree orientation. Over a load variation of 200 watts, the outlet temperature of the Freon-21 fluid varied by 7°F. Without variable conductance heat pipe (VCHP) control the temperature variation was 42°F. An alternate control system was also investigated which used a variable conductance heat pipe header attached to the heat pipe radiator panel. This system proved ineffectual due to the inability of the header to carry large loads when configured as a VCHP.

## 1 - INTRODUCTION

Heat pipe radiators are recognized as an attractive alternate to conventional pumped looped radiators in spacecraft thermal control systems. They have no moving parts, require no electrical power, do not generate noise or vibration, are insensitive to meteoroid penetration and are weight competitive. Of particular benefit is the ability of the heat pipe radiator to provide self-control of the heat source fluid. This can be done by building variable conductance into the heat distributing feeder heat pipes, building variable conductance into a heat pipe delivery header, or a hybrid of both. Although each of these methods offers different features, they all control fluid exit temperatures without the use of by-pass loops, valves, etc.

It has been shown that the availability of electrical power, above that supplied by the Orbiter, will vastly improve the utilization of Shuttle flights by allowing more payloads per flight. However, this requires additional Shuttle heat rejection capability. One method of providing this with minimum impact on Shuttle design is to use deployable radiators that would reject waste heat while Spacelab operations are performed from the orbiting Shuttle cargo bay. Using a heat pipe radiator, the load could be delivered by a fluid loop or a heat pipe header. The heat pipe header would have to be capable of flexing at least 90 degrees and providing high thermal transport capacity. A unique feature offered by the heat pipe radiator is minimum vibration environments that are necessary, for example, when conducting low-g space processing experiments.

This report describes the effort involved in the design, analysis, fabrication and testing of a 24 square foot heat pipe radiator system that has deployment capability. In addition, different methods of fluid temperature control are examined. Following the design and analysis of the radiator system, individual component heat pipe parts were fabricated and tested. The radiator was then assembled and performance tested in an ambient simulated radiation environment. Additional thermal vacuum testing has been planned by the National Aeronautics and Space Administration/Marshall Space Flight Center (NASA/MSFC) at their facilities.

## 2 - DESIGN

### 2.1 DESIGN REQUIREMENTS

The objectives of this program were to design, build and test a heat pipe radiator that: (1) incorporates a deployable, flexible heat pipe header, and (2) serves as an experimental research tool for investigating various methods of temperature control.

The radiator will interface with a pumped Freon-21 fluid heat source, extract heat from it and reject it to a space environment. The prime thermal requirement is to maintain the Freon-21 temperature exiting the radiator between 70 and 90°F over a load range of 200 to 400 watts in an environment that varies from -110 to -30°F. The design requirements are as follows:

- Panel area (single side heat rejection): 1.2 by 1.8m (4 by 6 ft)
- Surface properties:  $\alpha/\epsilon = 0.25/0.90$
- Head load
  - Maximum 400 watts
  - Minimum 200 watts
- Environment equivalent sink temperature
  - Maximum 430°R (-30°F)
  - Minimum 350°R (-100°F)
- Freon-21 flow rate: 0.063 Kg/s (500 lb/hr)
- Freon-21 outlet temperature
  - Maximum 90°F
  - Minimum 70°F
- Freon-21 inlet temperature (derived from inlet conditions)
  - Maximum 101°F
  - Minimum 75.5°F
- Heat pipe header bend requirement: 0 to 90 degrees.

Four methods of temperature control, as shown in Fig. 2-1, were evaluated. System A couples radiator panel variable conductance heat pipes (VCHP's) directly to a fluid line header; temperature control is provided by the panel VCHP's. (The shaded area represents the gas blocked or non-operating portion of the radiator.) System B uses a flexible single fluid heat pipe (SFHP) header to connect panel VCHP's to a fluid heat exchanger. Again, temperature control is provided by the panel VCHP's. System C uses panel SFHP's connected to a VCHP header. The VCHP header provides panel load control. System D is a hybrid that uses both panel VCHP's and a VCHP header for temperature regulation. In all systems that use the heat pipe header (B, C, and D), load is provided to the panel by a fluid heat exchanger attached to the header's evaporator section.

In addition, a fifth "no control" system (denoted by I) was evaluated to serve as a basis of comparison with the other four control systems. It is identical to System A except that the feeder pipes are single fluid devices. A summary of these systems is as follows:

<u>System</u>	<u>Header Type</u>	<u>Feeder Type</u>
A	Fluid (Freon-21)	VCHP
B	SFHP	VCHP
C	VCHP	SFHP
D	VCHP	SFHP
I	Fluid (Freon -21)	SFHP

Each pipe is required to operate either as a single fluid or variable conductance heat pipe. Therefore, each pipe is designed with a reservoir and is sealed with a valve to allow evacuation and recharging.

## 2.2 SYSTEM DESIGN

The overall configuration of the deployable heat pipe radiator is shown in Fig. 2.2. It consists of four separate detachable pieces of hardware: heat pipe panel, flexible heat pipe header, heat exchanger, and fluid header. The heat pipe panel can be attached to either the heat pipe header or the fluid header using removable clamps. Similarly, the heat exchanger is mechanically clamped to the evaporator section of the heat pipe header. An assembly drawing is presented in Fig. 2-3.

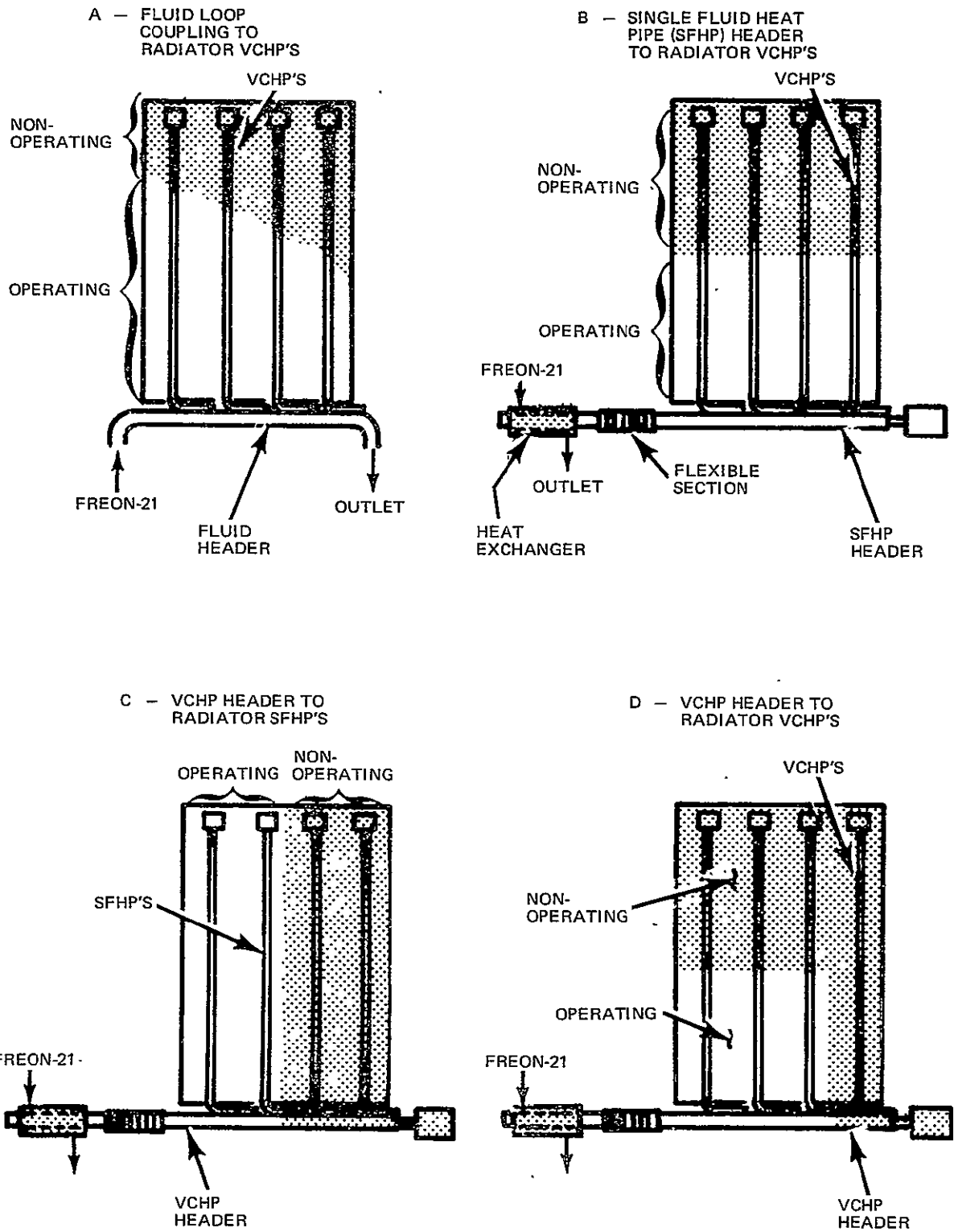


Fig. 2-1 Radiator Panel Operating Systems

ORIGINAL PAGE IS  
OF POOR QUALITY

ORIGINAL PAGE IS  
OF POOR QUALITY

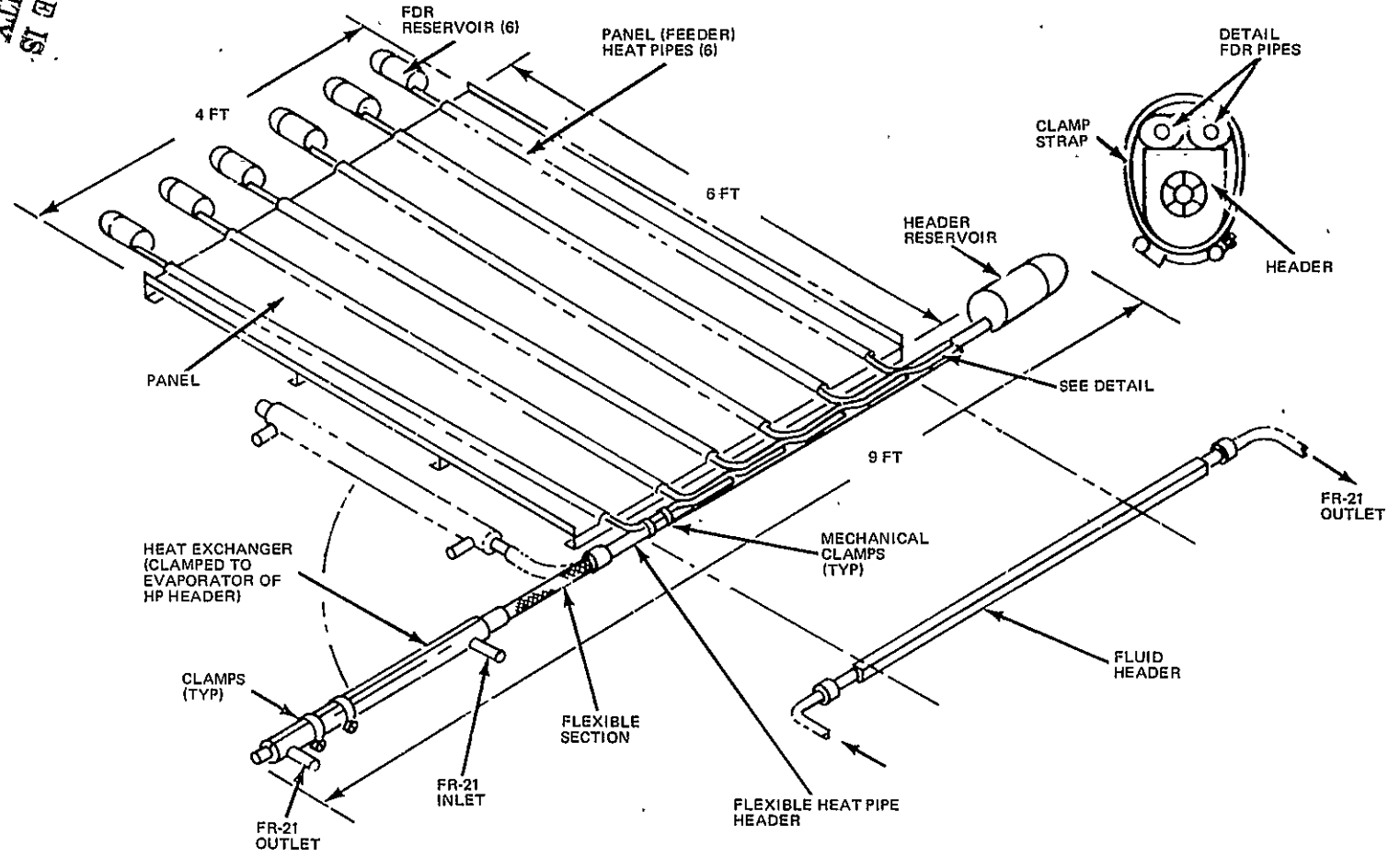


Fig. 2-2 Deployable Heat Pipe Radiator

Table 2-1 Heat Pipe Panel Design Details

OVERALL PANEL SIZE	4 X 6 FT
NUMBER OF FEEDER PIPES	6
SPACING BETWEEN PIPES	8 IN.
RADIATOR FIN MATERIAL	2024 T-3 ALUMINUM
RADIATOR FIN THICKNESS	0.032 IN.
FEEDER TO FIN ATTACHMENT	POLYURETHANE ADHESIVE
FIN TO FIN ATTACHMENT	RIVETS
FEEDER TYPE HEAT PIPES	EXTRUDED AL 6063 AXIAL GROOVES
WORKING FLUID	AMMONIA
LENGTH: EVAPORATOR	1 FT*
TRANSPORT	3 IN.
CONDENSER	6 FT
DIAMETER ACROSS FLATS	0.562 IN.
RESERVOIR MATERIAL	STAINLESS STEEL 321
RESERVOIR SIZE	3-IN. DIA X 6-IN. LONG
$V_r/V_c$	7.8
MAXIMUM DESIGN LOAD PER PIPE	67 WATTS OR 3,000 WATT-IN.
WEIGHT OF PANEL	13.1 Kg (28.8 LB)
WEIGHT PER UNIT AREA	5.9 Kg/m <sup>2</sup> (1.2 LB/FT <sup>2</sup> )

\*The Evaporator Length for Five of the Six Feeder Pipes is One Foot. The Last or End Feeder Pipe Has a Foreshortened Six In. Evaporator.

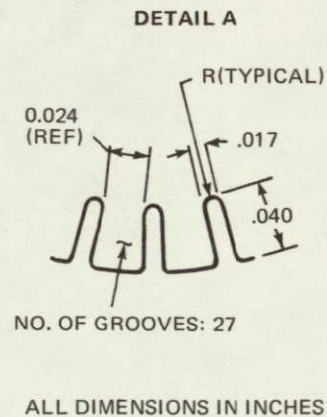
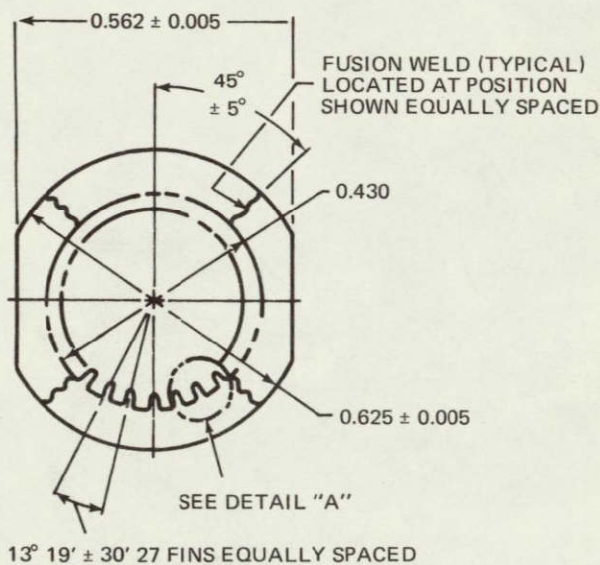


Fig. 2-4 Groove Pipe Extrusion

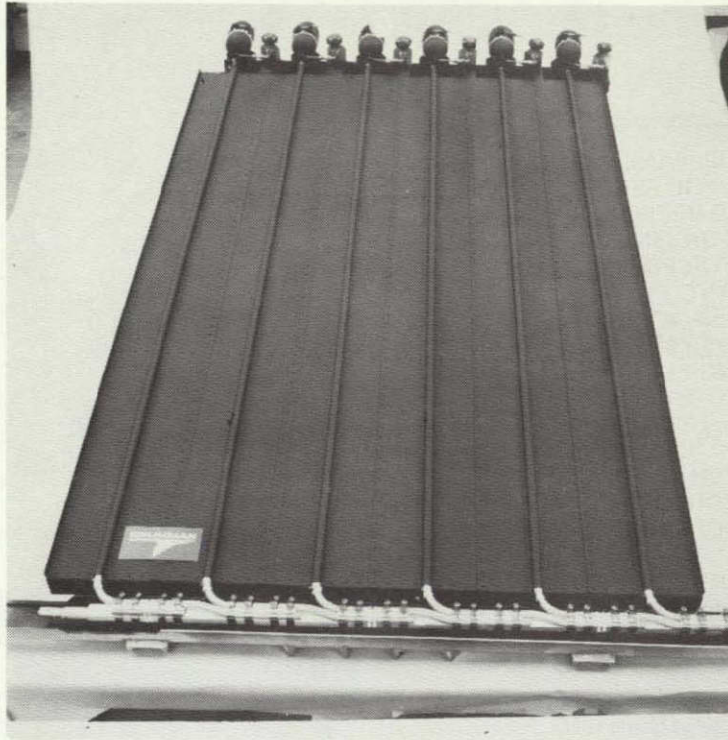


Fig. 2-5 Radiator Panel (Painted) Shown Clamped to Fluid Header

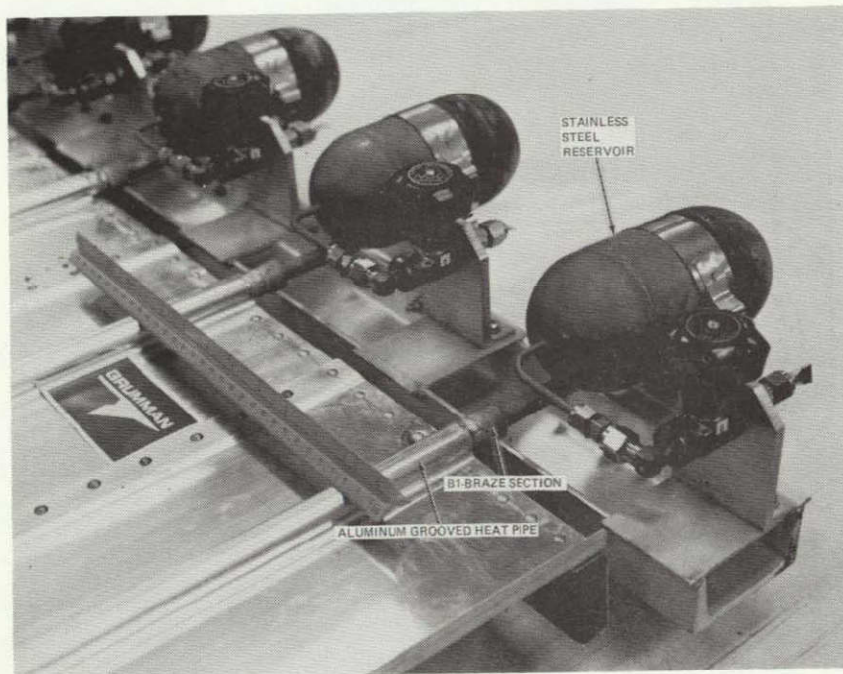


Fig. 2-6 Attachment of Stainless Steel Reservoirs to Aluminum Heat Pipes on Deployable Heat Pipe Radiator

artery can vent unwanted gas bubbles without destroying wick integrity. This is accomplished by using perforation dimensions (diameter to foil thickness ratio) such that the menisci on both sides of the hole interfere causing the liquid to drain from the hole, and permitting the bubble to vent. See Fig. 2-7 for foil details.

Based on the above considerations, a number of design features were incorporated to minimize the influence of non-condensable gas bubbles within the artery during VCHP operation. These included:

- (1) Design the artery with a sufficient number of spiral gaps(6) to carry a 600 watt load assuming the tunnel completely inoperative.
- (2) Provide shielding around the artery within the condenser to allow subcooling of returning condensate.
- (3) Provide a gas trap between the end of the flexible section and beginning of the condenser. In this region (see Fig. 2-7 and 2-8) the outer wrap of the artery is expanded and in contact with a cooled surface at the beginning of the condenser. Vent holes through the screen layers to the tunnel allow tunnel gas bubbles to collect in the gas trap region. Because this region is subcooled, relatively large quantities of gas can be collected and thus free the flow of liquid condensate through the tunnel. The vapor space in this region is restricted and can result in large pressure drops at high loads. Therefore, a vapor bypass tube is provided around the gas trap.
- (4) Provide a perforated foil at the evaporator end to vent gas bubbles that may migrate into the evaporator; foil thickness = 0.00076 cm (0.0003 in.); hole diameter = 0.0051 cm (0.002 in.).

### 2.2.3 Heat Exchanger

This unit is a two-piece aluminum clam shell design 0.76 m (30 in.) long that clamps over the circular evaporator section of the heat pipe header. Freon-21 flows through an annular section, 2.347 cm (0.924 in.) inside diameter by 2.855 cm (1.124 in.) outside diameter. Aluminum finning, 0.0152 cm (0.006 in.) thick, 15 fins per inch, is brazed in the annulus. A photograph of the heat exchanger is shown in Fig. 2-9. It is estimated that the heat exchanger effectiveness between the Freon-21 and ammonia vapor in the header is over 80 percent.

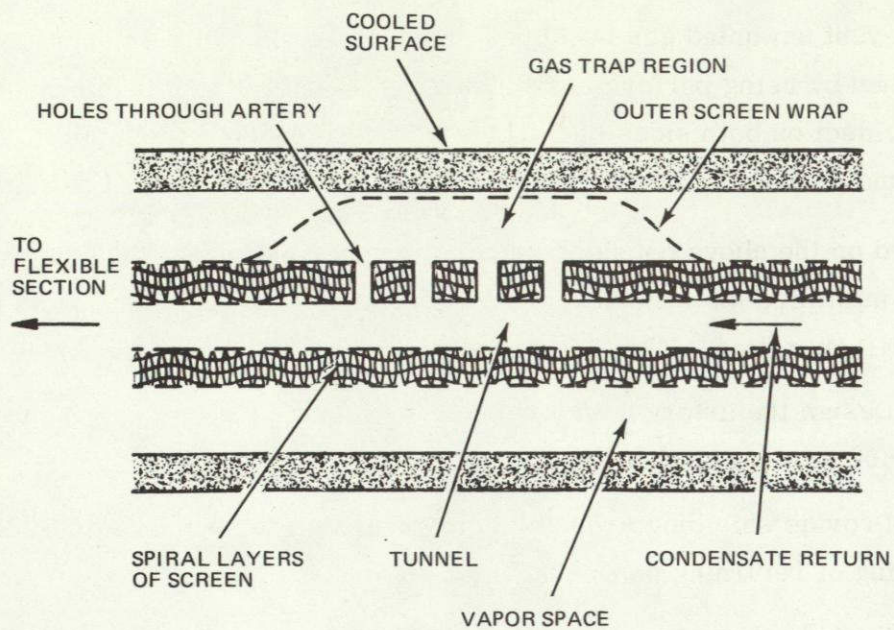


Fig. 2-8 Gas Trap Region of Deployable Header Heat Pipe

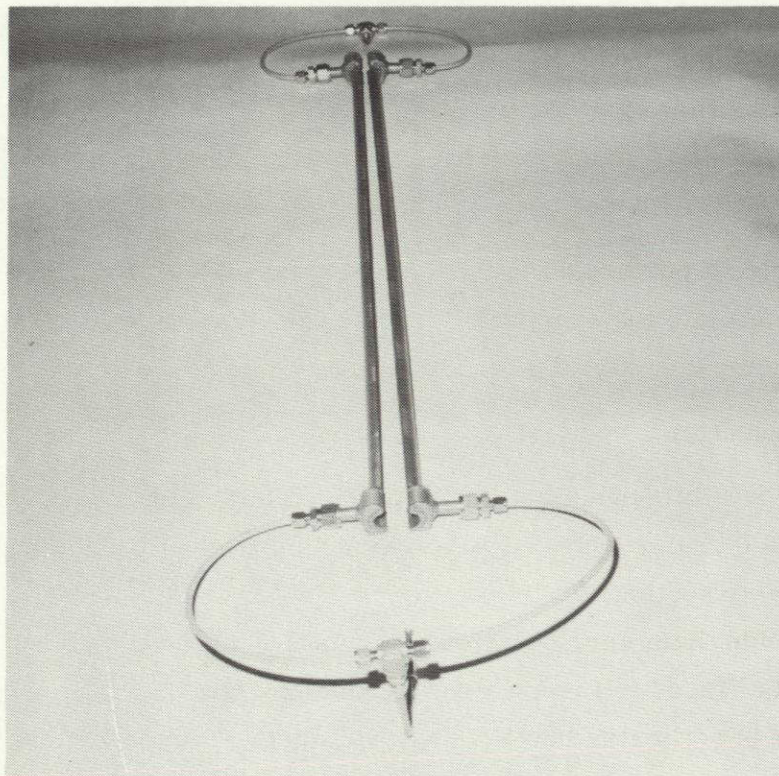


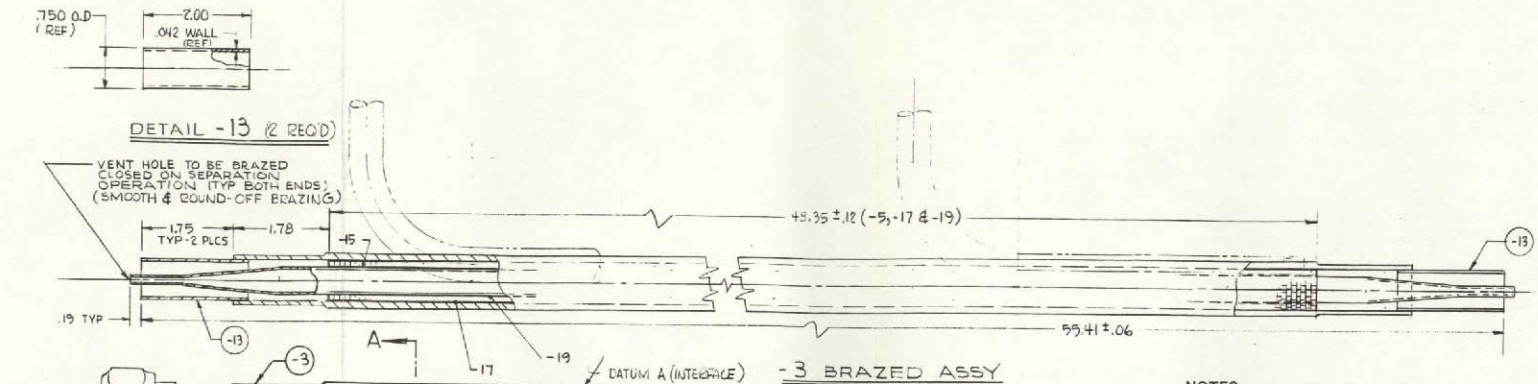
Fig. 2-9 Heat Exchanger (Clamps to Header Heat Pipe)

ORIGINAL PAGE IS  
OF POOR QUALITY

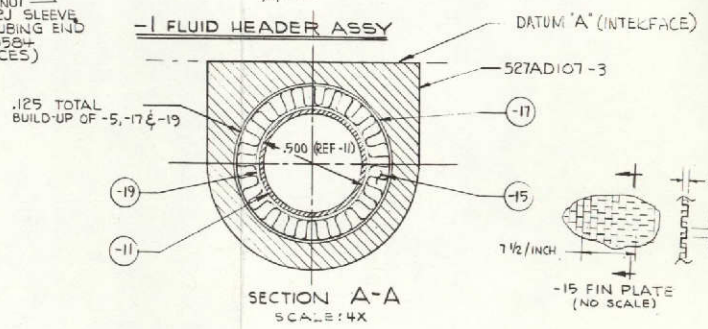
#### 2.2.4 Fluid Header

This aluminum unit is 1.22 m (48 in.) long and clamps directly to the six evaporators of the panel feeder pipes. It has a finned annular Freon-21 flow area 1.27 cm (0.5 in.) inside diameter by 1.91 cm (0.75 in.) outside diameter. Approximately 15 fins per inch are brazed into the annular region to improve heat transfer effectiveness. The outer surface of the fluid header, identical to that of the heat pipe header condenser, has a flat machined surface that is clamped to the feeder evaporators. Thermal grease is used as an interface material. A drawing of the fluid header is shown in Fig. 2-10.

The assembled radiator with the flexible heat pipe header and heat exchanger (System B) is shown in Fig. 2-11 with the header in the straight and bent positions.

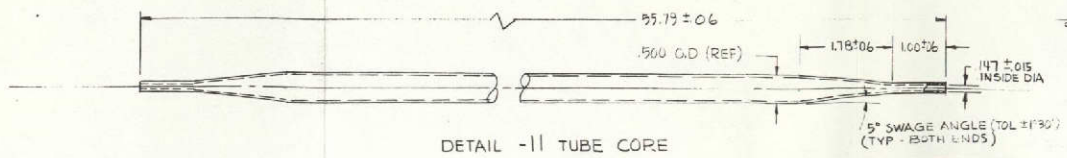


AN 3/8-12J NUT  
MS20519-12J SLEEVE  
FLARE -11 TUBING END  
PER MS35584  
(TYP 2 PLACES)



- NOTES
- (1) -3 ASSY SHALL BE COMPLETELY ALUMINUM BRAZED WITH ALL JOINTS TO BE SEALED TIGHT AGAINST 100 PSI FLUID PRESSURE.
  - (2) NEXT ASSY OF -1 IS 527AD100
  - (3) THE INTERFACE MATING SURFACE (DATUM "A") IS TO BE DIMENSIONALLY CONSTANT AND FREE OF DISTORTIONS FOR ITS ENTIRE LGTH
  - (4) -17 & -19 FILLER METAL THICKNESS TO BE SELECTED BY VENDOR DOING THE BRAZING

QTY	PART NO	NAME	MATERIAL	GOVT SPEC	STOCK SIZE	FINISH	WT
2	AN3/8-12J (REF)	NUT					1.1
2	MS20519-12J (REF)	SLEEVE					2.26
1	527AD107-3	HEAD PIP (FLUID)	AL A1Y 3003	SEE NOTE 4			1.5
1	-19	FILLER METAL	AL A1Y 3003	SEE NOTE 4			1.01
1	-17	FILLER METAL	AL A1Y 3003	SEE NOTE 4			1.01
1	-15	PLATE FIN	AL A1Y 8061-T6	WW-T-700/6	54x100 R.R. 10x25x.49.0		1.04
1	-13	TUBE	AL A1Y 8061-T6	WW-T-700/6	.750 O.D x .042 WALL x 2.5		1.75
1	-11	TUBE - CORE	AL A1Y 8061-T6	WW-T-700/6	.500 O.D x .020 WALL x 570		5.01

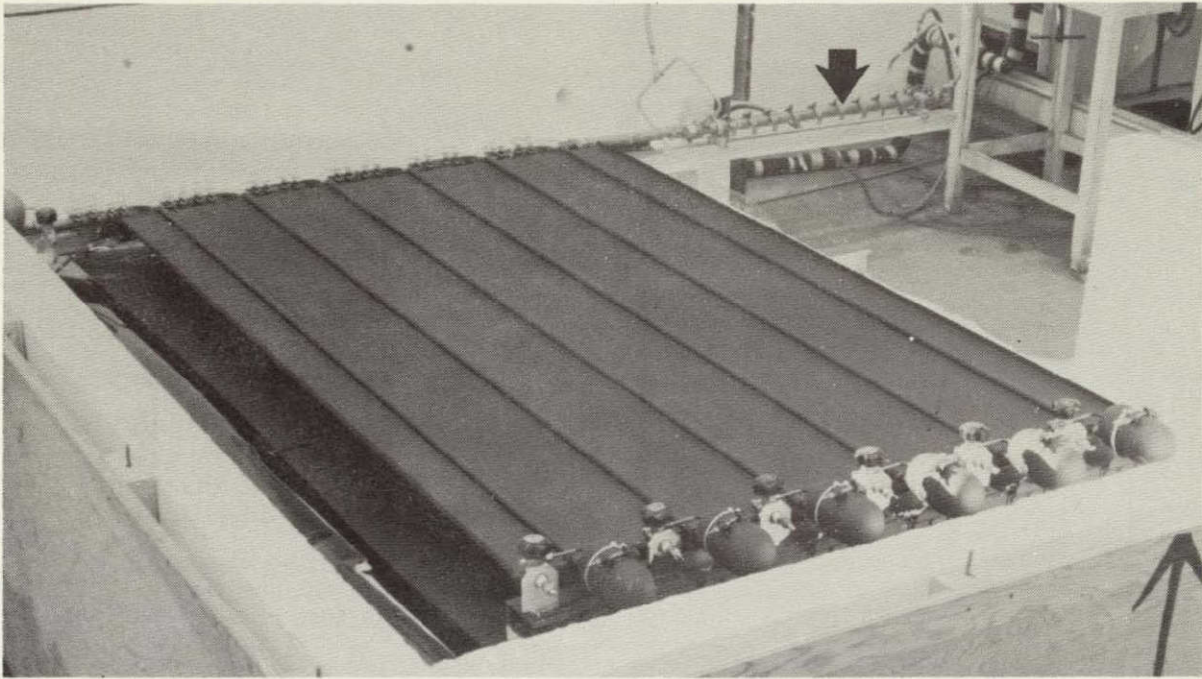


FOLDOUT FRAME

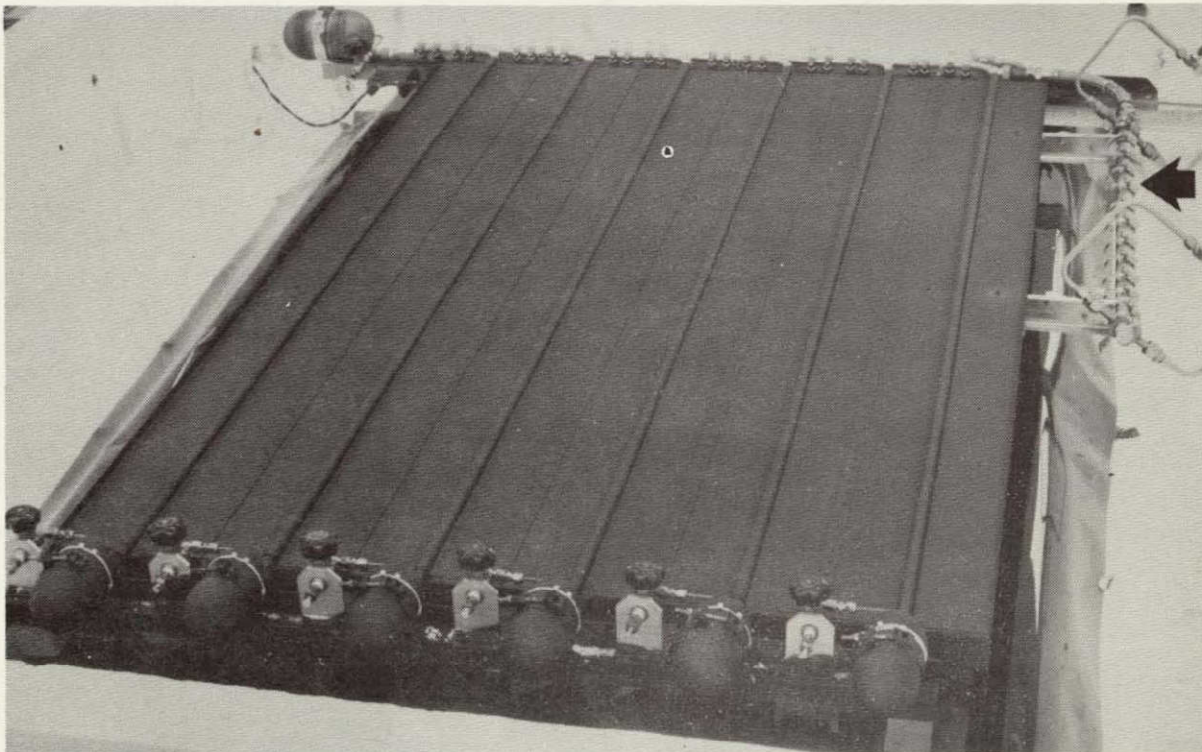
Fig. 2-10 Fluid Header Assembly Deployable Heat Pipe Radiator

FOLDOUT FRAME

2



A. DEPLOYABLE RADIATOR — HEADER PIPE STRAIGHT



B. HEADER PIPE BENT 90 DEG

Fig. 2-11 Four By Six Foot Deployable Radiator

ORIGINAL PAGE IS  
OF POOR QUALITY

## 3 - SYSTEM PERFORMANCE ANALYSIS

### 3.1 SUMMARY

This section presents a systems analysis of the deployable heat pipe (HP) radiator design. Computer programs were used for the analysis of four of the five operating modes of the panel. Comparison of results showed that for systems A (fluid header/VCHP feeder), B (HP header/VCHP feeder), and C (VCHP header/HP feeder) a much tighter temperature control could be obtained than that of System I, which represents a fixed conductance no control heat pipe radiator system (fluid header/HP feeder). The best control was provided by System C which essentially met the performance requirements calling for an outlet fluid temperature range of 70-90<sup>o</sup>F between 200 and 400 watts and an environment of -110<sup>o</sup>F to -30<sup>o</sup>F. Systems A and B did not provide tight enough temperature control. This is due to the higher temperature drop between the fluid and VCHP pipes in these systems compared to that in System C. Methods of varying temperature control are also presented.

### 3.2 DISCUSSION

The purpose of this analysis is to evaluate the various control systems available with the deployable heat pipe radiator. Computer runs were made for four of the five possible systems (D was the exception). These systems are summarized in Table 3-1 (See Fig. 2-1).

System I is a fixed conductance heat pipe radiator and fluid header which serves as a no-control panel for comparison purposes. The other systems represent gas loaded heat pipes that are completely passive; that is, they require no reservoir temperature control. System D was not analyzed because of the extensive program modifications required.

Each system was analyzed using a computer program which combines the overall systems thermal equations (Appendix A) with those defining the interface position of a gas loaded variable conductance heat pipe. Program input to each system consisted of physical dimensions of the various hardware components for that system. Examples of this include pipe lengths, reservoir volume, feeder to header contact area, and fin configuration for fluid header. Additional thermal data used is summarized in Table 3-2.

**Table 3-1 Performance of Various Radiator Control Systems**

SYSTEM	HEADER TYPE	FEEDER TYPE	OUTLET FLUID TEMP VARIATION, °F
A	FLUID (FREON-21)	VCHP	28
B	SINGLE FLUID HP	VCHP	31
C	VCHP	SINGLE FLUID HP	20
D	VCHP	VCHP	—
I	FLUID (FREON-21)	SINGLE FLUID HP	83

**Table 3-2 Thermal Data Input**

PARAMETER	VALUE	UNITS
HEADER EVAPORATOR FILM COEFFICIENT	2,000	BTU/HR-FT <sup>2</sup> °F
HEADER CONDENSER FILM COEFFICIENT	2,400	BTU/HR-FT <sup>2</sup> °F
HEADER/HX CONTACT CONDUCTANCE	1,000	BTU/HR-FT <sup>2</sup> °F
HEADER/FEEDER CONTACT CONDUCTANCE	1,000	BTU/HR-FT <sup>2</sup> °F
FEEDER EVAPORATOR FILM COEFFICIENT	1,530	BTU/HR-FT <sup>2</sup> °F
FEEDER CONDENSER FILM COEFFICIENT	1,675	BTU/HR-FT <sup>2</sup> °F
POLYURETHANE BOND CONDUCTANCE	300	BTU/HR-FT <sup>2</sup> °F
CONTROL GAS CHARGE	0.0437 (HDR)	LB
CONTROL GAS CHARGE	0.0135 (FDR)	LB

Using the previous parameters and a given sink temperature, the fluid (Freon-21) inlet temperature, which in systems B and C is inputted to the heat exchanger and in systems A and I to the fluid line header, was varied and the response of the system determined. Output included fluid outlet temperature, header vapor temperature, feeder vapor temperature, radiator temperature and load. Runs were made at both extremes of radiator environment ( $-30^{\circ}\text{F}$  and  $-110^{\circ}\text{F}$ ) and at an intermediate temperature of  $-70^{\circ}\text{F}$ . A fluid flow rate of 500 lb/hr was used for all runs.

The performance requirements call for an outlet fluid temperature of  $70^{\circ}\text{F}$  to  $90^{\circ}\text{F}$  over a load range of 200 to 400 watts with an environment range of  $-110^{\circ}\text{F}$  to  $-30^{\circ}\text{F}$ . A summary of results from the computer runs with regard to these performance requirements appears in Fig. 3-1 and Table 3-1 for each of the four configurations (two additional runs involving modifications of configuration B are also shown and will be discussed later). Figures 3-2 through 3-4 represent comparison plots of fluid outlet temperature versus load for all four systems at each of the three radiator environments. Figures 3-5 through 3-8 are separate plots for each configuration of fluid inlet, fluid outlet, vapor and average radiator temperatures versus load at the  $-70^{\circ}\text{F}$  environment.

As seen from the results of Figures 3-2 through 3-4, a significantly tighter control of the fluid outlet temperature is obtained for systems A, B and C over that of system I. System C provides the best control of outlet temperature, and basically meets the performance requirements. The outlet temperature range of system C can easily be lowered by slightly lowering the control gas charge. Systems A and B provide good temperature control but not enough to meet the design goal of 70 to  $90^{\circ}\text{F}$ . This is because the panel was primarily designed for system C and as a result performed somewhat less than optimum when configured in systems A and B, as Fig. 3-2 through 3-4 show. The wider control tolerance is the result of a higher temperature drop between the fluid and the VCHP vapor in systems A and B compared to C.

Best control results when there is a minimum thermal resistance between the fluid and VCHP vapor. This is because the VCHP vapor inherently reacts to load and environment changes attempting to maintain itself at constant temperatures. The fluid temperature, coupled to the VCHP vapor by a thermal resistance, will vary over a range which is proportional to the magnitude of that resistance i. e.,  $T_{\text{fluid}} = Q \cdot R + T_{\text{vap}}$ . The higher the resistance the wider the fluid temperature variation.

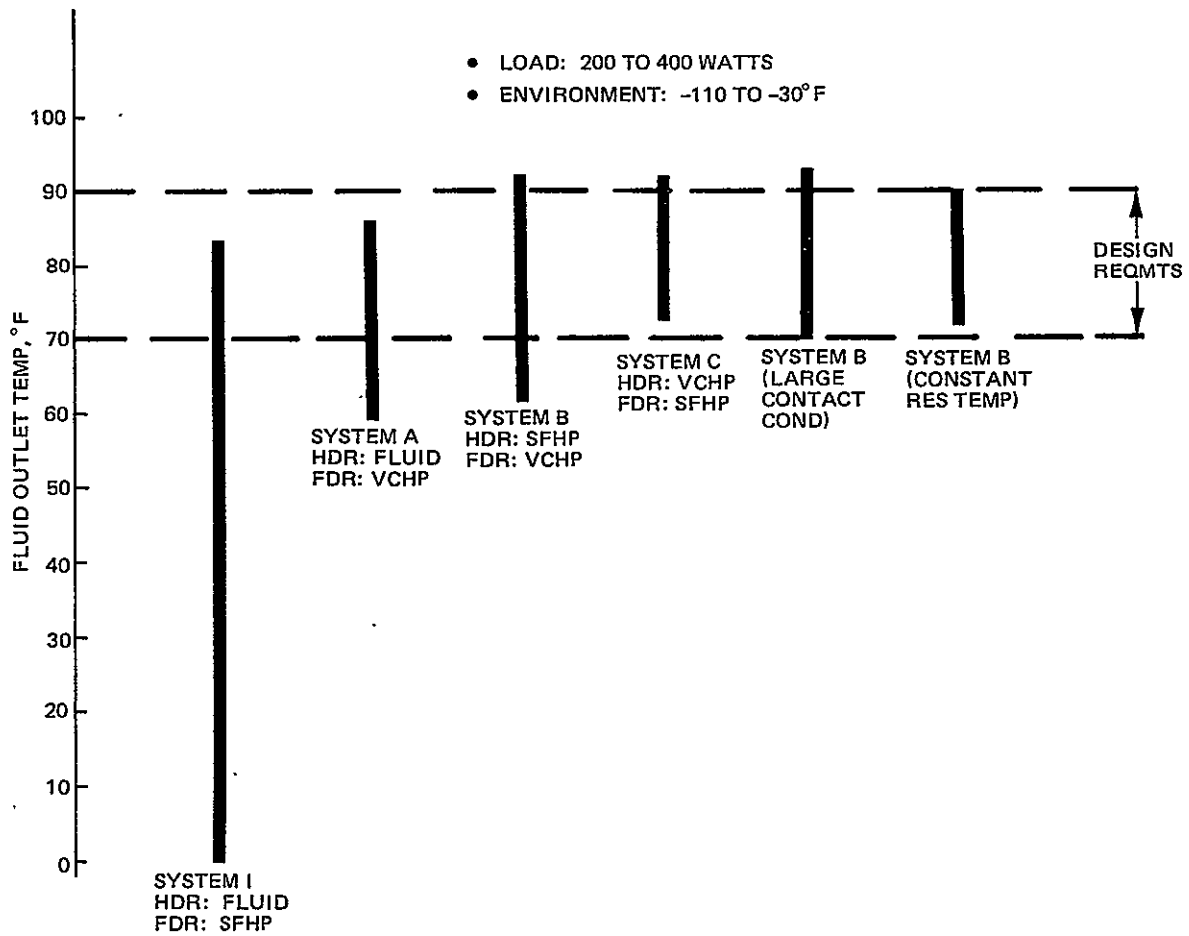


Fig. 3-1 Analytical Performance Summary of Deployable Radiator Systems

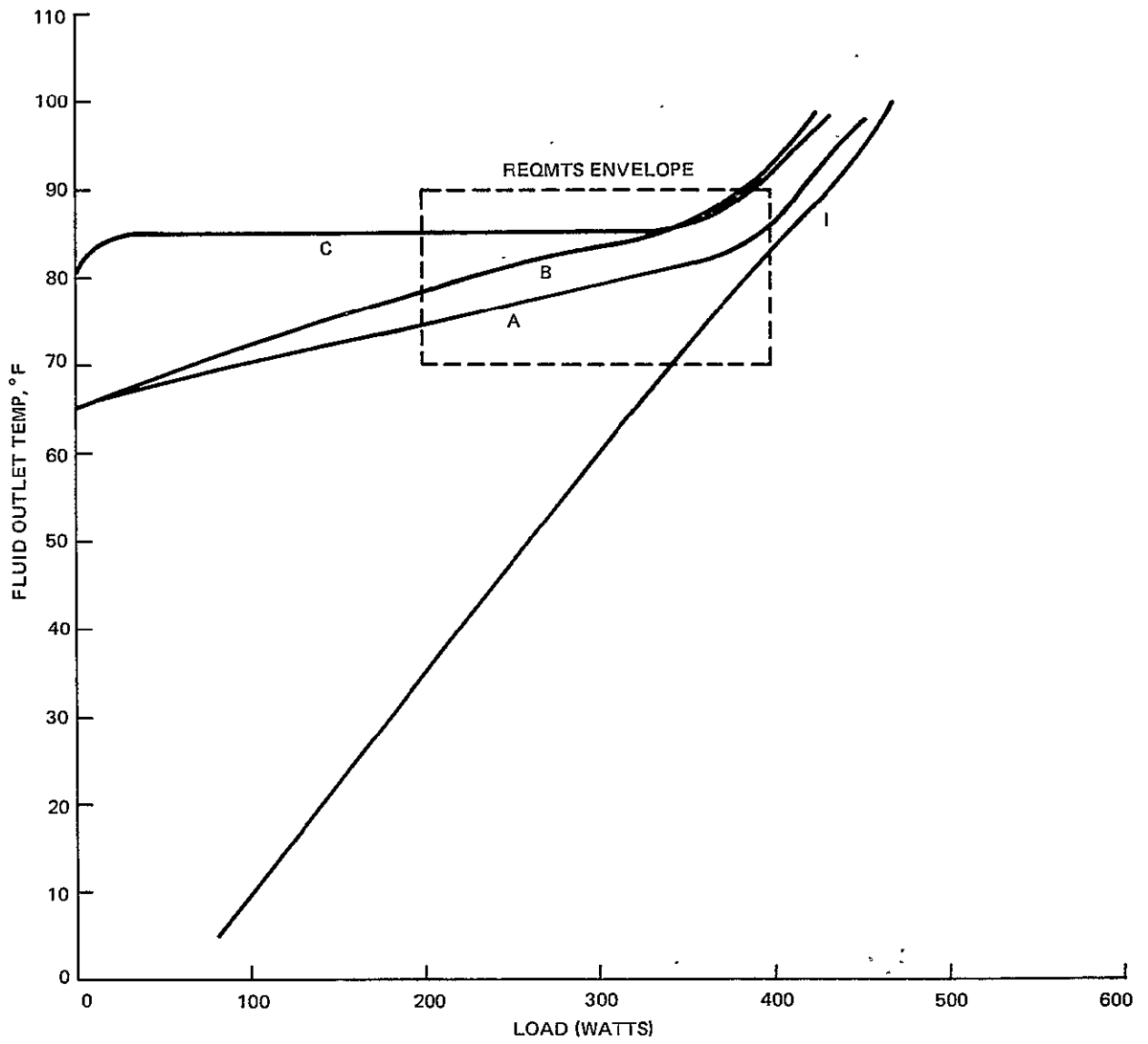


Fig. 3-2 Fluid Outlet Temperature vs Load,  $T_{env} = -30^{\circ}F$

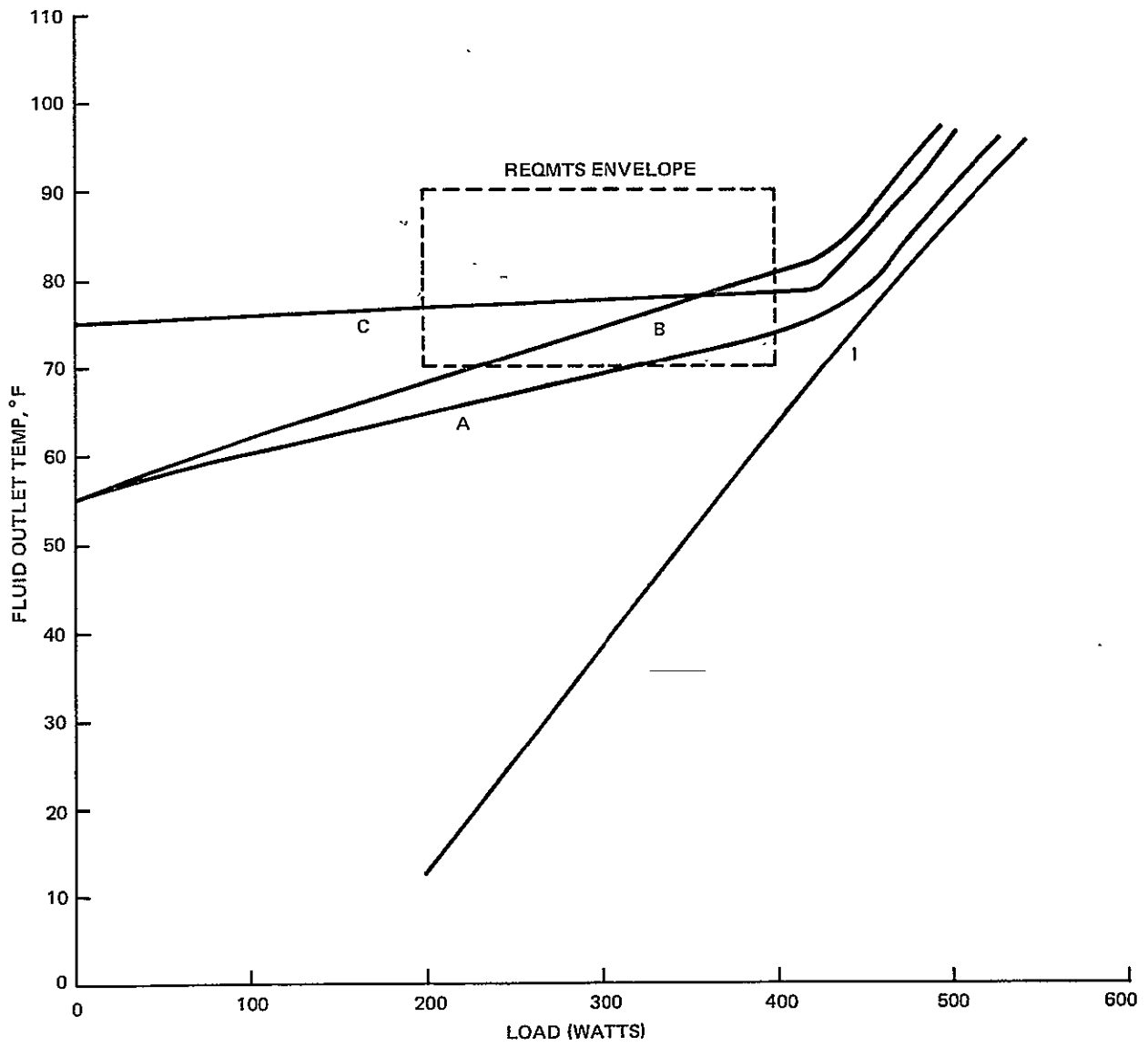


Fig. 3-3 Fluid Outlet Temperature vs Load,  $T_{env} = -70^{\circ}F$

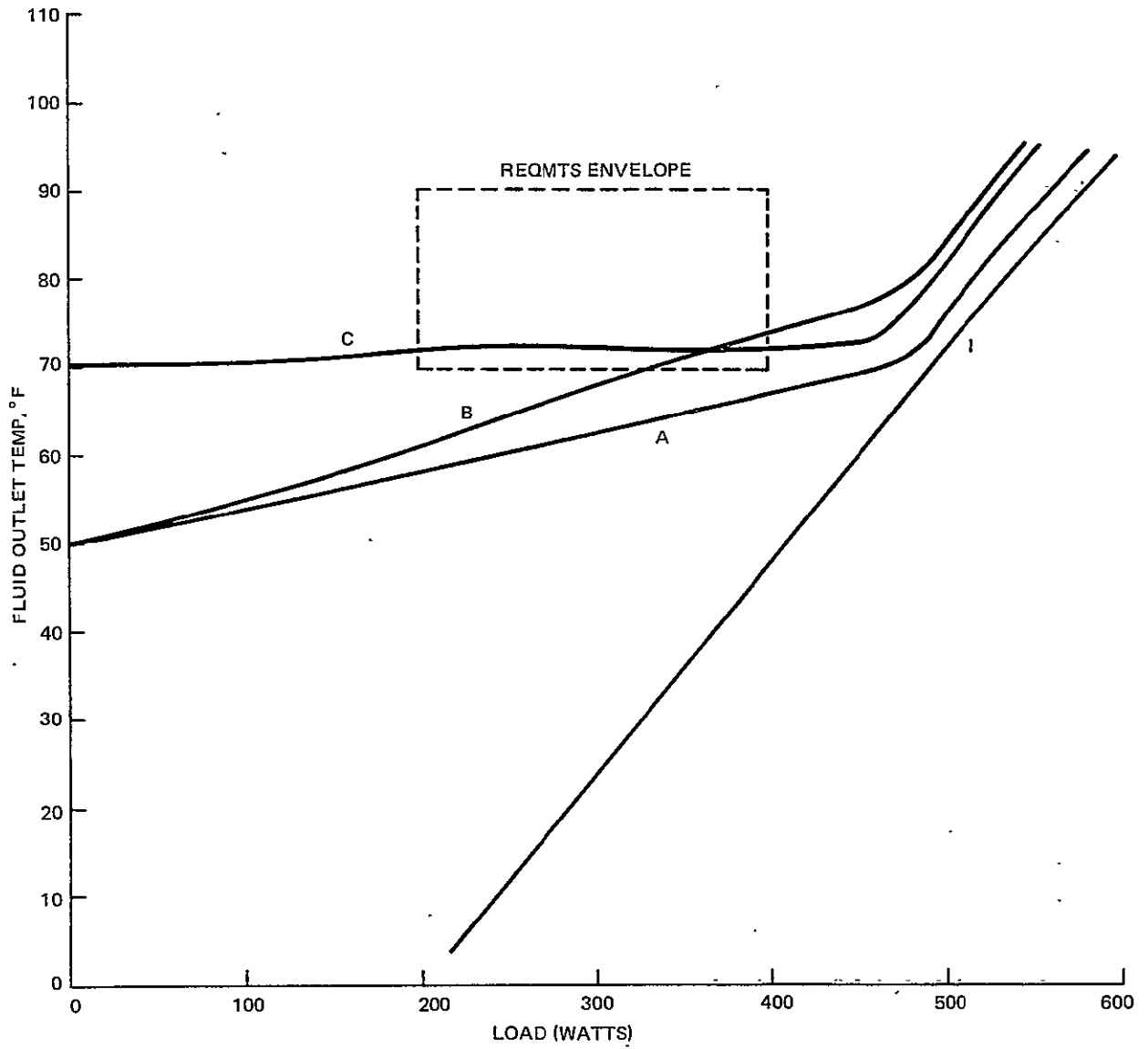


Fig. 3-4 Fluid Outlet Temperature vs Load,  $T_{env} = -110^{\circ}\text{F}$

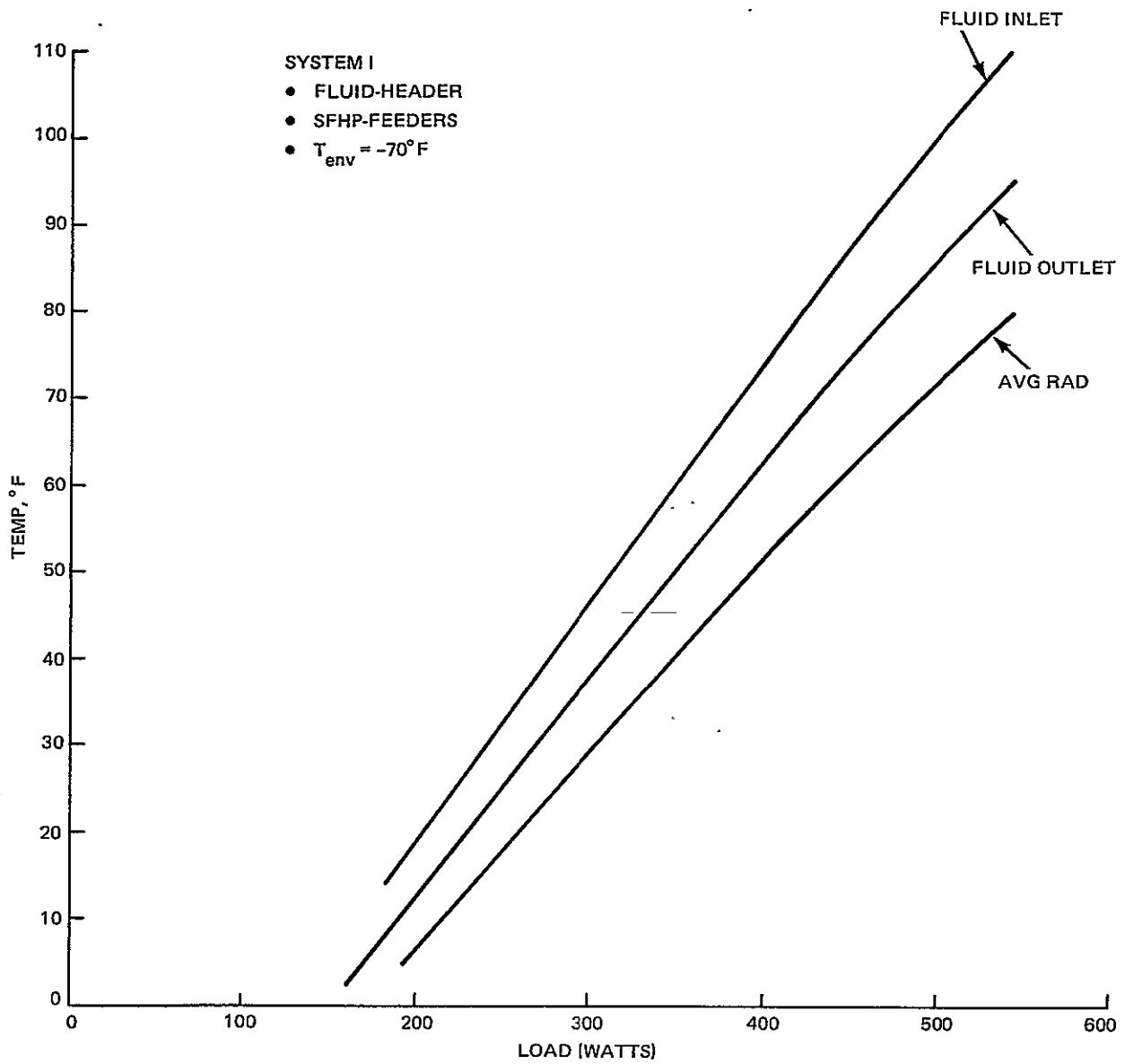


Fig. 3-5 System I Temperatures vs Load

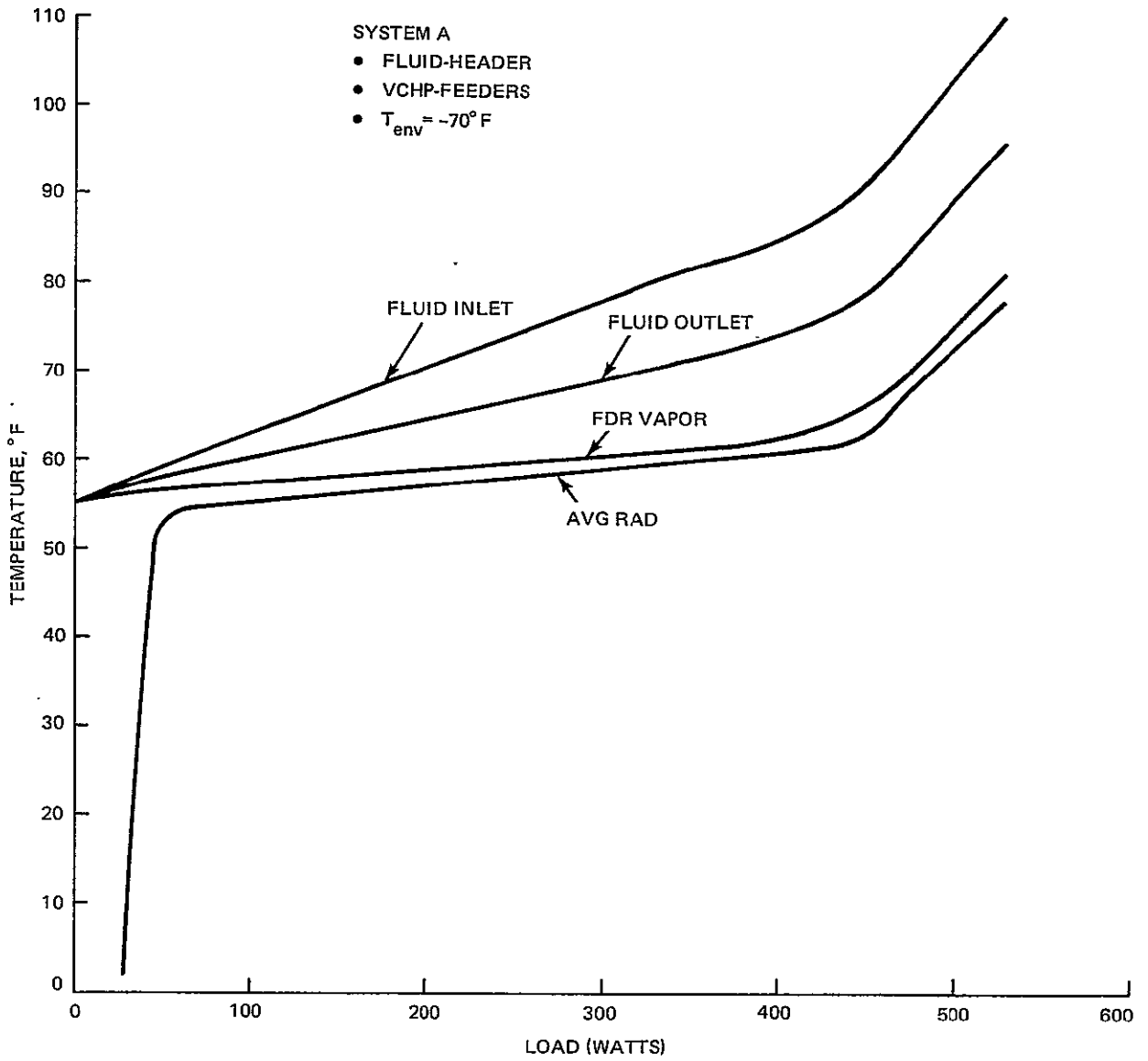


Fig. 3-6 System A Temperatures vs Load

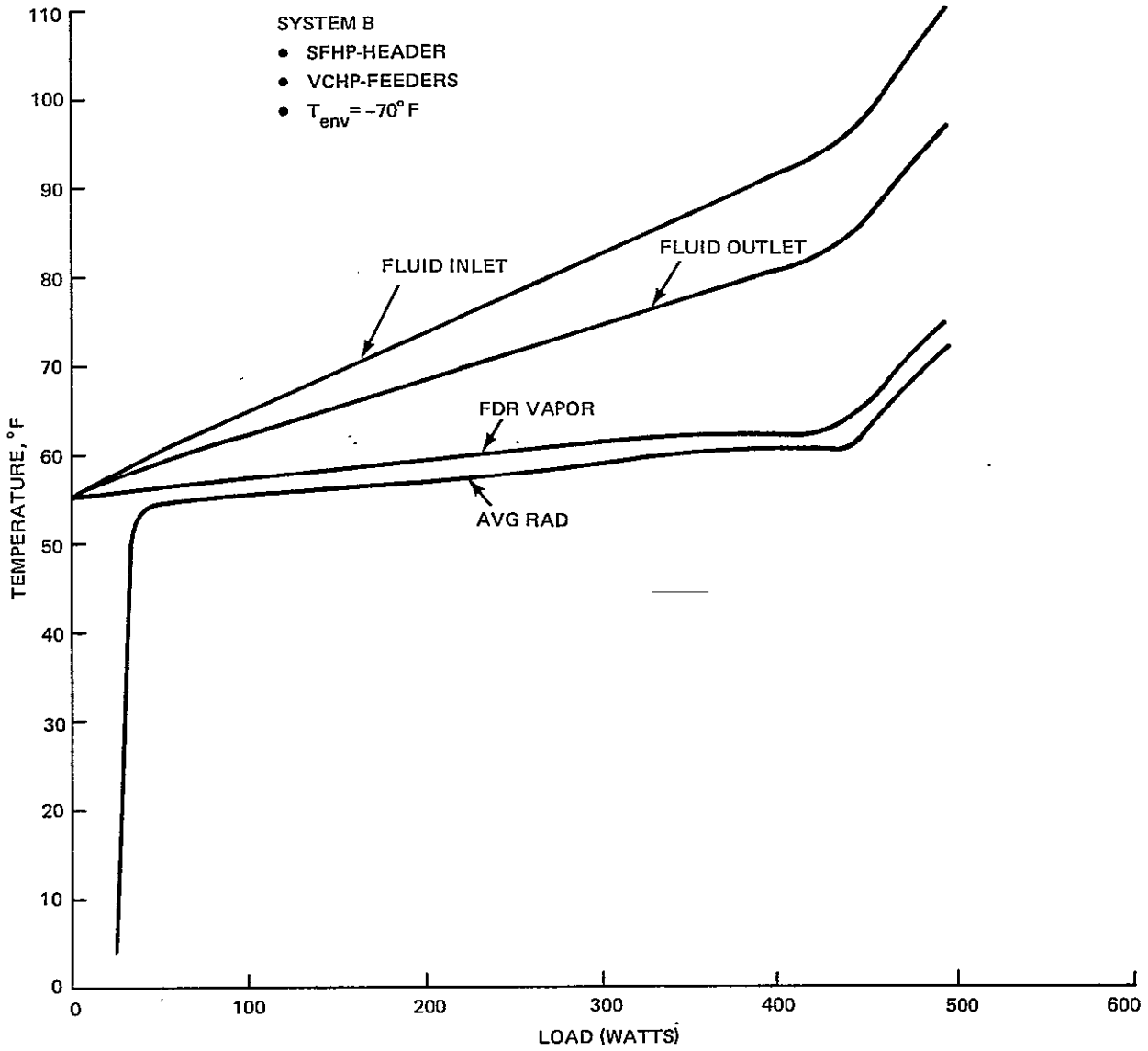


Fig. 3-7 System B Temperatures vs Load

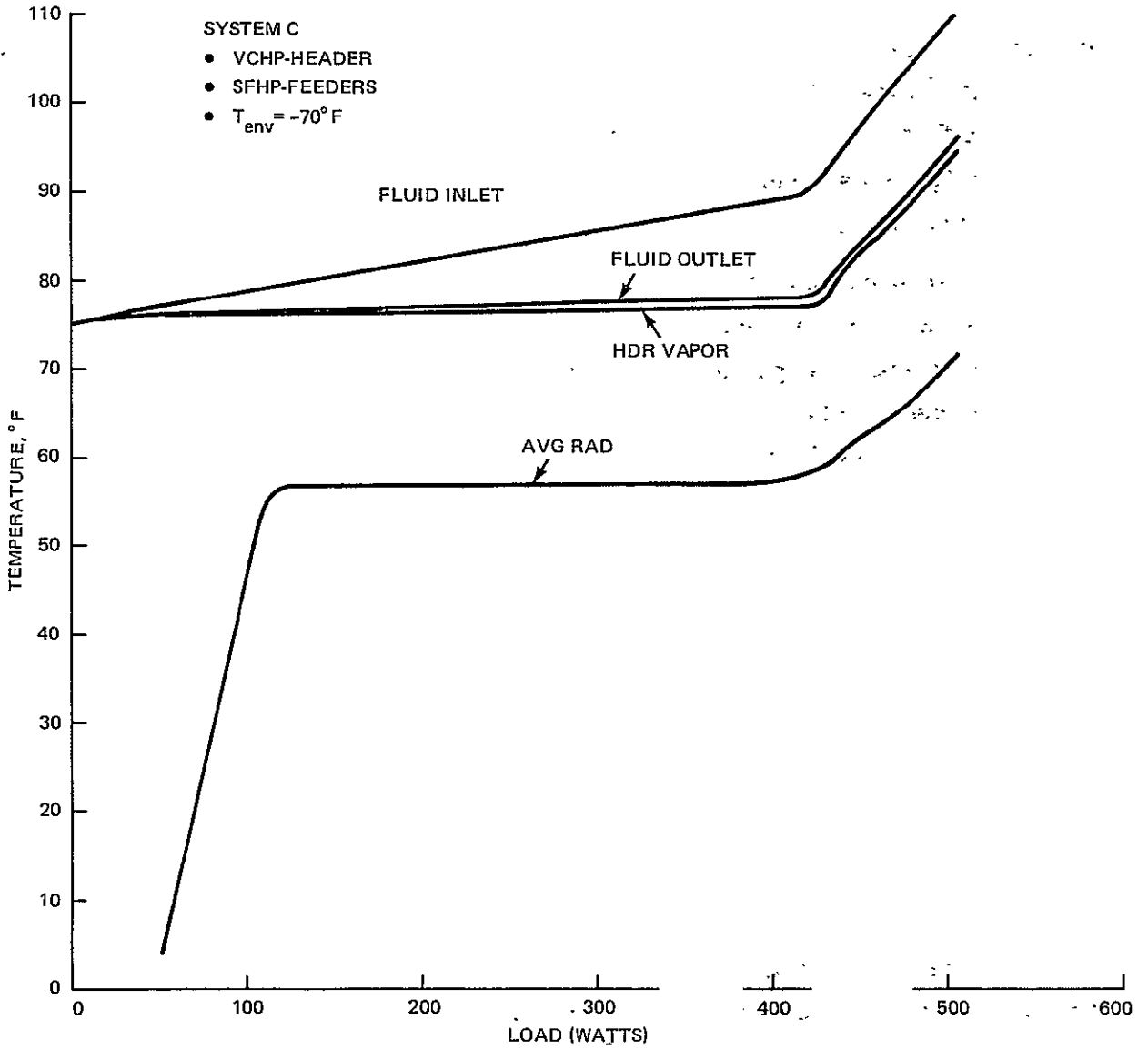


Fig. 3-8 System C Temperatures vs Load

A high thermal resistance is displayed in Fig. 3-7 for system B which shows a temperature drop of  $13^{\circ}\text{F}$  between the fluid outlet and the VCHP feeder vapor temperature at 300 watts. In comparison, as Fig. 3-8 shows, the temperature drop between the fluid outlet and the VCHP header vapor for system C is only  $1^{\circ}\text{F}$ . This is due to three additional resistances that configuration B has, namely, the header condenser film, the header to feeder contact conductance, and the feeder evaporator film. Of the three, the contact conductance represents the largest resistance.

A run was made to see the effect of reducing this resistance, which can be done by using a metallurgical bond between the header and feeders, double sided radiators, etc. Using a large value of contact conductance and increasing the nitrogen control gas charge from 0.0135 to 0.0175 lb resulted in a panel performance that essentially met the design goals. This is seen in Fig. 3-1 for system B modified with a large contact conductance.

The performance of system A is somewhat better than that of system B. As seen in Fig. 3-6, the average temperature drop between the fluid outlet and VCHP vapor (feeder pipes) is approximately  $8^{\circ}\text{F}$  at 300 watts compared to  $1^{\circ}\text{F}$  for system C. In this case, the higher resistance is also due to the header to feeder contact conductance, as well as the one sided heat input from the fluid header to the feeders and the feeder evaporator film.

Aside from decreasing the resistance between the fluid and VCHP vapor, finer temperature control can also be obtained by narrowing the temperature range of the reservoir. This was demonstrated for system B where the reservoir temperature was held constant at  $-51^{\circ}\text{F}$ . Fig. 3-1 summarizes the result which shows that system B (with constant reservoir temperature) meets the performance requirements of  $70$  to  $90^{\circ}\text{F}$ . Constant reservoir temperature can be provided, if necessary, by using a thermostatically controlled heater.

Two points are worth noting. In Figures 3-2 through 3-7 the curves for systems A, B and C turn upward and parallel curve I at the high power levels. This indicates that the interface has progressed beyond the condenser and into the reservoir. Under these conditions the pipe operates as though it were a single fluid device. Secondly,

the nitrogen control gas charge in the VCHP's for systems A, B and C were selected primarily to meet the upper design point of a 90<sup>o</sup>F fluid outlet temperature at 400 watts and a -30<sup>o</sup>F environment (See Fig. 3-1 and 3-2). This results in lower fluid outlet temperatures for systems A and B at the lower end of the design point (200 watts and -110<sup>o</sup>F environment). By increasing the gas charge, the operating range of the pipe could just as easily be raised so that it overlaps the performance requirements.

### 3.3 Conclusions

- Systems A, B and C provide significant temperature control over system I
- System C provides the best control, essentially meeting the design goals
- Systems A and B provide good temperature control but are outside the design goal. This is because the hardware was primarily designed for system C and performed somewhat less than optimum when configured in systems A and B. The temperature drop between the fluid and VCHP was higher in both systems A and B than in system C, thereby accounting for the wider control tolerance
- If required, finer temperature control can be achieved for systems A, B and C by
  - Providing a narrower temperature range for the reservoir
  - Reducing the thermal resistance between the fluid and the VCHP, e.g., double sided radiator, brazed joints, etc.

## 4 - COMPONENT TESTS

### 4.1 FEEDER HEAT PIPE TESTS

Prior to assembly of the radiator panel, acceptance tests were performed on each of the six grooved feeder pipes. All pipes were tested for proper capacity in the single fluid mode. Two pipes (Serial No. 01 and 05) were further tested in the VCHP mode to assure no performance degradation due to non-condensibles. One of these pipes (Serial No. 01) was also tested in the straight and final "L-shaped" configuration to determine the effects, if any, of bending the grooved pipe.

Tests were conducted with one sided electrical heat input on the 0.3m (1 ft) evaporator. Heat was removed by submerging the 1.8m (6 ft) condenser in a water trough covering half the circumference. Figure 4-1 shows the instrumentation drawing. Figure 4-2 shows maximum sustained load versus tilt for the same pipe (Serial No. 01) in three different configurations. The straight pipe, single fluid, tilt data (data point o) is extrapolated to zero tilt to yield a value of about 130 watts. This is well above the 67 watt requirement for the 400 watt panel. Actual test data at zero tilt shows a higher load of 180 watts. However, this can be misleading since puddling effects enhance performance at zero tilt. Adding nitrogen control gas to the pipe provided a variable conductance heat pipe (VCHP), which exhibited no degradation in performance as evidenced by the  $\Delta$  data points. Subsequent bending of the pipe and testing in the VCHP mode also showed no degradation below single fluid performance. In the VCHP mode, the interface was positioned so that at least three-fourths of the condenser length was active. This results in a pumping length comparable to the single fluid case. Results for the other five pipes are shown in Fig. 4-3 through 4-5. In all cases the design requirement of 67 watts at zero tilt was met.

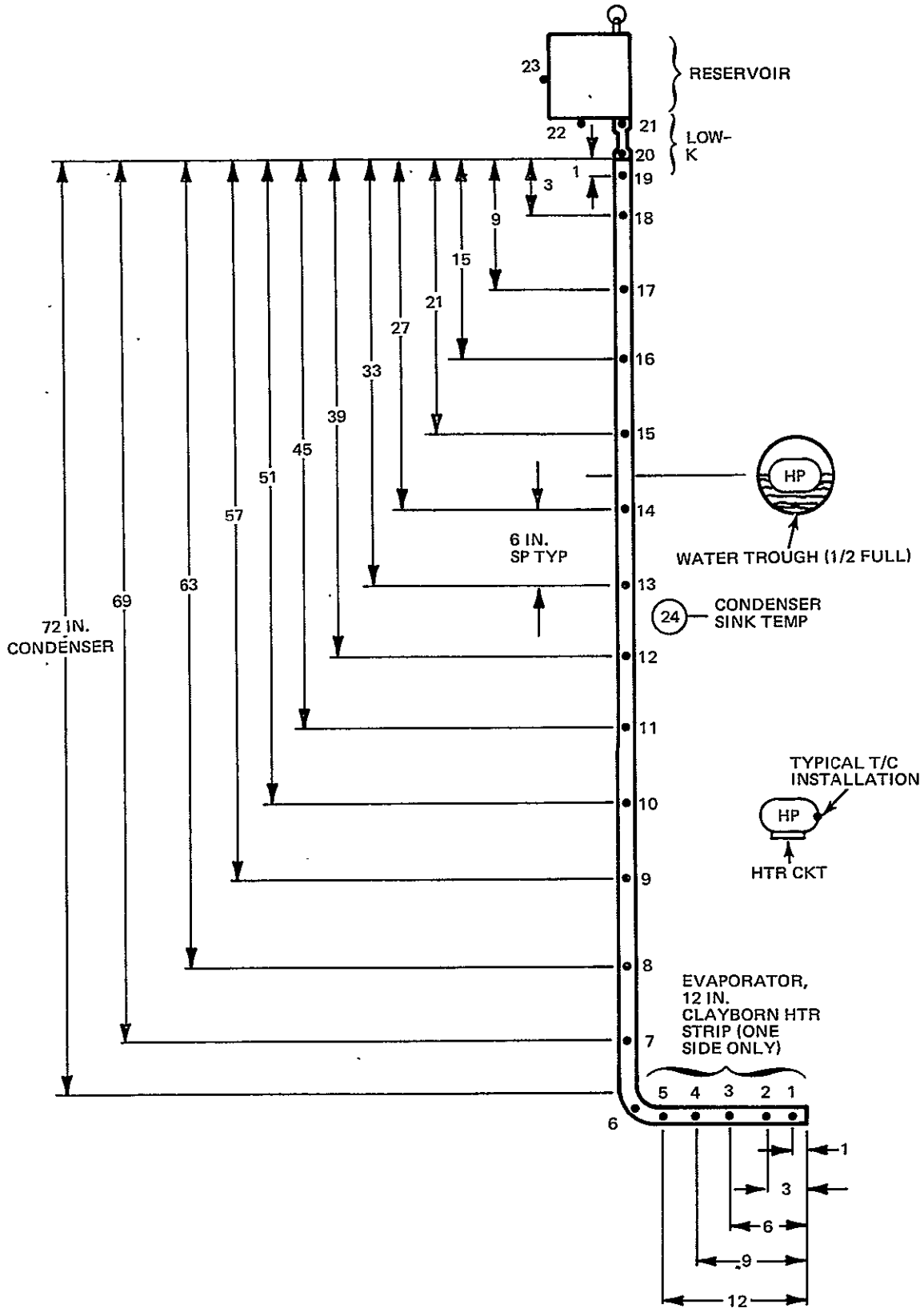


Fig. 4-1 Feeder Heat Pipe Instrumentation Set-Up

- SINGLE SIDE HEAT INPUT/REMOVAL
- PIPE SERIAL NUMBER 01

DATA POINT	PIPE CONFIGURATION	CHARGE	
		NH <sub>3</sub>	N <sub>2</sub>
○- SFHP	STRAIGHT	44.2 gm	—
△- VCHP	STRAIGHT	44.2 gm	0.0135 LB
▲- VCHP	BENT "L" SHAPE	44.8 gm	0.0135 LB

SFHP = SINGLE FLUID HEAT PIPE

VCHP = VARIABLE CONDUCTANCE HEAT PIPE

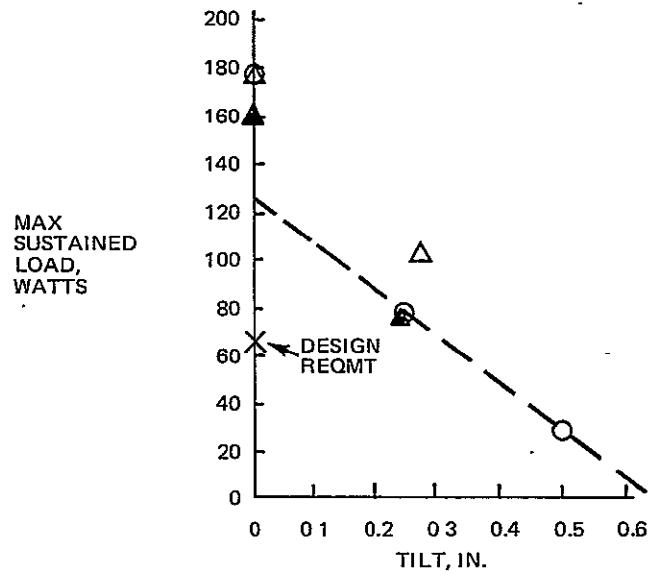


Fig. 4-2 Feeder Heat Pipe Component Test Results

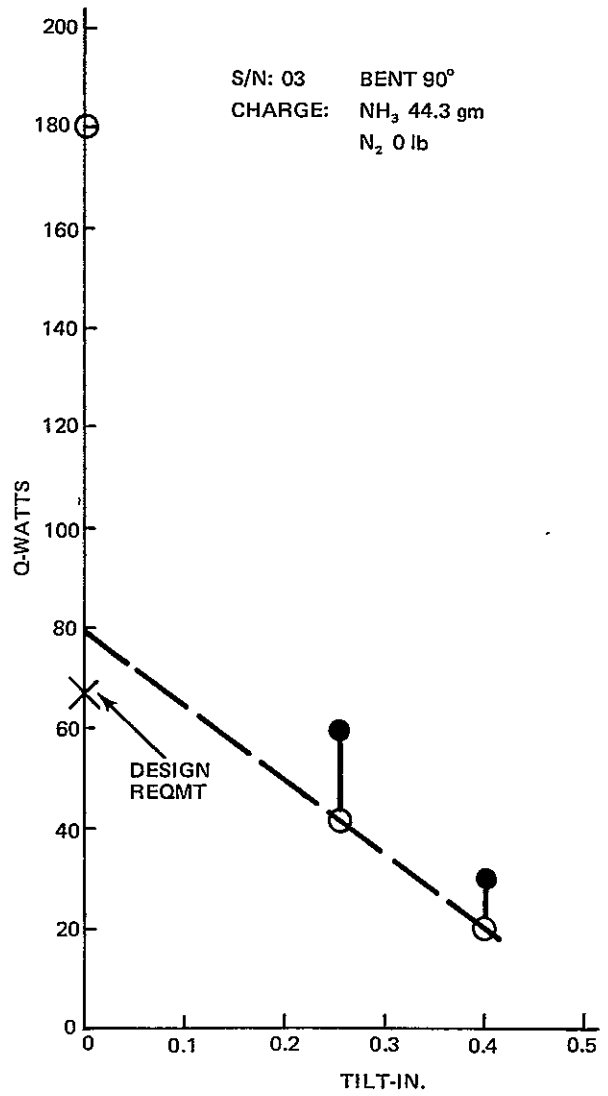
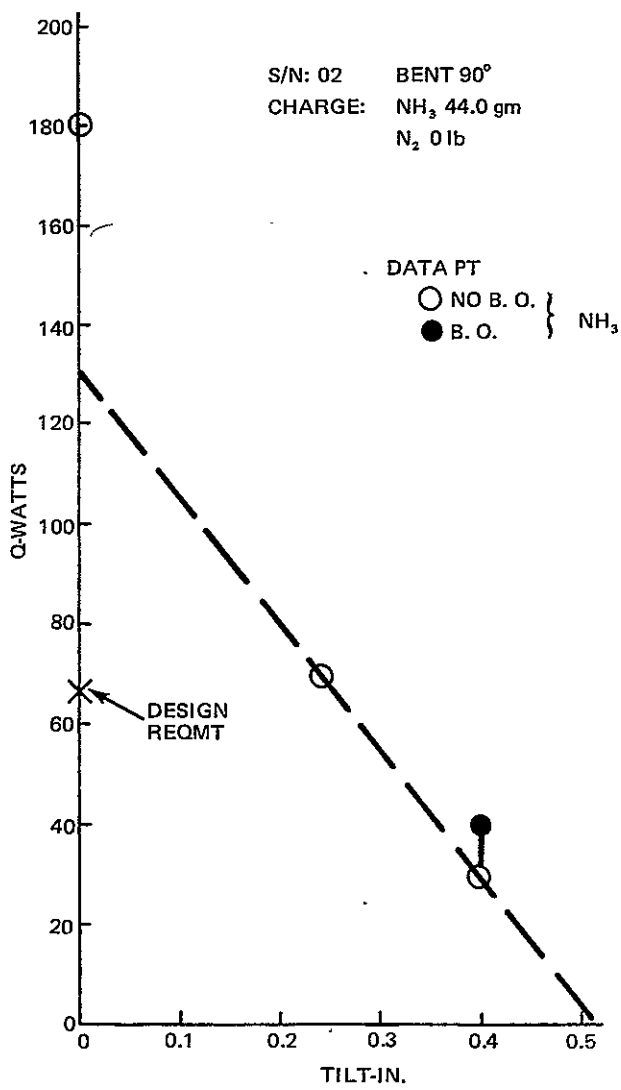


Fig. 4-3 Feeder Heat Pipe Performance (S/N 02; 03)

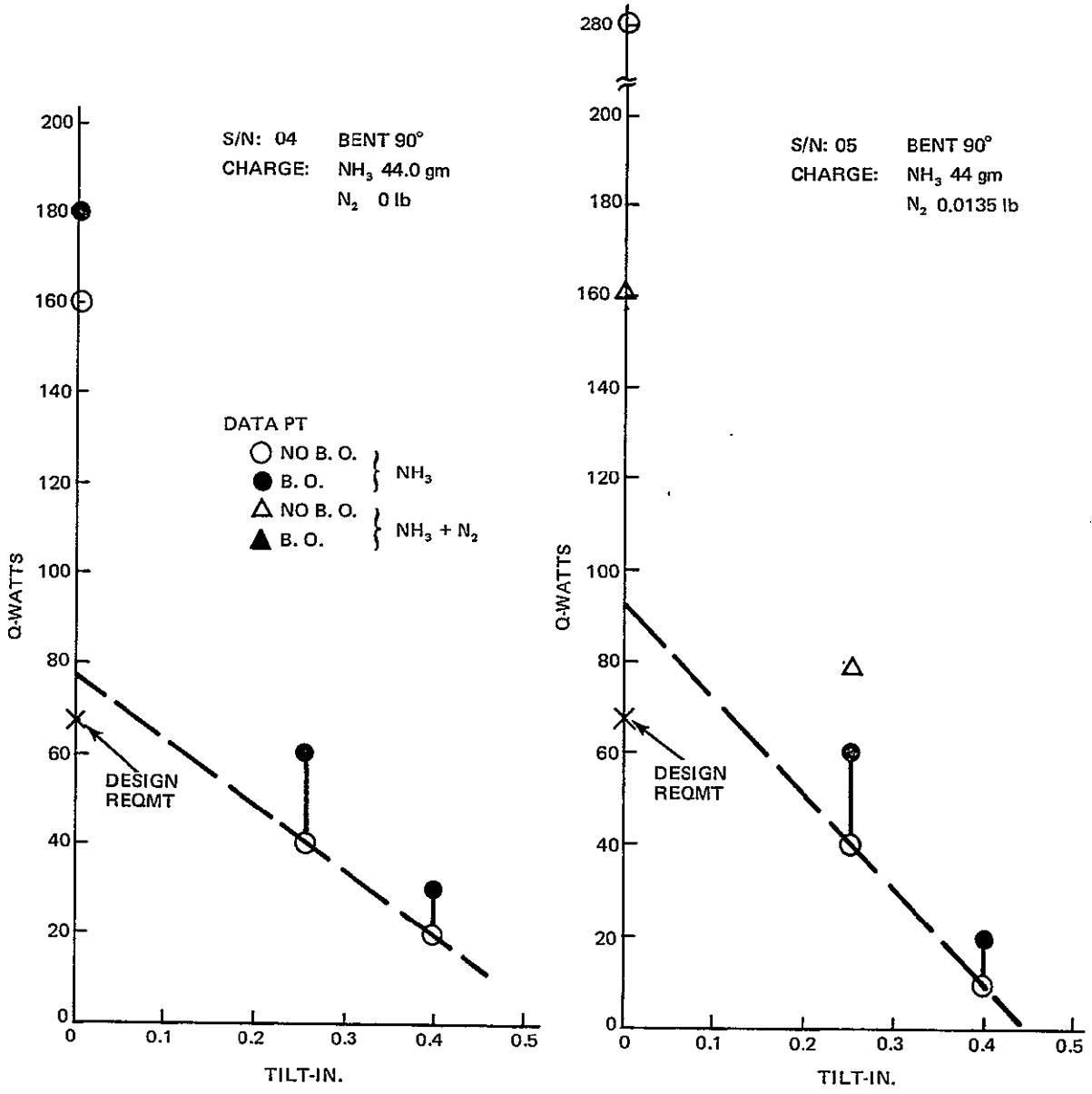


Fig. 4-4 Feeder Heat Pipe Performance (S/N 04; 05)

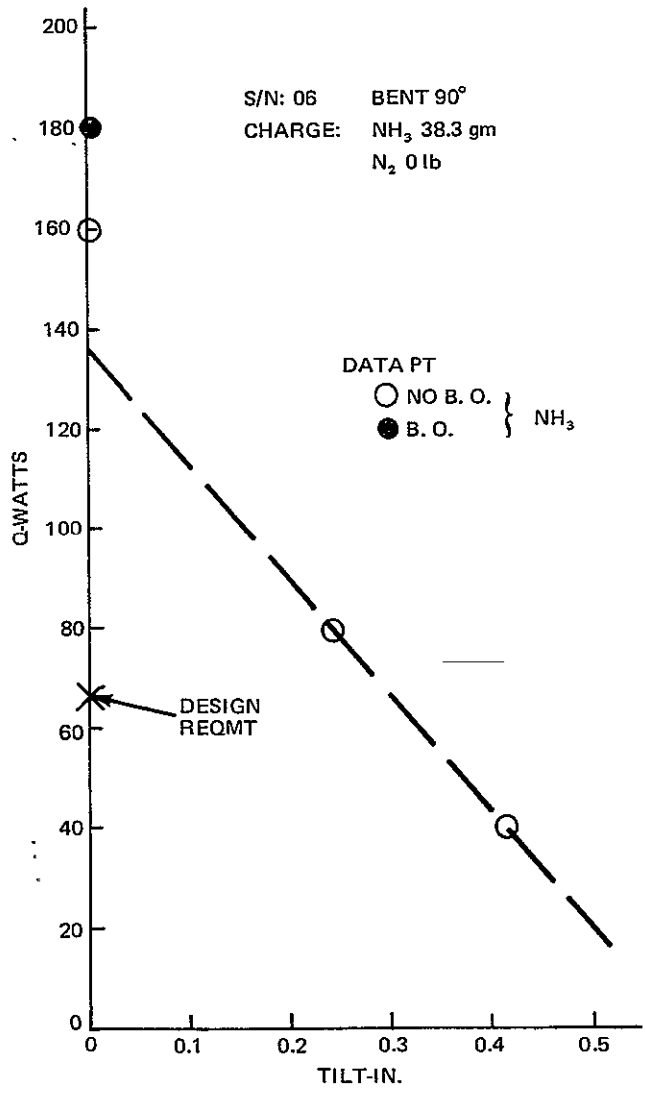


Fig. 4-5 Feeder Heat Pipe Performance (S/N 06)

The temperature distribution along (Serial No. 01) pipe in the VCHP mode is shown in Fig. 4-6 at three different power levels. At 20 watts, the vapor/gas interface is located near the beginning of the condenser. At 80 watts, the interface moves along the condenser exposing a larger condensing area to the water heat sink. Finally at 160 watts, the entire condenser length is active. During these power changes, it is noticed that the evaporator temperature, as expected, remained unchanged at an average value of about 62.5°F. Also, at 160 watts, the temperature differential between the evaporator and condenser is only about 2°F.

The thermocouple temperature data is presented in Table 4-1 for Serial No. 01 pipe, bent 90 degrees for both the single fluid and VCHP test conditions. This data was typical for the other five feeder pipes.

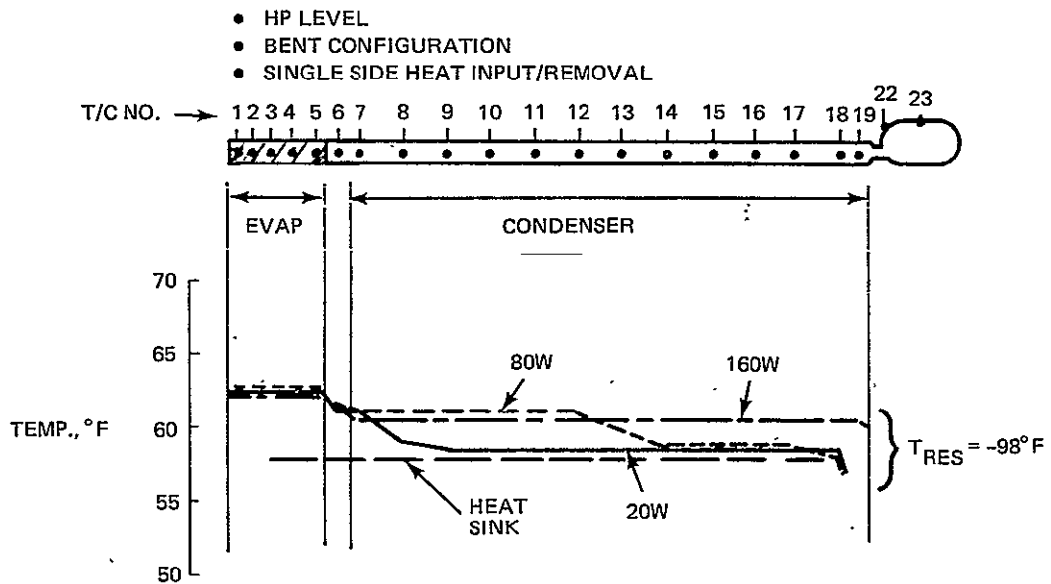


Fig. 4-6 Feeder VCHP Test Results – Temperature Profile

Table 4-1 Feeder Heat Pipe Bench Test Data (S/NO.01) – Bent

TEST MODE:	SINGLE FLUID	SINGLE FLUID	SINGLE FLUID	VCHP*	VCHP*	VCHP*
Tilt (in.)	0	1/4"	1/2"	0	0	0
I (AMPS)	3.84	2.86	1.56	1.28	2.56	3.62
V (VOLTS)	47	35	19	15.6	31	44
Q (WATTS)	180	100	80	25	80	160
T/C #						
EVAPORATOR	1	62.5	60	61.5	62.5	62.5
	2	63	61	59.5	62	63
	3	62	60	58	62	62.8
	4	63	60	58	62.5	63
	5	64	61	58.5	62.5	63
TRANSPORT	6	61.5	59	57	61	61.5
	7	61	59	57	61	61
	8	60.5	59	57	59	61
	9	60.5	58.5	57	58.5	61
	10	61	59.5	57	58.5	61.5
CONDENSER	11	61	59.5	57	58.5	61
	12	61	59.5	57	58.5	61
	13	61	59	57	58.5	60
	14	61	58	57	58.5	58.5
	15	61	58.5	57	58.5	58.5
	16	61	58.5	57	58.5	58.5
	17	61	58.5	56.5	58.5	58.5
	18	61.5	58.5	57	58	58
LOW-K	19	60.5	58	57	57	57
	20	59.5	58	57	54	54.5
	21	61.5	60	58.5	-4	-6
RESERVOIR	22	64.5	62.5	61	-85.5	-89
	23	64	62	60	-97	-96
HEAT SINK	24	57	57	56	59	58.5
ROLL NO.	8	9	9	9	9	9
DATE	9/30/74	10/1/74	10/1/74	10/2/74	10/2/74	10/2/74
TIME	PM	AM	AM	AM	AM	AM
Ammonia Charge (GMS): 44						
*Nitrogen Gas Charge (lb): 0.0135						

## 4.2 FLEXIBLE HEAT PIPE HEADER TESTS

The purpose of these tests was to determine single fluid and variable conductance performance with the pipe oriented in a straight configuration and flexed at a 90 degree angle. In the flexed orientation, the evaporator was always tested in a horizontal plane on level or tilted above the condenser. Electrical heat input was provided around the entire circumference of the 76.2 cm (30 in.) evaporator. Heat was removed by submerging the condenser in a flowing water trough. During some tests, a water spray was used to lower the pipe temperature during high power runs. A thermocouple installation drawing is presented in Fig. 4-7.

Figure 4-8 shows the test results obtained with the pipe charged only with ammonia. The maximum sustained capacity was about 950 watts at zero tilt with the pipe in a straight configuration. This was well above the 400 watt panel requirement. Strong performance was also noticed at high tilts, which unlike the longitudinally grooved pipe, is characteristic of the fine pore size obtainable with screen wicks. With the pipe flexed at a 90 degree angle, (see Fig. 4-9) no degradation in performance was noticed as shown by the data points at 0.5 in. and 1.0-in. tilts. Although in these tests power was turned off while the pipe was repositioned, subsequent tests revealed that the pipe remained primed during repeated slow flexing of the evaporator between its straight and angled positions. Thermocouple data in the straight and flexed configuration is presented in Table 4-2.

After the single fluid test sequences, nitrogen was added to the pipe to allow VCHP testing. In this mode, only loads as high as 300 watts could be obtained. It was apparent that the tunnel was unprimed and it is probable that a portion of the spiral gaps were also unprimed, since the full gap capacity was estimated to be about 600 watts. Failure to prime was attributed to the presence of gas bubbles within the artery as well as high pressure oscillations which were subsequently recorded at relatively low power (150 watts) levels. Appendix C documents the pressure oscillations that were observed with and without the presence of nitrogen control gas. Efforts to vent the gas bubbles through the perforated evaporator end foil or collect them in the gas trap proved unsuccessful.

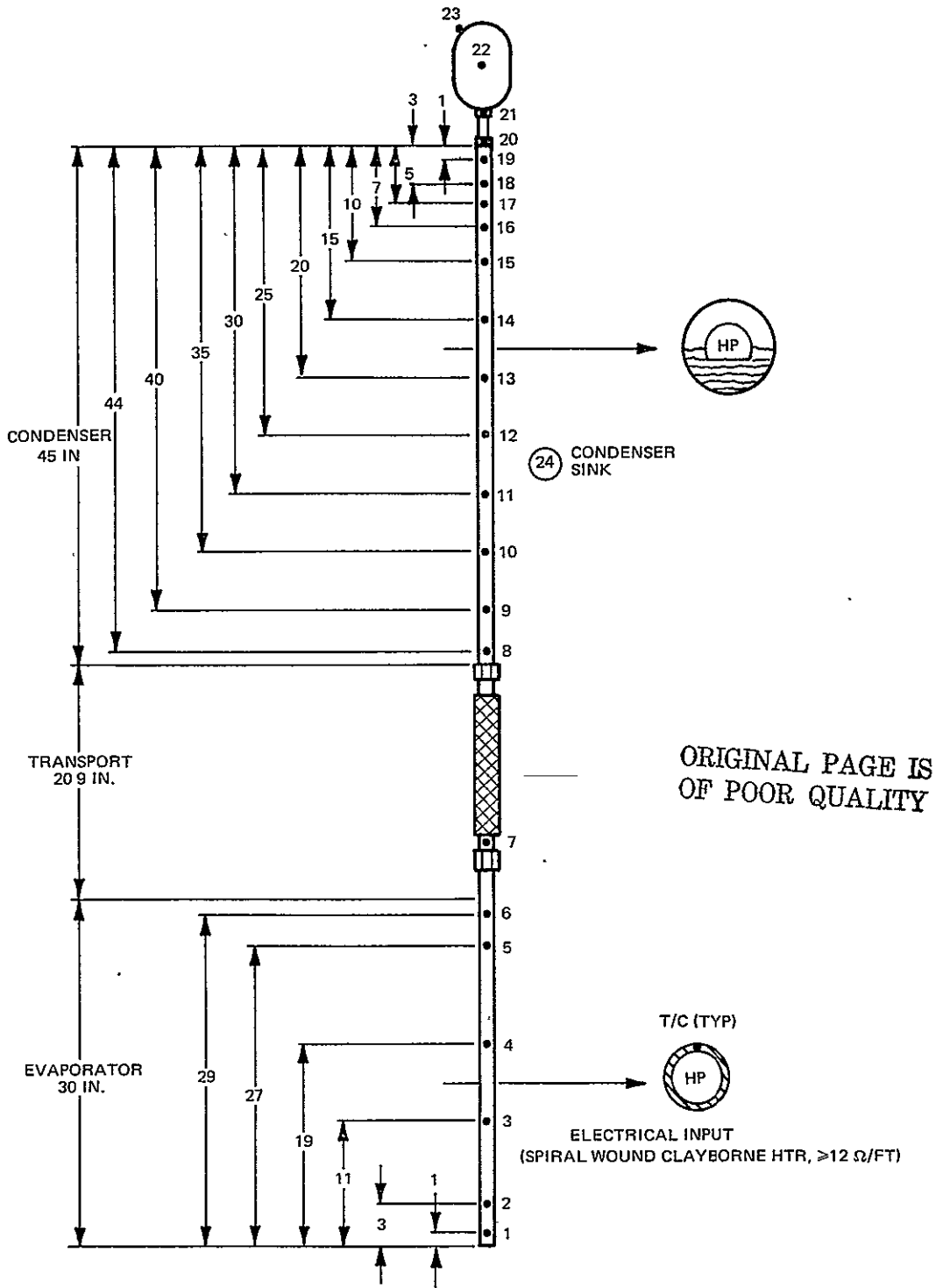


Fig. 4-7 Header Heat Pipe Instrumentation Set-Up

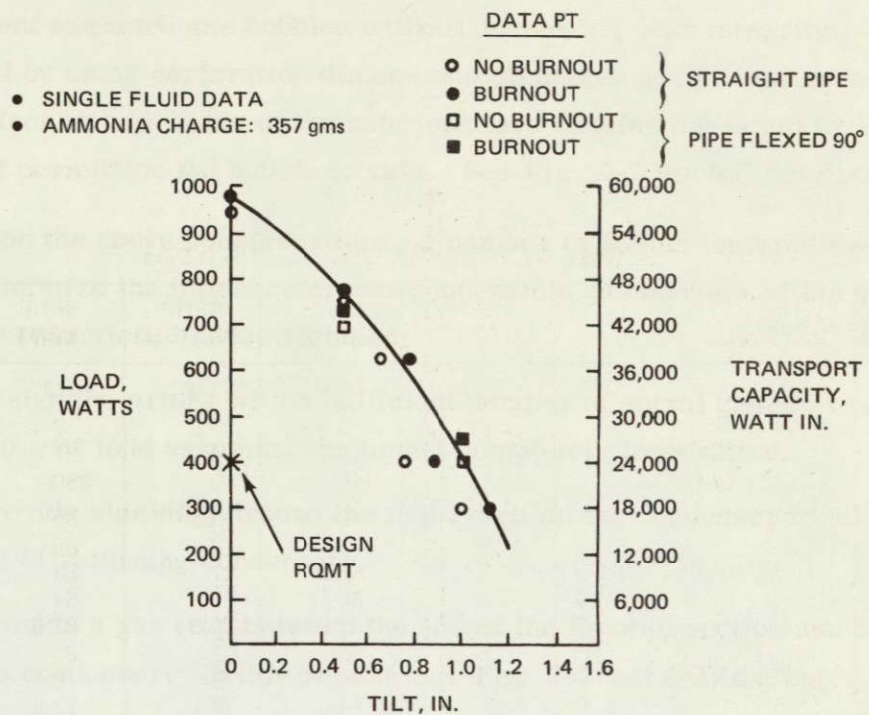


Fig. 4-8 Flexible Heat Pipe Header Test Results

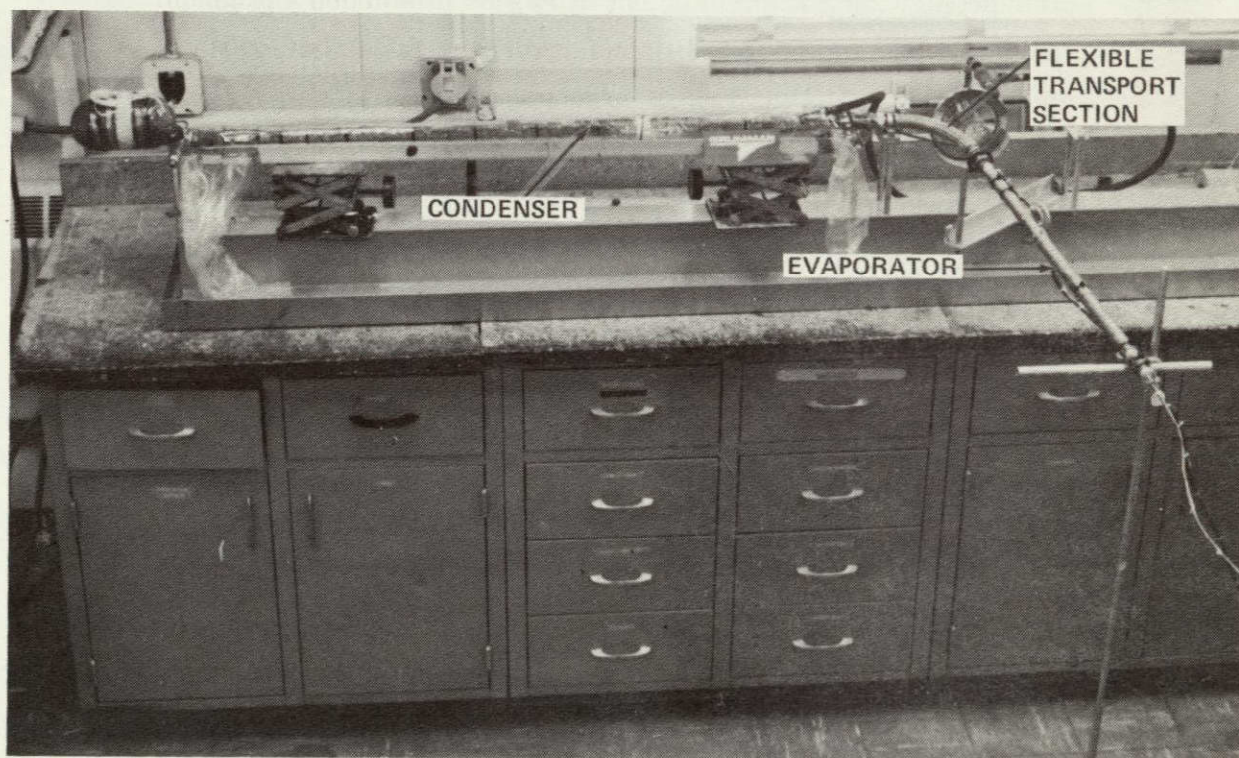


Fig. 4-9 Flexible Header Heat Pipe Shown Bent 90 Degrees During Acceptance Test

Table 4-2 Header Heat Pipe Bench Test Data

TEST MODE:	SFHP STRAIGHT	SFHP STRAIGHT	SFHP STRAIGHT	SFHP BENT	
TILT (IN.)	LEVEL	LEVEL	1/2"	1/2"	
I (AMPS)	7.5	9.3	7.5	7.4	
V (VOLTS)	88	10.2	88	87	
Q (WATTS)	660	945	660	650	
TC #					
EVAPORATOR	1	74.5	82	79.5	85
	2	71.5	78	78	80
	3	75.5	83.5	81	84
	4	77.0	86	81	84
	5	75.5	83.5	81.5	83.5
	6	76.5	85	82	85
TRANSPORT	7	70.0	75	75	78
	8	68.5	74	74	77.5
	9	67.0	68	66	71
CONDENSER	10	68	73.5	74	76
	11	69	74	74.5	77.5
	12	67.5	72.5	73.5	76.5
	13	68	73.5	74	77
	14	68	73	74	77
	15	68	72.5	73	76
	16	68	73	73	76
	17	68.5	73.5	74	77
	18	-	-	-	-
LOW-K	19	68	72	73	77
	20	66	71	71.5	76
RESERVOIR	21	69	74	74.5	77
	22	70.5	75	75	77.5
HEAT SINK	23	70.5	75	75	77.5
	24	55	56	56	66.5
ROLL NO.	4	4	4	5	
DATE	10/30/74	10/30/74	10/30/74	11/1/74	
TIME	1407	1522	1158	1158	

AMMONIA CHARGE (GMS): 357

## 5 - RADIATOR SYSTEM TESTS

After assembling the feeder pipes into the panel, tests were performed for systems A and B. In addition, a "no-control" system (denoted by I) was tested which was identical to system A except that the feeder pipes were single fluid devices, charged only with ammonia. Although not having any variable conductance control capability, this system was tested to serve as a basis of comparison with the other two control systems, A and B. Systems C and D were not tested due to the inability of the header to satisfactorily operate in the VCHP mode. These tests were essentially acceptance tests to check the overall performance of each system. More thorough thermal vacuum tests are planned by NASA/MSFC.

Testing was done at ambient pressure in an insulated box to simulate a radiation environment. Fig. 5-1 shows the schematic of the test set-up. The radiator was installed horizontally in the box above a 0.318 cm (0.125 in.) thick aluminum cold plate. The underside of the radiator transferred heat to the cold plate which was cooled by a LN<sub>2</sub>/distribution system. The upper side of the radiator was insulated. This arrangement, which is the opposite of normal orientation (upper side is radiator), minimized convection between the radiator and the cold plate thereby producing a more realistic radiation coupling. Both sides of the radiator and the reservoirs were coated with Z306, a black paint with a 0.85 emittance. The heat source was supplied by a 0.063 kg/s (500 lb/hr) temperature controlled Freon-21 loop coupled either to the fluid header (in systems I and A) or the heat pipe header heat exchanger (in system B). A total of 45 thermocouples were used for systems A and I tests while 48 thermocouples were used for system B tests. Figure 5-2 shows the thermocouple locations. Included in the total are four thermocouples used to monitor the cold plate temperature (environment).

A typical test run consisted of setting and maintaining the cold plate to a temperature between -30°F and -110°F. The Freon-21 inlet temperature was then adjusted to a steady value of about 60°F and a flow of 500 lb/hr. When steady state was reached, data from all 48 thermocouples were recorded.

1/8 ALUMINUM ALY

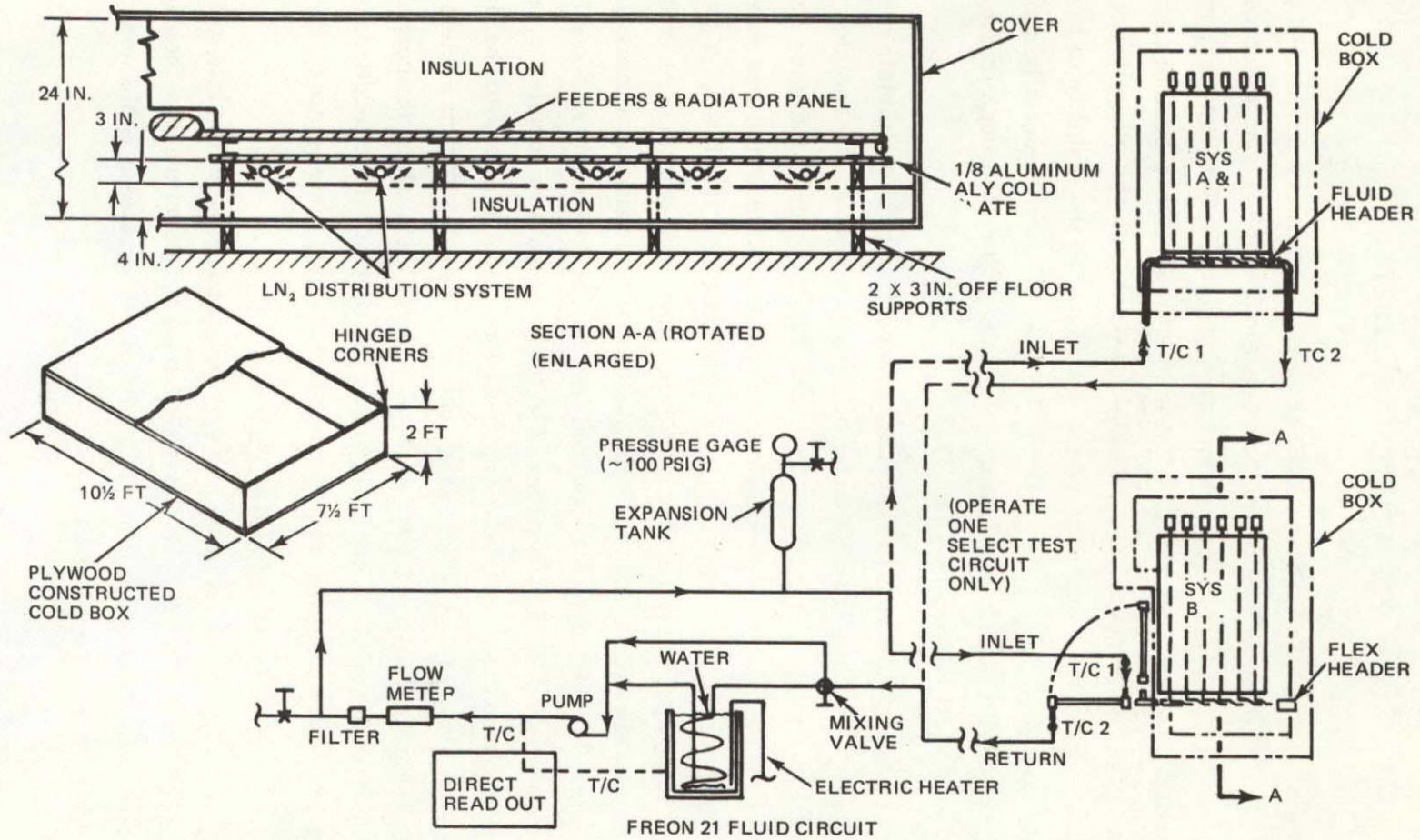


Fig. 5-1 Cold Box Testing Arrangement for Systems A, B, and I

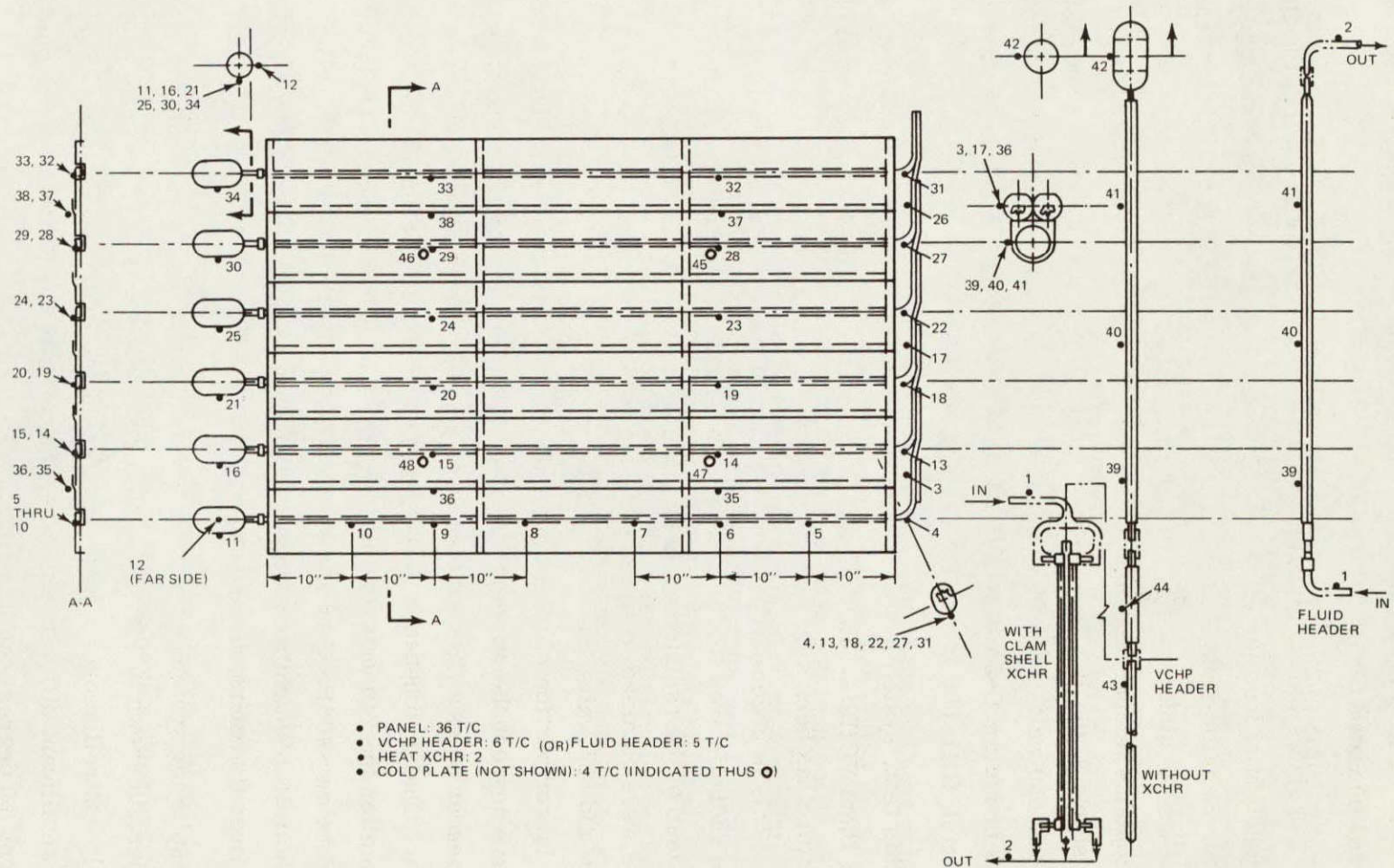


Fig. 5-2 Thermocouple Locations : Copper Constantan Type T/C

Approximately six runs were made with the inlet at 60°F, 70°F, 80°F, 90°F, 100°F and 110°F. These values extended below and above the required load range of 200 watts to 400 watts.

Figure 5-3 shows the steady state response of the Freon-21 exiting the fluid header as a function of load for system I. As expected, the response was typical of a fixed conductor radiator/fluid loop panel. At low loads the Freon-21 outlet temperature approaches the sink temperature, which in this case was between -84°F to -70°F. Appendix D contains temperature maps (°F) for all thermocouples for system I tests as well as systems A and B. Two maps, Figures D-1 and D-2, are presented for system I at 370 and 650 watts respectively. (In some cases, inconsistencies in data appear, such as in Figure D-2 where T/C 41 is lower than T/C 2. This is attributed to poor contact of T/C 41.)

After this test, system A was evaluated by adding nitrogen to each of the feeder pipes making them VCHP's. Results for this system (Fig. 5-3) show that the outlet fluid temperature has been significantly controlled over a load range from near zero to 600 watts. This is accomplished by the action of the VCHP's automatically adjusting the active radiator area to changes in load. Figure 5-4 shows an approximate temperature map of the radiator at three different power levels of 240, 440 and 590 watts. These were obtained from temperature maps in Figures D-4, D-5, and D-6. (Maps at zero and 625 watts are also included in Figures D-3 and D-7.) As the load increases, a larger portion of the radiator above 50°F is activated. Also, those feeder pipes which are nearest the warmer Freon-21 inlet have longer active condensers than downstream feeder pipes. The temperatures along the first or most upstream feeder pipe is shown. (Distance between thermocouples is about 25.4 cm (10 in).) Note that at the interface for the 240 watt profile, the pipe temperature changes sharply from above 50°F to below -40°F. At near zero load (Fig. D-3), the inlet and outlet temperatures were both 55.5°F while the panel, which was essentially shut-off, was about -50 to -20°F over its entire surface.

Test results for system B, which uses the flexible heat pipe header in place of the fluid header, is shown in Fig. 5-5. It is seen that the outlet Freon-21 temperature was effectively controlled over a load range extending to about 850 watts. Furthermore, there was no significant difference in performance with the flexible header pipe in a straight or bent (90 degree) configuration.

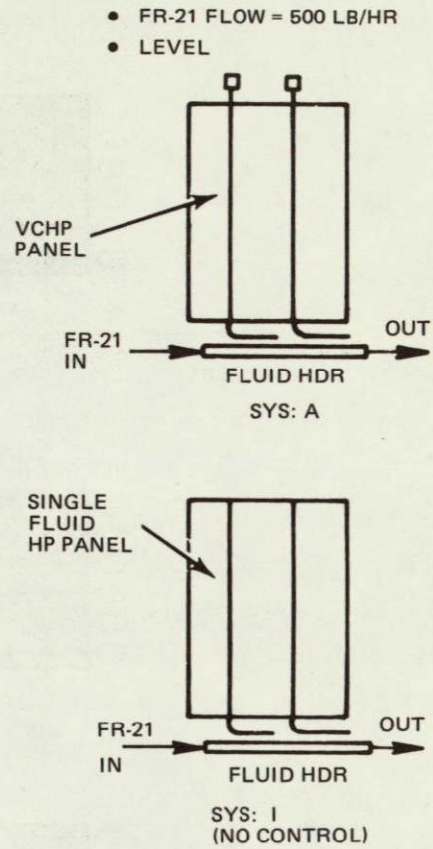
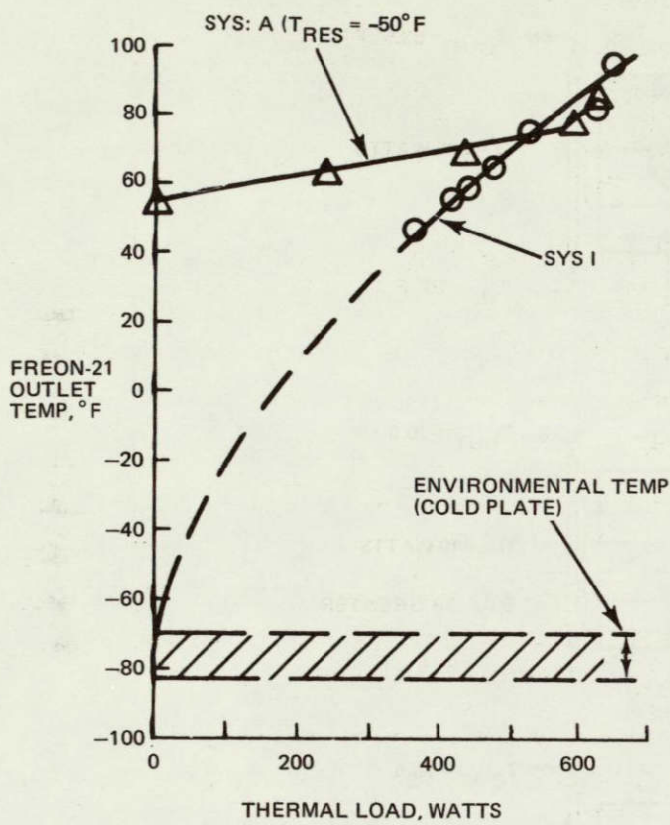


Fig. 5-3 Radiator Systems A and I Test Results

- SYSTEM A: FLUID HDR/VCHP FEEDERS
- FREON-21 FLOW RATE: 500 LB/HR
- SINK TEMP:  $-71^{\circ}\text{F}$  TO  $-91^{\circ}\text{F}$

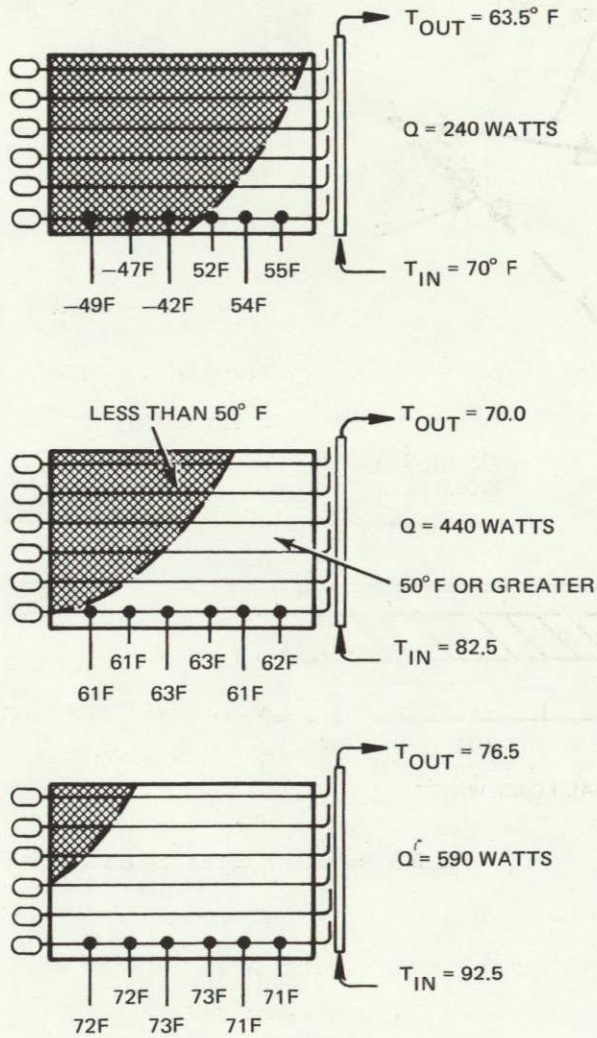


Fig. 5-4 System A Test Results – Panel Temperature Pattern

ORIGINAL PAGE IS  
OF POOR QUALITY

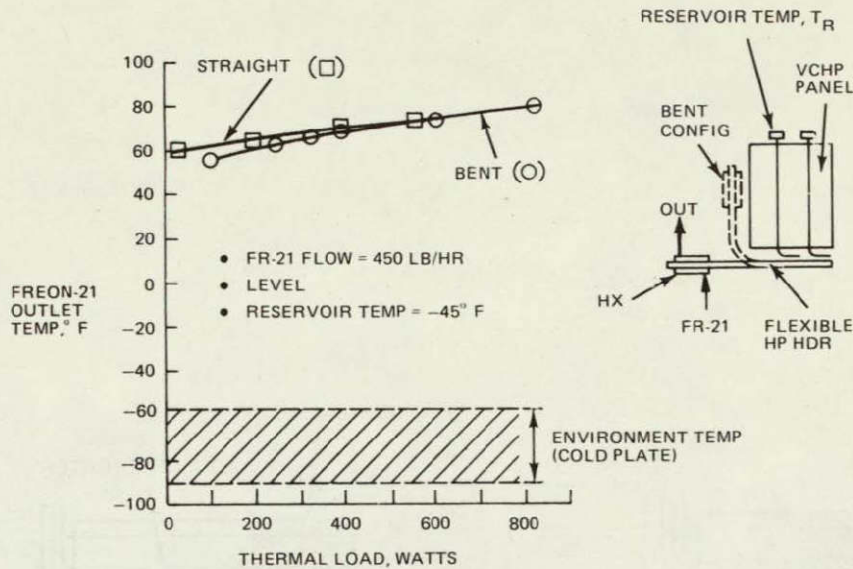


Fig. 5-5 Radiator System B Test Results

Although the Freon-21 temperature response is similar for both systems A and B, there is a basic difference in the manner in which the radiator area responds. This is shown in Fig. 5-6 where a panel profile for configuration B is depicted at two power levels of 198 and 462 watts. As power increases, the active radiator area increases. However, unlike system A, the active area increases more uniformly across its 1.2m (4 ft) width. This is because the condenser of the heat pipe header supplies a uniform temperature heat source to the radiator as opposed to continually decreasing temperature heat source supplied by the fluid header in system A. The temperature distribution along the first pipe is also shown, indicating the drop off in temperature across the interface. Figures D-8, -9, and -10 depict temperature maps for the straight configuration at 198, 313, and 462 watts. Figures D-11, D-12 and D-13 depict temperature maps for the bent configuration at 99, 396 and 692 watts.

The overall performance summary of systems A and B are given in Table 5-1 along with the no-control system I. It is obvious that systems A and B provide effective outlet temperature control over that of system I. There is also no significant difference in performance between system A and either the straight or deployed orientation of system B. Although it appears that the Freon-21 outlet temperature was below the minimum design goal value of 70°F, final evaluation of panel thermal performance can only be done in a thermal vacuum test environment, where other factors which affect outlet temperature response, such as reservoir temperature and system heat losses can be properly examined.

- SYSTEM B: HP HDR/VCHP FEEDERS
- FREON-21 FLOW RATE: 446 LB/HR
- SINK TEMP:  $-45^{\circ}\text{F}$  TO  $-95^{\circ}\text{F}$
- HDR PIPE – STRAIGHT

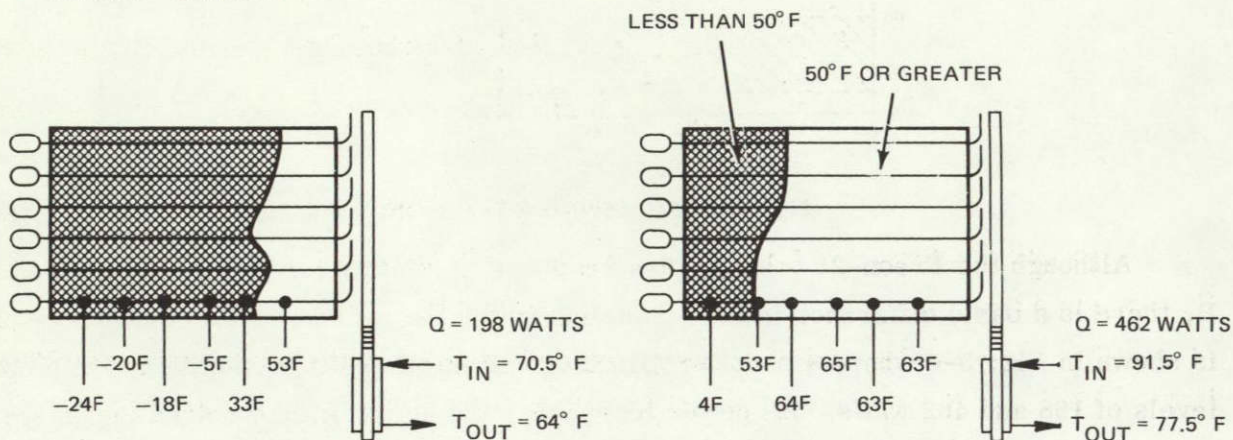


Fig. 5-6 System B Test Results – Panel Temperature Pattern

Table 5-1 Performance Summary of Radiator Systems

SYSTEM	FREON-21 OUTLET TEMPERATURE, $^{\circ}\text{F}$		$\Delta T$ , $^{\circ}\text{F}$
	AT 200W	AT 400W	
1 (NO CONTROL)	8	50	42
A (FLUID HEADER)	62	69	7
B (HP HDR-STRAIGHT)	64	71	7
B (HP HDR-BENT)	62	70	8

## 6 - CONCLUSIONS

- Two completely passive heat pipe radiator systems have been built which successfully demonstrated effective temperature control of a fluid loop heat source
  - System A - Fluid header coupled to a radiator composed of VCHP's
  - System B - Heat pipe header coupled to a radiator composed of VCHP's
- The heat pipe header of System B has a flexible section that allows radiator deployment over a 90 degree bend. Single fluid transport capacities of about 850 watts, corresponding to 51,000 watt-in. have been achieved in a 90 degree bent orientation
- Each system has demonstrated the ability to provide near complete radiator shut down in cold environments, thereby preventing fluid loop freeze-up in low power situations
- Although thermal performance of both systems A and B were similar, detailed evaluation must be made in more refined thermal vacuum tests
- Radiator concepts that provide temperature control using large capacity variable conductance heat pipe headers are not attractive at the present time because of the unreliable nature of artery type VCHP's. On the other hand, longitudinally grooved pipes, although smaller in capacity, perform reliably in the VCHP mode.

## 7 - REFERENCES

1. Edelstein, F., Roukis, J. G., and Loose, J. D.: "The Development of a 150,000 Watt-Inch Variable Conductance Heat Pipe for Space Vehicle Thermal Control", ASME Paper 72-ENAv-14.
2. Kosson, R., Hembach, R., Edelstein, F.: and Loose, J. D. "Development of a High Capacity Variable Conductance Heat Pipe", AIAA Paper 73-728.
3. Eninger, J. E.: "Menisci Coalescence as a Mechanism for Venting Noncondensable Gas From Heat-Pipe Arteries", AIAA Paper No. 74-748.
4. "Heat Pipe Radiator - Final Report" by Grumman Aerospace Corp. for NASA/JSC, Contract NAS9-12848, October 1973.
5. "Space Shuttle Heat Pipe Thermal Control Systems - Final Report" by Grumman Aerospace Corp. for NASA/JSC, Contract NAS9-12801, October 1973.

## APPENDIX A - DEPLOYABLE HEAT PIPE RADIATOR - PANEL DESIGN SELECTION

### SUMMARY

This analysis details the selection of the basic panel design for the deployable heat pipe radiator. It considers concepts that use either a fluid header or a heat pipe header and provides parametric performance analyses for each basic type.

The recommended panel design, which is suitable for any operating mode, uses a 0.032-in. thick aluminum panel with six heat pipes. The pipes are coupled to the fluid or HP header with mechanical attachments, whose efficiency have a strong impact on panel performance.

### INTRODUCTION

The objective of this tradeoff study is to determine the number of panel feeder heat pipes and the panel fin thickness that will best satisfy the performance requirements of the deployable heat pipe radiator. These requirements are summarized in Table A-1. The four possible operating modes are included in this preliminary design study (see Fig. 2-1).

The basic panel design, in terms of the number of heat pipes and fin thickness, is dictated by successful operation at the maximum load (400 watts) and maximum environment ( $-30^{\circ}\text{F}$  sink) condition. If the panel can be designed to provide the necessary fin root temperature to reject the maximum load in the warmest environment, then it can be made to function properly under less severe combinations of load and environment. As seen in Fig. 2-1, only two generic categories need be considered for operation at maximum load and environment since all panels will be fully open, utilizing all of the available 24 square feet surface area. One category (Category I) uses a direct coupling to a fluid line header (System A). The other category (Category II) uses a HP header to couple the panel to the fluid loop (Systems B, C and D). At the extreme operating condition Systems B, C and D are indistinguishable when considering the temperature drops through each system, since the VCHP's and SFHP's have exactly the same active lengths.

## RESULTS

The major factors which dictate the thermal design of the heat pipe radiator panel are the fin root temperature, thermal load and the environment. This is illustrated in Fig. A-1 which shows the net heat rejection per unit area as a function of fin root temperature for several values of fin effectiveness ( $\eta_F$ ) at the warmest (-30°F) and coldest (-110°F) environments. Considering the critical design case (400 watts, -30°F sink) and a completely active 24 square foot area, about 57 BTU/hr must be rejected from each square foot of area. Assuming a fin effectiveness of 0.90 (a reasonable design target), a root temperature of 62°F is needed to reject the 400 watt load to the -30°F environment. This means that the panel design, no matter what category, must result in a minimum fin root temperature of 62°F if it is to meet the critical design case heat rejection requirements. A lower fin effectiveness would require a higher fin root temperature for the same heat rejection. For example, 73°F is needed at  $\eta_F = 0.80$  and 83°F at  $\eta_F = 0.70$ . This means that the overall system temperature drop from the fluid inlet to the fin root must be further minimized in order to accommodate lower effectiveness values---that means decreasing thermal resistances.

Figure A-2 is a general design curve that relates the panel design, in terms of number of heat pipes and panel fin thickness, to fin effectiveness. It assumes a 4 ft x 6 ft aluminum panel with a 0.90 surface emittance and a ratio of sink to root temperature ( $T_S/T_R$ ) of unity. The latter assumption insures conservative results since the effectiveness increases as the ratio  $T_S/T_R$  decreases from 1.0, all other things being equal. From Figure A-3, the requirement for a 62°F root temperature and a 0.90 effectiveness can be met either by a 0.032-in. thick fin and six heat pipes, or a relatively thick 0.048-in. fin and five heat pipes. Four heat pipes don't come close to meeting the 0.90 requirement for any reasonable thickness. Figures A-1 and A-2 can be used together to relate panel heat rejection capability and root temperature to the required panel design. This was done for the critical design case and the results are summarized in Table A-2.

It now remains to be seen if Category I and II systems can be designed to give the necessary fin root temperatures that will meet the heat rejection requirements. This can be done by analyzing the temperature drops through each system, from fluid inlet to fin root, and comparing the available fin root temperature with the minimum required value, as given in Table A-2.

Table A-1 – Performance Requirements Summary

	MAX	MIN
LOAD, Q, WATTS	400	200
FREON-21 FLOW RATE, LB/HR	500	500
FLUID OUTLET TEMP, °F	90	70
FLUID INLET TEMP, °F	101	75.5
SINK TEMP, °F	-30	-110

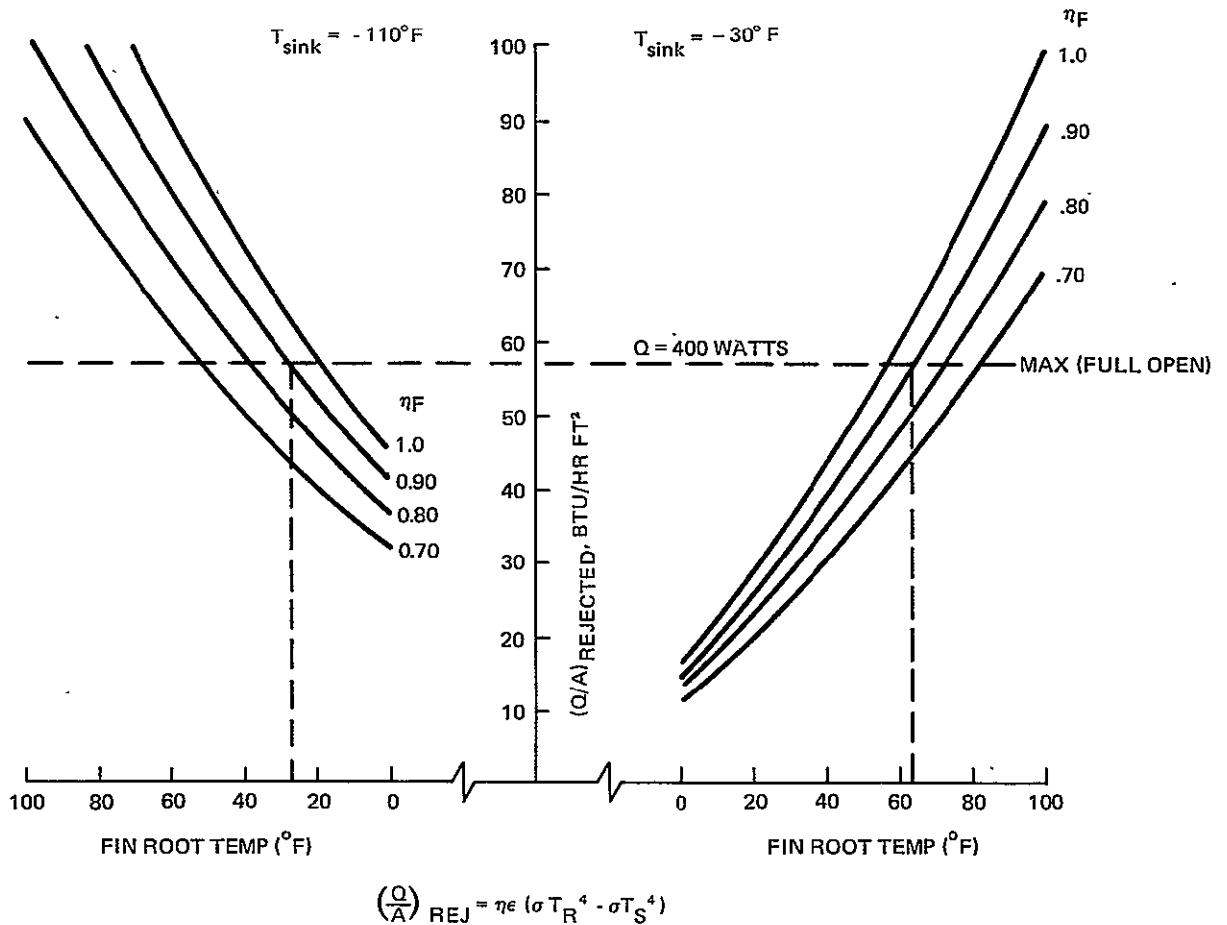


Fig. A-1 Heat Pipe Radiator Panel Heat Rejection Capability

- ALUMINUM PANEL, 4 FT x 6 FT
- $\epsilon = 0.90$
- $K = 100 \text{ BTU/HR FT } ^\circ\text{F}$
- $\frac{T_S}{T_R} = 1.0$
- SINGLE SIDE REJECTION

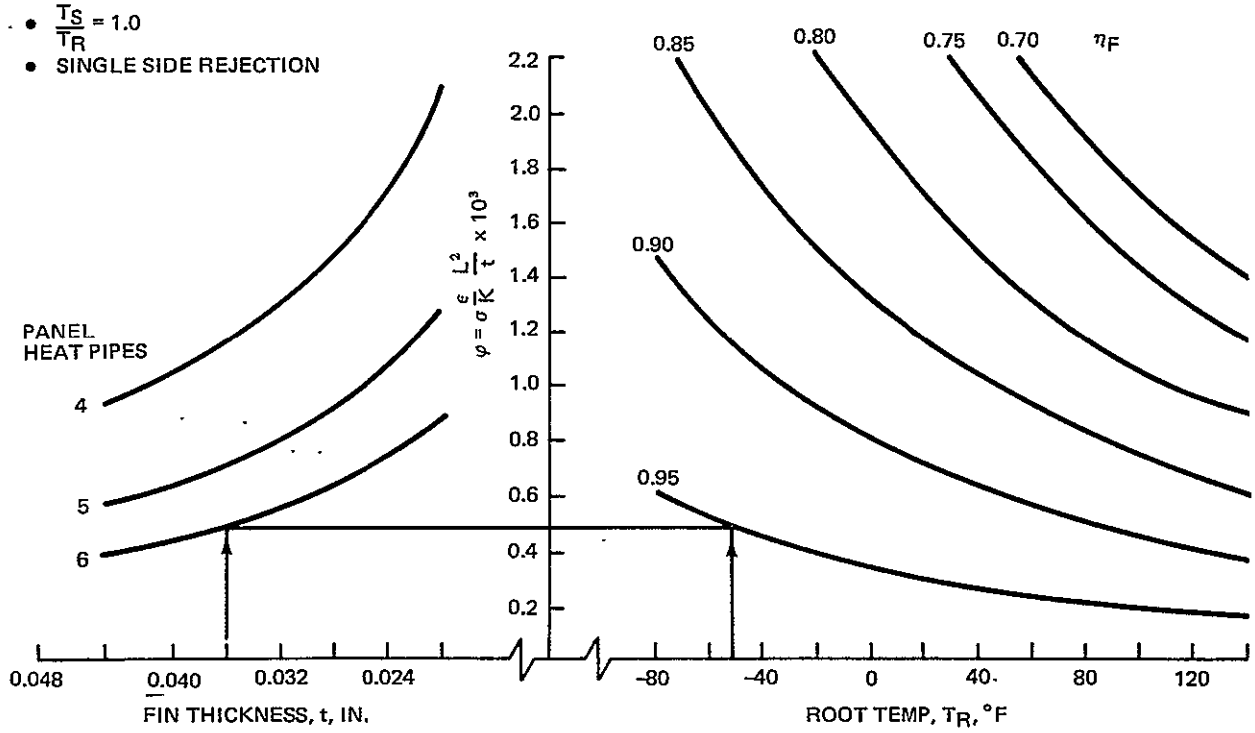


Fig. A-2 Radiator Fin Effectiveness ( $\eta_F$ )

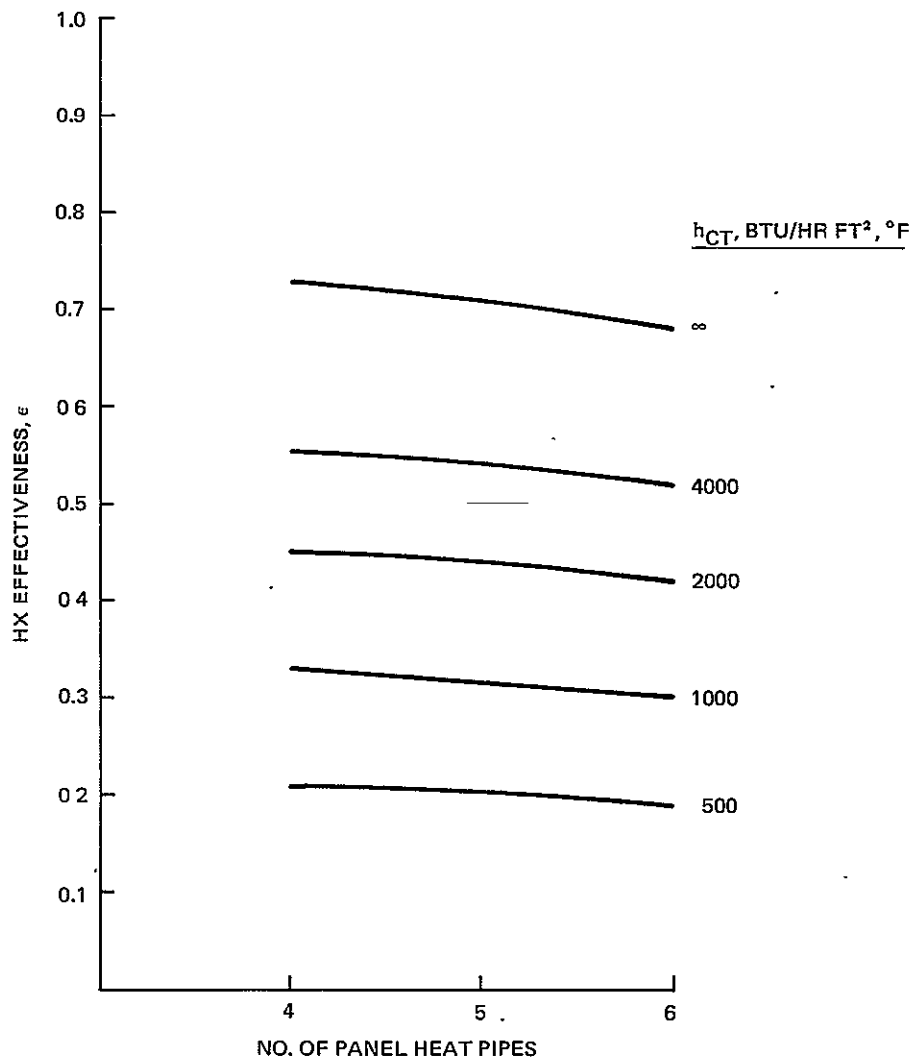
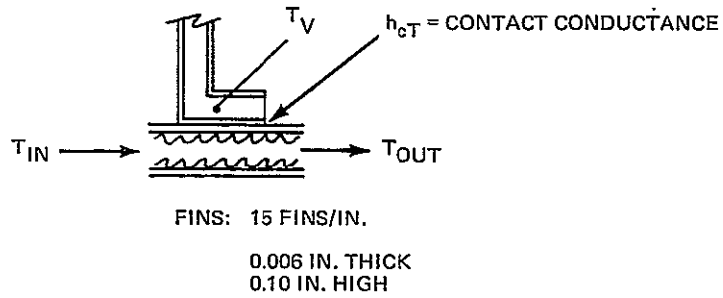


Fig. A-3 Heat Exchanger Effectiveness – Finned Tube Header to Panel Heat Pipe

Table A-2 Heat Pipe Panel Requirements,  
 $Q_{rej} = 400$  Watts,  $T_{sink} = -30^{\circ}\text{F}$

$\eta_F$	$T_{ROOT}$ ( $^{\circ}\text{F}$ )	NO. OF HEAT PIPES	$t$ (IN.)
0.9	62	6	0.032
		5	0.048
0.8	73	6	0.016*
		5	0.024
		4	0.036
0.7	83	6	0.016*
		5	0.016*
		4	0.024

\*Minimum allowable thickness for fabrication

### Category I (System A) Performance

Assuming a properly finned fluid tube header, the most critical parameter affecting the fin root temperature, and thus the panel heat rejection capability, is the contact conductance at the fluid tube to HP evaporator interface. As seen in Fig. A-3, the heat exchanger effectiveness from fluid to HP vapor is a strong function of the interface conductance,  $h_{CT}$ . The number of pipes has little effect since the overall heat transfer lengths are about the same, varying from 40 in. (four HP's with 10-in. long evaporators) to 36 in. (six HP's with 6-in. evaporators). The generalized expression giving fin root temperature as a function of various system parameters is given below and developed in detail at the end of this Appendix.

$$T_R = T_{IN} - \frac{Q/MC_p}{\epsilon} - \left(\frac{Q}{N}\right) \left[ \frac{1}{(\eta hA)_c} + \frac{1}{h_p A_p} \right]$$

It has been solved for the 400 watt design case and the results are plotted in Fig. A-4, which gives fin root temperature as a function of number of panel heat pipes for several values of interface contact conductance,  $h_{CT}$ . As seen from the figure, a contact conductance of 1000 BTU/Hr Ft<sup>2</sup>°F results in a fin root temperature of at least 62.5°F, depending on the number of HP's. Higher values of  $h_{CT}$  yield correspondingly higher fin root temperatures. Reasonable combinations of  $h_{CT}$  and number of HP's that result in acceptable root temperatures, as determined from Fig. A-4, are given in Table A-3.

Table A-3 Category I, Available Root Temperatures

$h_{ct}$ (BTU/HR FT <sup>2</sup> °F)	NO. HEAT PIPES	$T_R$ (°F)
1000	6	62.5
1000	5	64
1000	4	65
2000	6	73
2000	5	73.5
2000	4	74

- SYSTEM A – FLUID LINE TO PANEL VCHP'S
- MAX LOAD, MAX ENVIRONMENT CONDITION
- $T_{IN} = 101^\circ\text{F}$ ,  $Q = 400$  WATTS,  $T_{SINK} = -30^\circ\text{F}$
- ACTIVE AREA = 24 FT<sup>2</sup>

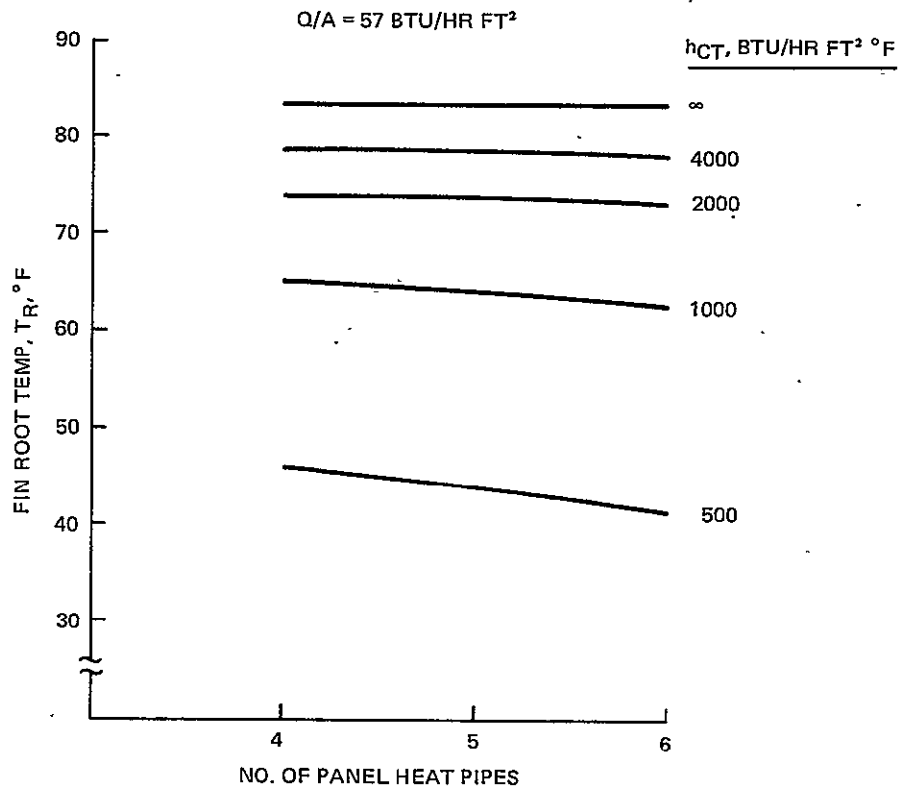


Fig. A-4 Heat Pipe Radiator Performance

The necessary design for Category I panel can be determined when Table A-3, the available root temperature, is compared with Table A-2, the required root temperature. From Table A-2, a fin effectiveness of 0.9 needs a 62°F root and an effectiveness of 0.8 needs a 73°F root. From Table A-3, the lower value of  $h_{CT}$  (1000 BTU/Hr Ft<sup>2</sup>°F) will only yield a 62.5 to 65°F root temperature, the higher 73°F root temperature can only be obtained by doubling  $h_{CT}$  to 2000 BTU/Hr Ft<sup>2</sup>°F. Values of contact conductance on the order of 1000 BTU/Hr Ft<sup>2</sup>°F have been demonstrated with a previous radiator panel using mechanical clamps (ref. 5) and it would be reasonable to limit the design of the deployable panel to this demonstrated value. From Table A-3, the constraint of a limiting 1000 BTU/Hr Ft<sup>2</sup>°F value of contact conductance limits the panel to an available root temperature of 62.5°F. From Table A-2, this means using either six heat pipes and a 0.032-in. fin or five heat pipes and a 0.048-in. fin to get a 0.90 fin effectiveness.

Consideration must now be given to the required heat transport capacity per heat pipe before a final decision is reached on panel design. Using the 400 watt maximum load, the load per heat pipe will be 67 watts (3000 watt-in.) with six pipes and 80 watts (3600 watt-in.) with five pipes. Since the demonstrated transport capacity of the longitudinally grooved pipes with a single fluid (NH<sub>3</sub>) is 5000 watt-in., limiting each HP to the lowest requirement will result in the greatest design margin. This is especially important when the heat pipes are operated as VCHP's since there might be some performance degradation due to the presence of the nitrogen control gas.

Considering the greater performance margin available using six HP's and the lighter gage panel required, a six HP panel design is recommended for Category I. The following summarizes the recommended design for the panel.

#### Category I Recommendations

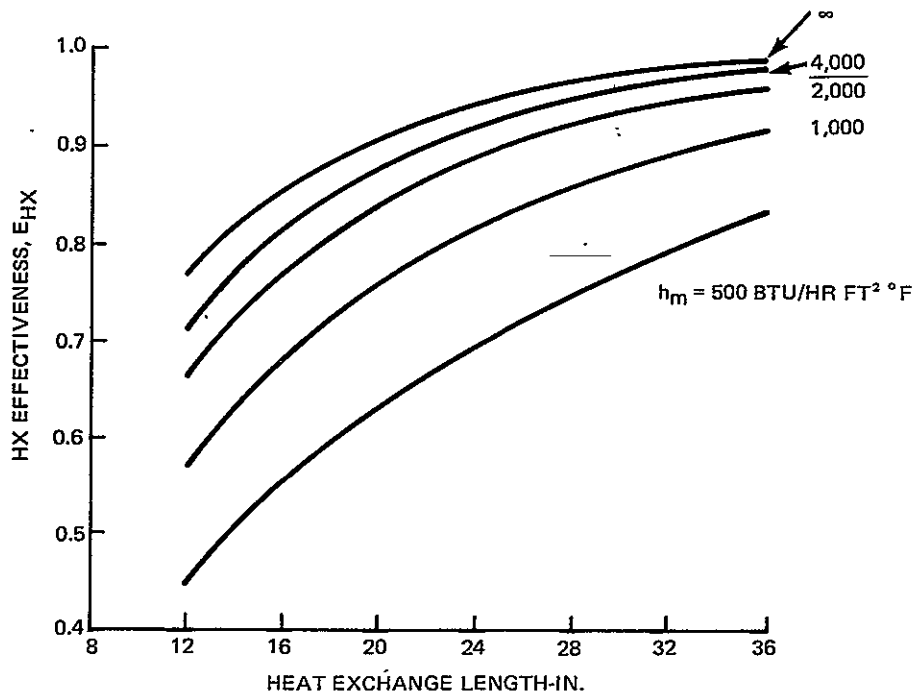
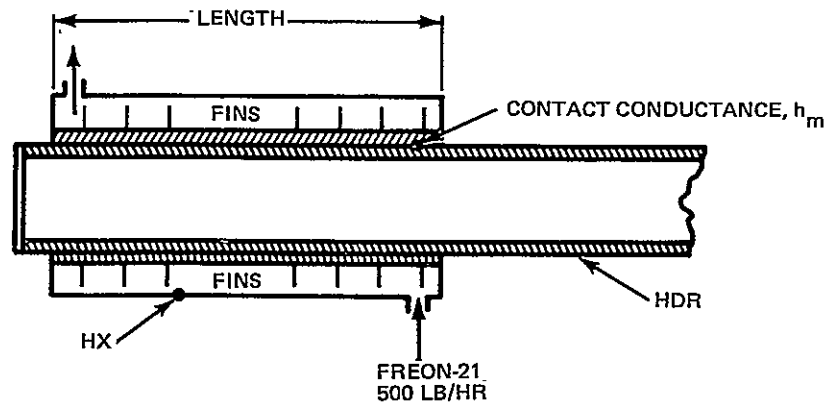
No. of HP's: Six

Aluminum fin thickness: 0.032 in.

#### Category II (Systems B, C and D) Performance

The category II panel may not be as efficient as Category I due to the insertion of an additional thermal resistance, the HP header. However, this inefficiency can be overcome if the fluid heat exchanger is properly designed to give a high enough value of effectiveness. Since the heat exchanger is removable, there is an additional





- HDR I.D. = 1.0 IN.
- FINS: 15 PER IN. (3003 Al)  
0.006 - IN. THICK  
0.10 - IN. HIGH
- HDR FILM COEFFICIENT = 2,000 BTU/HR FT<sup>2</sup> °F

Fig. A-5 Heat Exchanger Effectiveness

ORIGINAL PAGE IS  
OF POOR QUALITY

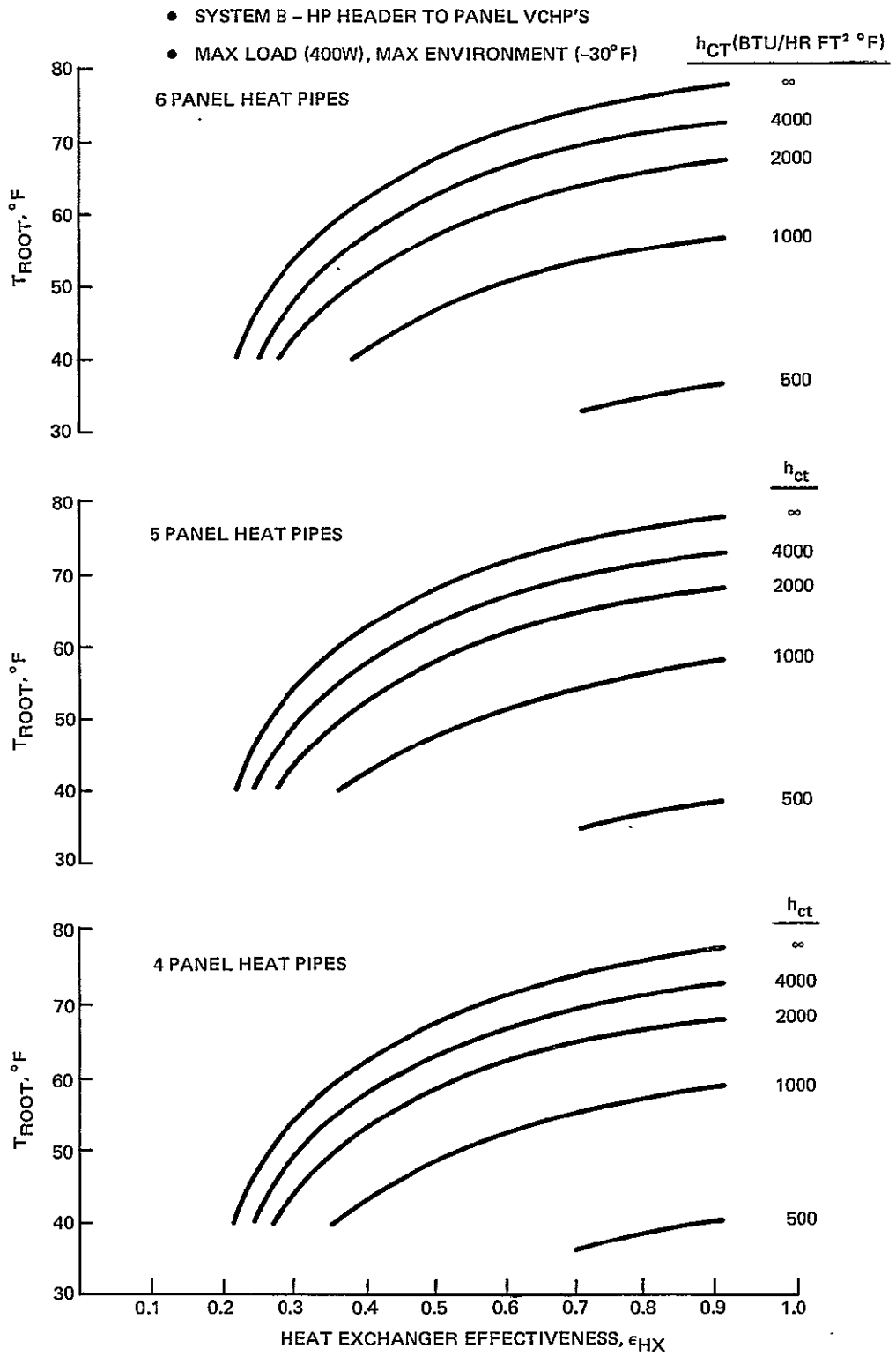


Fig. A-6 Heat Pipe Radiator Performance

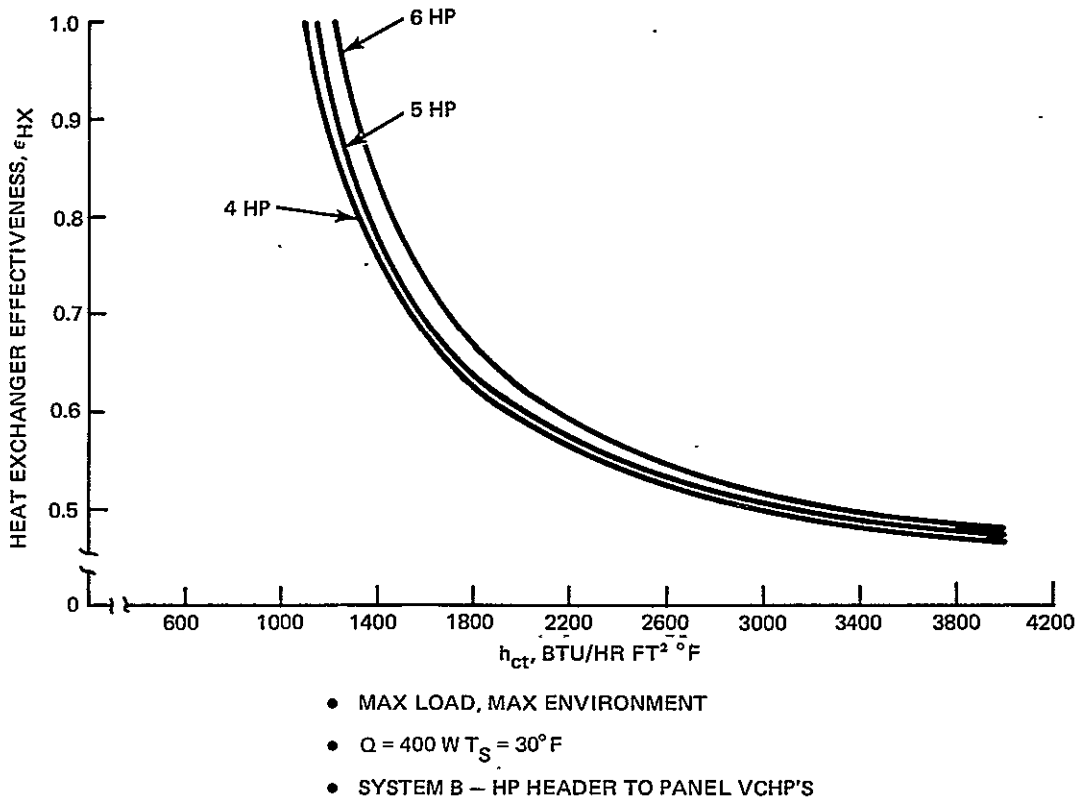


Fig. A-7 Heat Pipe Radiator Design Requirements for  $T_{\text{ROOT}} = 62^\circ\text{F}$ , System B

Table A-4 Category II, Design for  $T_R = 62^\circ\text{F}$

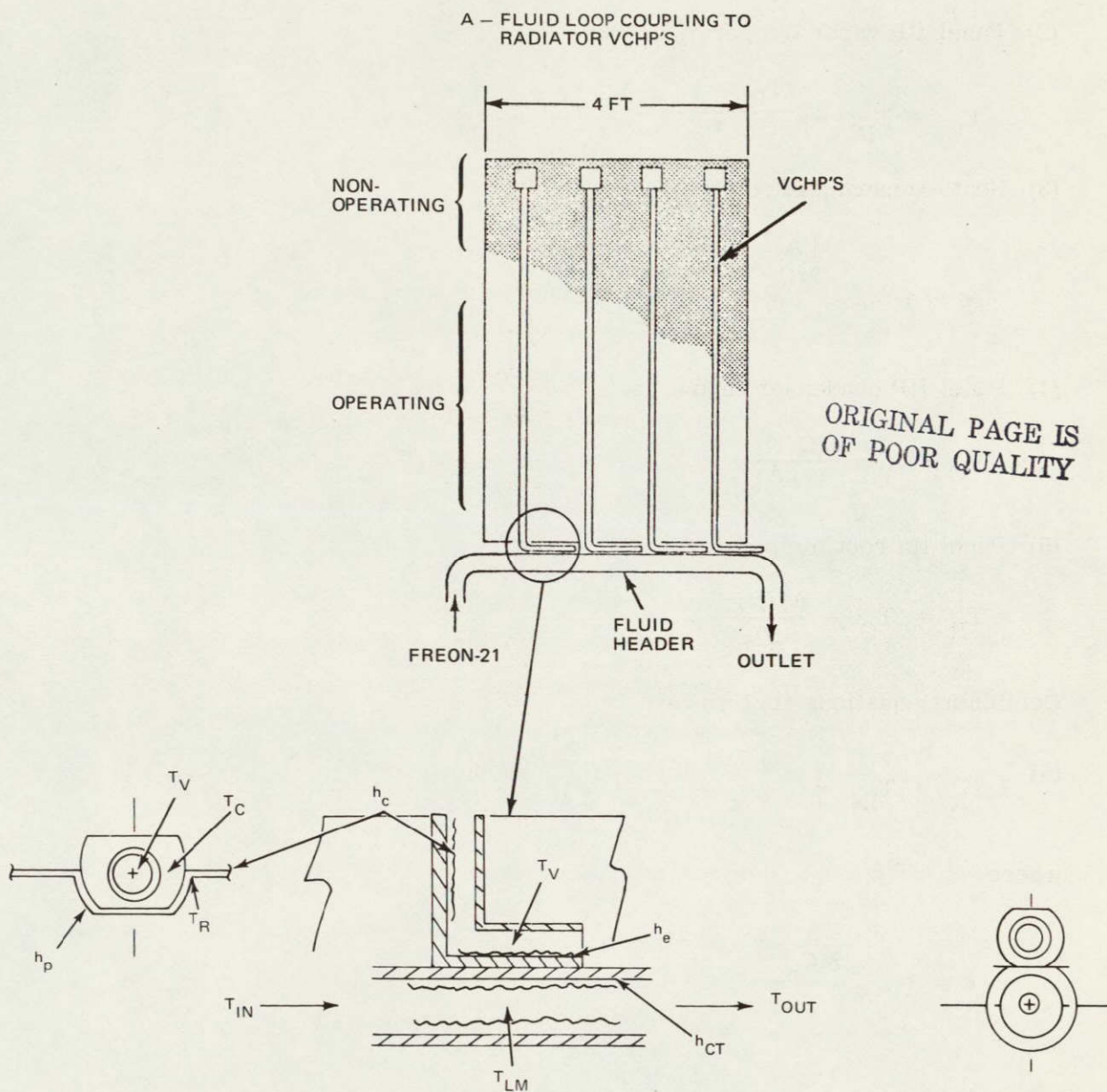
$\epsilon_{\text{HX}}$	NO. HEAT PIPES	$h_{\text{ct}}$ (BTU/HR FT <sup>2</sup> °F)
0.8	6	1450
0.8	5	1360
0.8	4	1320
0.9	6	1310
0.9	5	1230
0.9	4	1180

## CONCLUSIONS

A 0.032-in. thick aluminum panel with six panel heat pipes can best meet the requirements of the deployable HP radiator for any of the operating systems considered. The category II panel requires values of contact conductance ( $h_{\text{CT}}$ ) about 35 percent greater than the Category I panel in order to provide the same fin root temperature. This is due to the addition of the HP header and clamp-on heat exchanger which represent additional thermal resistances and higher temperature drops.

## DERIVATION OF EXPRESSION FOR FIN ROOT TEMPERATURE

- Category I - Fluid Line Header to Radiator Panel VCHP's



Assumption - Since the overall temperature drop across the panel is only 11°F at the maximum, the panel load is assumed to be equally distributed among the panel feeder heat pipes. Although the load per pipe actually varies in relation to position nearest the fluid inlet, the variation is small and hence ignored.

The heat transfer equations for category I (System A) can be expressed as follows:

(1) Heat transfer from fluid

$$Q = MC_p (T_{IN} - T_{OUT})$$

(2) Panel HP vapor temperature

$$T_V = T_{IN} - \frac{(T_{IN} - T_{OUT})}{\epsilon}$$

(3) Heat exchanger effectiveness

$$\epsilon = 1 - e^{-\frac{UA}{MC_p}} = \frac{T_{IN} - T_{OUT}}{T_{IN} - T_V}$$

(4) Panel HP condenser temperature

$$T_C = T_V - \frac{(Q/N)}{(\eta hA)_c}$$

(5) Panel fin root temperature

$$T_R = T_C - \frac{(Q/N)}{h_p A_p}$$

Combining equations (1) thru (5):

$$(6) \quad T_R = T_{IN} - \frac{Q/MC_p}{\epsilon} - \left(\frac{Q}{N}\right) \left[ \frac{1}{(\eta hA)_c} + \frac{1}{h_p A_p} \right]$$

where

$$\epsilon = 1 - e^{-\frac{UA}{MC_p}}$$

and

$$U = \frac{1}{\frac{A_e}{(\eta_o h_o A_o)_X} + \frac{A_e}{h_{CT} A_{CT}} + \frac{1}{e h_e}}$$

The construction of the fluid header consists of a nominal one inch ID aluminum tube (0.125-in. wall) containing a finned annulus that serves as the flow passage. The annulus is 0.10-in. wide and holds 0.006-in. thick aluminum fins at 15 fins per inch. These are the same type fins that were used on the VCHP header for the NASA/Houston HP Radiator (Ref. 4) and have proven performance characteristics. The heat exchanger parameters that were used in the analysis reflect the design Freon-21 flow rate of 500 lb/hr.

The panel feeder heat pipes are made from a grooved aluminum extrusion containing 27 longitudinal grooves. See Fig. 2-4 for details of the heat pipe cross-section, showing dimensions that were used in the tradeoff studies. The same panel heat pipe was used in the evaluation of all the alternative design concepts.

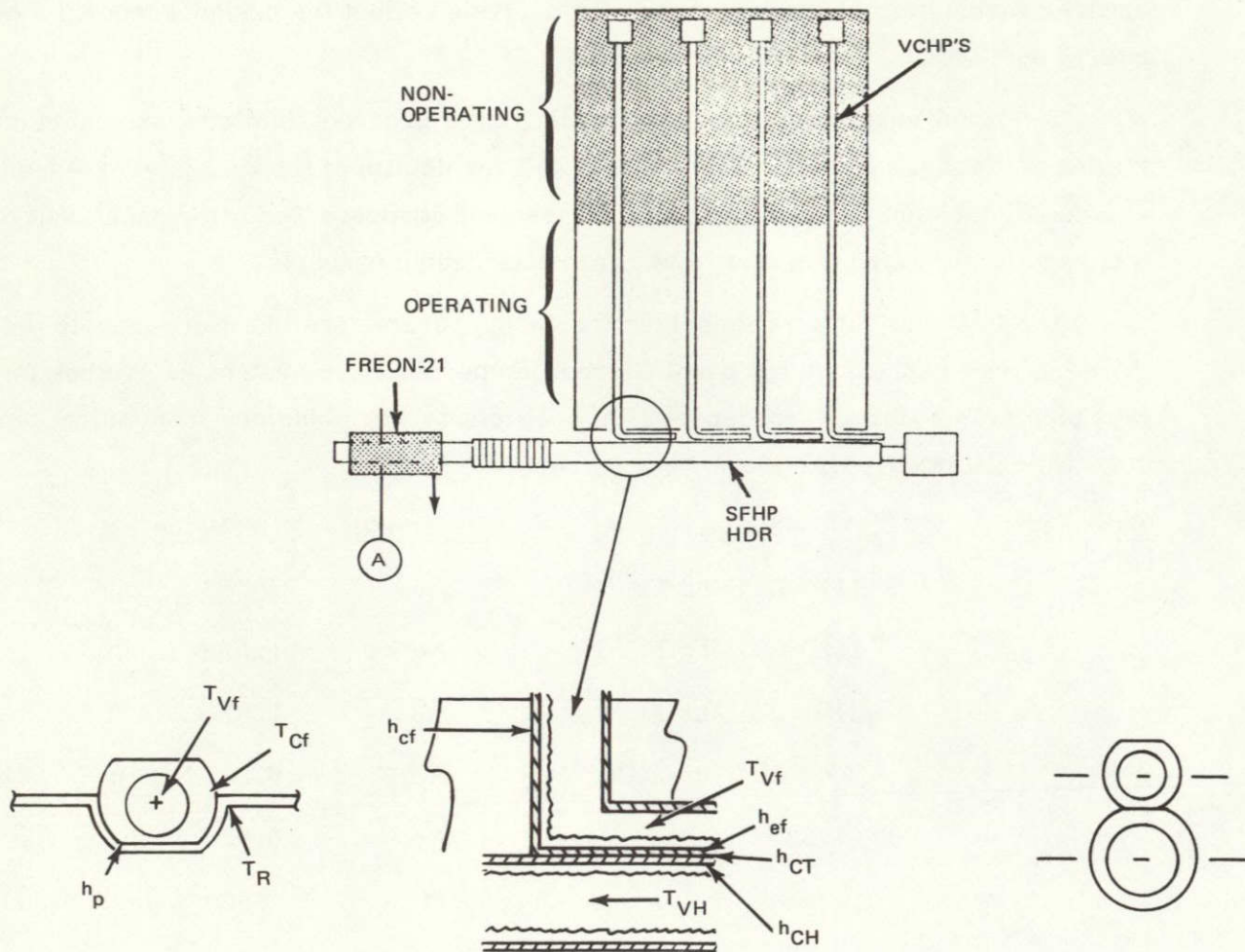
The following table summarizes the design parameters that were used to determine the final expression for panel fin root temperature for system A. Values for heat pipe evaporator and condenser film coefficients were obtained from actual test data while all other parameters were calculated.

<u>Parameter</u>	<u>Value</u>	<u>Parameter</u>	<u>Value</u>
$h_c$	1675 BTU/hr Ft <sup>2</sup> °F	Ao	0.08L <sub>HX</sub> in. <sup>2</sup>
$h_e$	1530 BTU/hr Ft <sup>2</sup> °F	Ae	1.57 N L <sub>e</sub> in. <sup>2</sup>
$h_o$	315 BTU/hr Ft <sup>2</sup> °F	Ac	1.57 L <sub>c</sub> in. <sup>2</sup>
$h_p$	300 BTU/hr Ft <sup>2</sup> °F	A <sub>CT</sub>	0.262 NL <sub>e</sub> in. <sup>2</sup>
$\eta_c$	0.733	Ap	0.970 L <sub>c</sub> in. <sup>2</sup>
$\eta_o$	0.391	M	500 lb/hr
$\eta_x$	0.840	Cp	0.25 BTU/lb °F

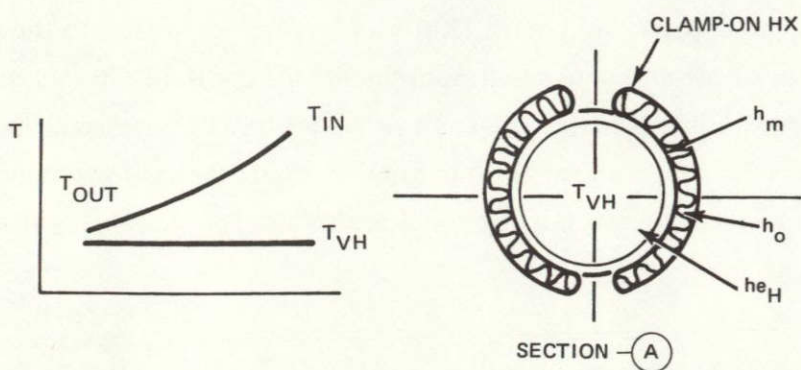
The evaporator length (Le) was varied according to the number of panel heat pipes in order to make maximum use of all available heat transfer area. A minimum evaporator length of six in. each is possible with six panel heat pipes; 7.6 in. with five pipes, and 10 in. with four pipes. Thus, using fewer heat pipes actually results in increased total evaporator heat transfer area with a corresponding benefit in temperature drop.

● Category II - Heat Pipe Header to Radiator Panel VCHP's

B - SINGLE FLUID HEAT PIPE (SFHP) HEADER TO RADIATOR VCHP'S



ORIGINAL PAGE IS  
OF POOR QUALITY



The heat transfer equations for Category II (Systems B, C and D) are expressed as follows:

- (1) Heat transfer from fluid

$$Q = MC_p (T_{IN} - T_{OUT})$$

- (2) HP Header vapor temperature

$$T_{V_H} = T_{IN} - \frac{(T_{IN} - T_{OUT})}{\epsilon}$$

- (3) Heat exchanger effectiveness

$$\epsilon = 1 - e^{-\frac{UA}{MC_p}} = \frac{T_{IN} - T_{OUT}}{T_{IN} - T_V}$$

- (4) Header condenser temperature

$$T_{C_H} = T_V - \frac{Q/N}{(\eta hA)_{CH}}$$

- (5) Panel HP evaporator temperature

$$T_{e_f} = T_{C_H} - \frac{Q/N}{h_{CT} A_{CT}}$$

- (6) Panel HP Vapor temperature

$$T_{V_f} = T_{e_f} - \frac{Q/N}{(\eta hA)_{e_f}}$$

- (7) Panel HP condenser temperature

$$T_{c_f} = T_{V_f} - \frac{Q/N}{(\eta hA)_{c_f}}$$

- (8) Panel fin root temperature

$$T_R = T_{c_f} - \frac{Q/N}{h_p A_p}$$

Combining equations (1) thru (8):

$$(9) \quad T_R = T_{IN} - \frac{Q/MC_p}{\epsilon} \frac{Q}{N} \left[ \frac{1}{(\eta hA)_{CH}} + \frac{1}{h_{CT} A_{CT}} + \frac{1}{(\eta hA)_{ef}} + \frac{1}{(\eta hA)_{cf}} + \frac{1}{h_p A_p} \right]$$

where

$$\epsilon = 1 - e^{-\frac{UA_{eH}}{MC_p}}$$

and

$$U = \frac{1}{\frac{A_{eH}}{(\eta hA)_o} + \frac{A_{eH}}{h_m A_m} + \frac{1}{h_{eH}}}$$

The clamp-on heat exchanger for the category II panels uses the same internal finning that was specified for the System A fluid header. The fins are 0.006-in. thick aluminum, 0.10-in. wide and spaced 15 fins per inch. The panel heat pipes also use the grooved aluminum extrusion. (See Fig. 2-4.)

The following table summarizes the design parameters that were used to determine the final expression for the panel fin root temperature. Once again the values for evaporator and condenser film heat transfer coefficients were obtained from actual published test data while other parameters ( $\eta$ , A) were calculated.

<u>Parameter</u>	<u>Value</u>	<u>Parameter</u>	<u>Value</u>
$h_{cf}$	1675 BTU/hr Ft <sup>2</sup> °F	$A_o$	0.089 L <sub>HX</sub> in. <sup>2</sup>
$h_{CH}$	2400 BTU/hr Ft <sup>2</sup> °F	$A_{ef}$	1.57 L <sub>ef</sub> in. <sup>2</sup>
$h_{ef}$	1530 BTU/hr Ft <sup>2</sup> °F	$A_{eH}$	3.14 L <sub>eH</sub> in. <sup>2</sup>
$h_{eH}$	2000 BTU/hr Ft <sup>2</sup> °F	$A_{cf}$	1.57 L <sub>cf</sub> in. <sup>2</sup>
$h_o$	327 BTU/hr Ft <sup>2</sup> °F	$A_{CH}$	3.14 L <sub>ef</sub> in. <sup>2</sup>
$h_p$	300 BTU/hr Ft <sup>2</sup> °F	$A_{CT}$	0.262 L <sub>ef</sub> in. <sup>2</sup>
$\eta_{cf}$	0.733	$A_M$	2.95 L <sub>HX</sub> in. <sup>2</sup>
$\eta_{CH}$	0.216	$A_p$	0.970 L <sub>cf</sub> in. <sup>2</sup>
$\eta_{ef}$	0.391	M	500 lb/hr
$\eta_o$	0.820	$C_p$	0.25 BTU/lb°F

## APPENDIX B - DEPLOYABLE HEAT PIPE RADIATOR CONTROL REQUIREMENTS

This analysis summarizes the control requirements for the deployable heat pipe (HP) radiator in terms of: (1) active area, (2) control gas interface location, (3) reservoir equilibrium temperature, and (4) reservoir volumes.

### Panel Active Area Requirements

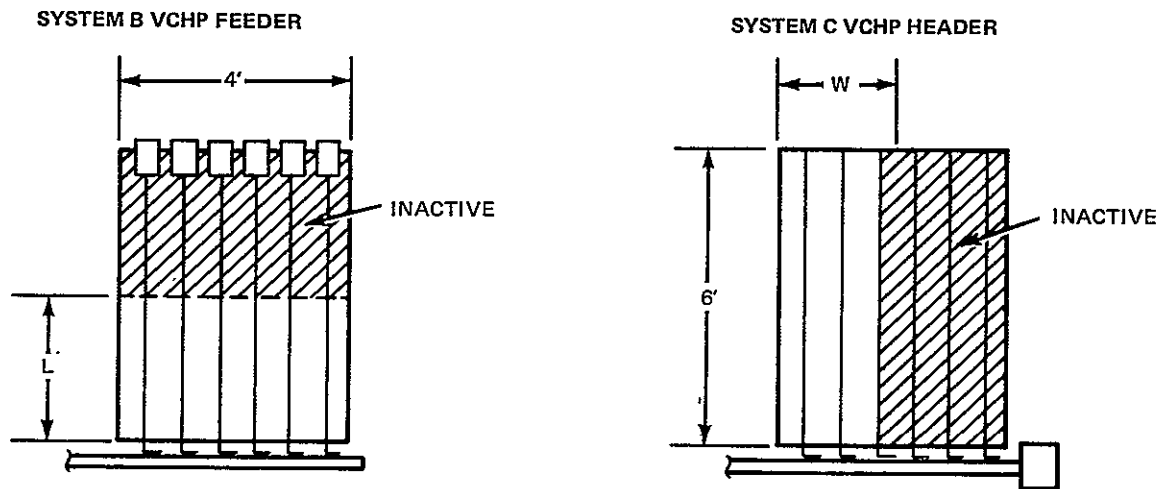
Proper design of the VCHP control reservoir depends upon the necessary active panel area required for heat rejection. There are two possible panel configurations and four operating extremes which scope the complete problem. Using the results of Appendix A, in particular Fig. A-1 and eq. 9, the panel active area requirements have been determined. The two panel configurations analyzed were: System B-all VCHP feeder HP's with a single fluid heat pipe (SFHP) header and System C-VCHP header with SFHP feeders. Each was examined for the combinations of max/min load and max/min environment and the results are summarized in Fig. B-1. The corresponding active panel fin root temperatures are also given.

### Control Gas Interface Location

Control gas interface positions which are consistent with the area requirements of Fig. B-1 are given in Fig. B-2 (for System C) and Fig. B-3 (for System B). In each figure the required position of the interface is indicated for the possible combinations of load and environment. The condenser is fully opened for the high load, high environment condition and least opened for the low load, low environment case. The maximum required interface movement is 28 in. for the VCHP header of System C (Fig. B-2) and 46 in. for the VCHP feeders of System B (Fig. B-3).

### Reservoir Equilibrium Temperatures

Ideally the equilibrium temperature of the control gas reservoir should be the same as the environmental sink temperature. This means an ideal reservoir temperature of  $-30^{\circ}\text{F}$  for the high environment case (fully opened condenser) and  $-110^{\circ}\text{F}$  for the low environment case (partially closed condenser). However, in actuality the reservoir temperatures that correspond to these operating extremes will be somewhat warmer than the ideal due to heat conduction from the condenser into the reservoir.



Q (WATTS)	T <sub>SINK</sub> (°F)	T <sub>ROOT</sub> (°F)	AREA (FT <sup>2</sup> )	(FT)	AREA (FT <sup>2</sup> )	(FT)	NO. ACTIVE HEAT PIPES
400	-30	62	24	6	24	4	6
400	-110	56.7	16.6	4.2	17.5	2.9	5
200	-30	49.3	13.4	3.3	14.8	2.5	4
200	-110	42.6	8.9	2.22	10.1	1.68	3

Fig. B-1 Active Area Requirements, Deployable Heat Pipe Radiator

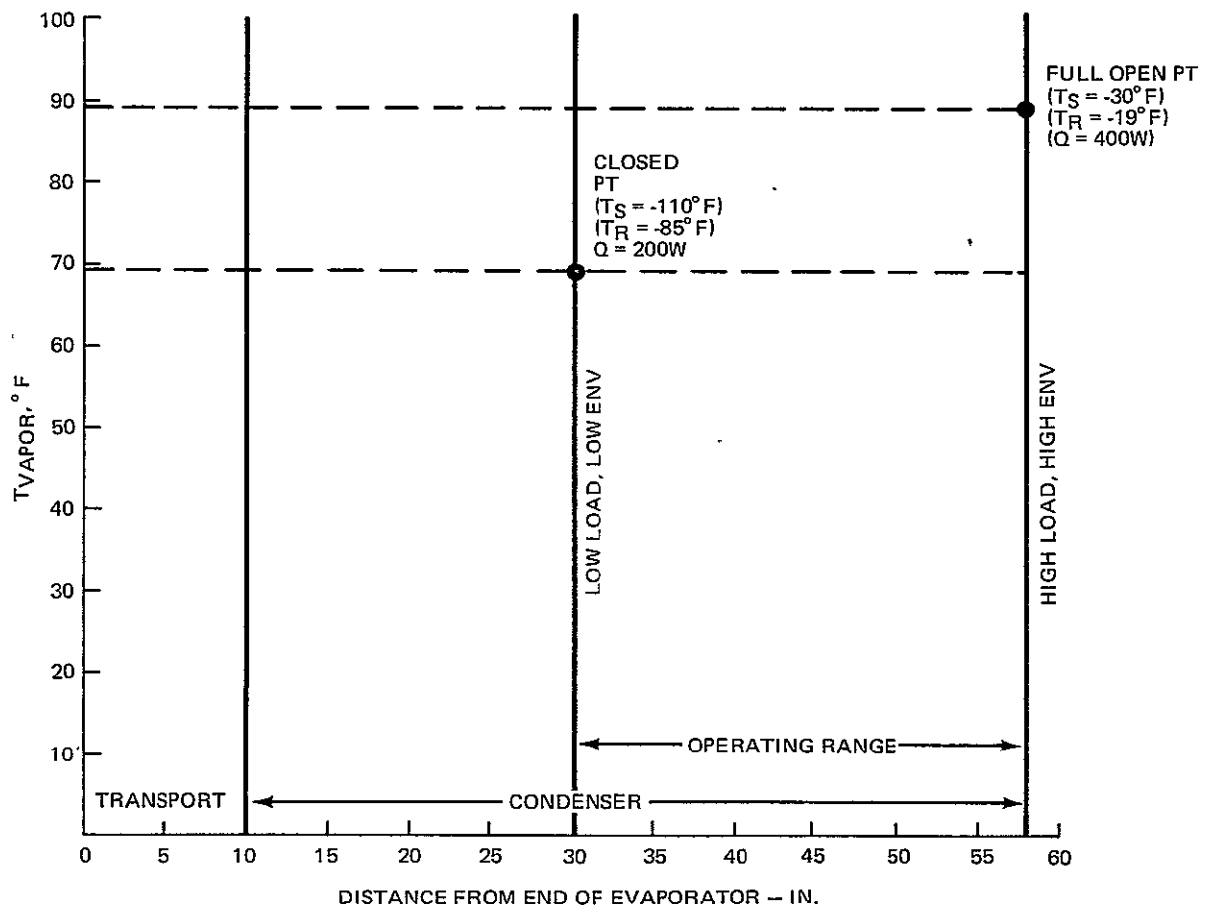


Fig. B-2 Operating Range, System C — VCHP Header

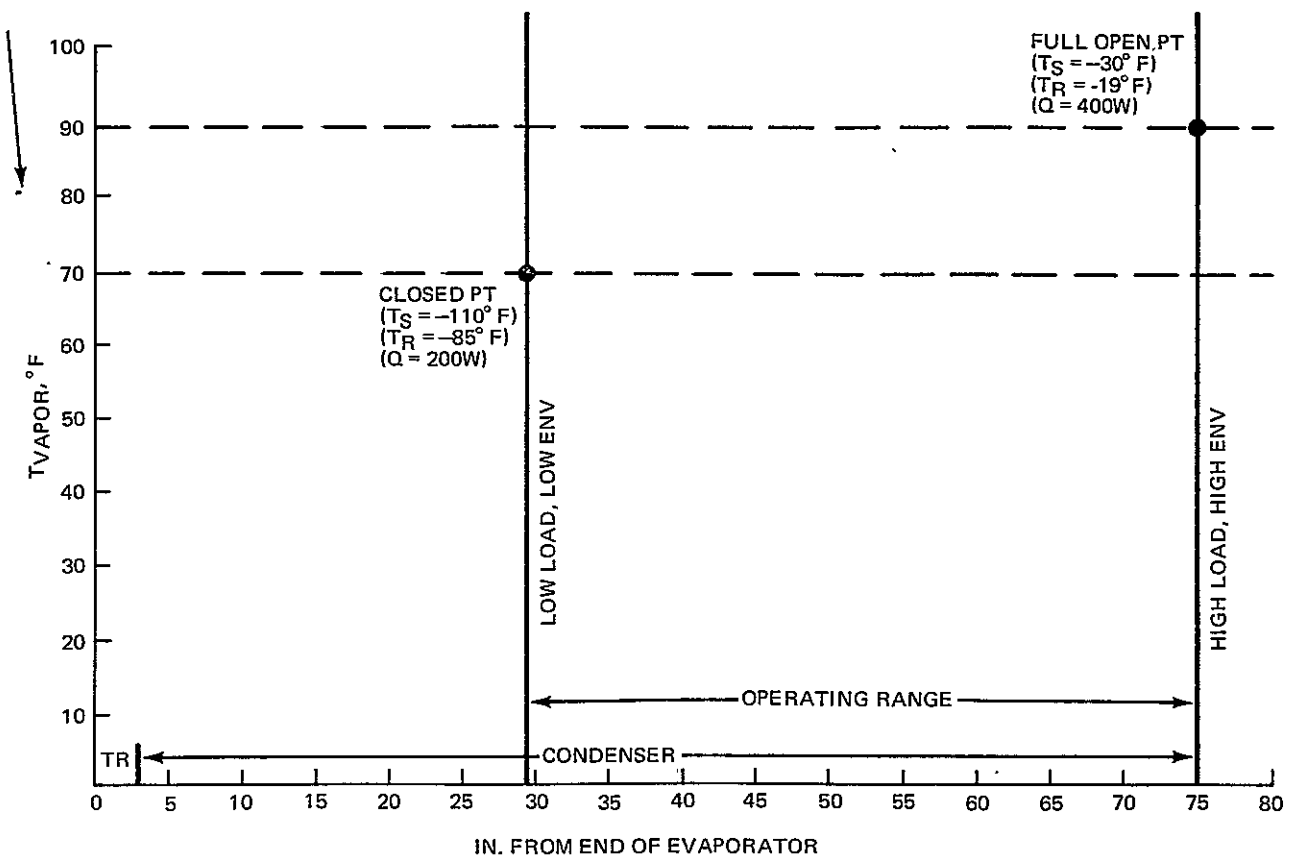


Fig. B-3 Operating Range, System B VCHP Feeder

Although a low thermal conductivity section is provided between the condenser and the reservoir to limit conduction and insure a "cold" reservoir, there still will be a small heat gain. The effect of this heat conduction on reservoir temperature is shown in Fig. B-4. At the extreme interface locations the actual reservoir temperatures were determined to be  $-19^{\circ}\text{F}$  (for the fully opened condenser and warm environment) and  $-85^{\circ}\text{F}$  (for the partially closed condenser and cold environment).

The heat gains that correspond to the above reservoir temperatures were calculated using the following design parameters:

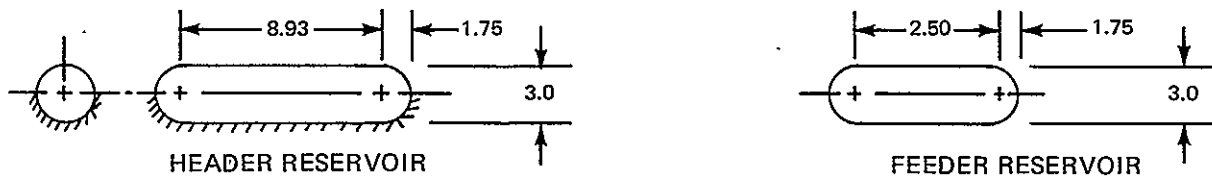
	<u>Header Reservoir</u>	<u>Feeder Reservoir</u>
● Reservoir heat rejection area, in. <sup>2</sup>	58.5	28.26
● Low-k section (SS)		
- tube OD, in.	0.750	0.437
- wall thickness, in.	0.028	0.028
- tube length, in.	2.43	2.85
● Vapor Temp, $^{\circ}\text{F}$		
- condenser open	89	89
- condenser closed	69	69

#### Reservoir Volumes

The required reservoir volumes for the header and feeder HP's were determined by using the 360/67 VCHP Interface Location Program. The program calculates the required  $V_R/V_C$  ratio corresponding to the prescribed reservoir temperatures, vapor temperatures, and interface locations for the extreme operating conditions. The reservoir volume,  $V_R$ , is then obtained from the  $V_R/V_C$  ratio and the blocked condenser vapor space volume,  $V_C$ .

Two conditions were examined: one assumed ideal reservoir temperatures (without losses), and the other used the predicted reservoir temperatures which included the effects of heat leaks to the reservoir. The following table summarizes the results:

	<u>Ideal</u>	<u>Predicted</u>
● Vapor Temp, °F		
- max	89	89
- min	69	69
● Reservoir Temp, °F		
- max	-30	-19
- min	-110	-85
	Header HP	Feeder HP
● Blocked Condenser		
Vapor Space		
- Length, In.	28	46
- Volume, In. 3	6.53	4.17
● $V_R/V_C$ Ratio		
- Without Heat Leaks	14.7	14.7
- With Heat Leaks	7.8	7.8



The actual reservoir designs will reflect a  $V_R/V_C$  of eight for the feeder heat pipes and 12 for the header HP. Using a larger than predicted  $V_R/V_C$  value for the header will increase its control sensitivity as a VCHP (i. e., smaller vapor temperature change needed for full interface movement). It will also insure that adequate reservoir volume remains to provide control in the event of partial artery depriming. Since depriming is not a problem with the feeder heat pipes (no arteries), the need for a larger than predicted reservoir volume is obviated.

The resulting absolute reservoir volumes required are 78.4 in<sup>3</sup> for the header and 33.4 in<sup>3</sup> for each feeder heat pipe. These volumes are provided by the configurations shown below, which are also consistent with the surface areas that were used to determine reservoir equilibrium temperatures.

The effect of reservoir temperature variation on  $V_R/V_C$  ratio is illustrated in Fig. B-5. As seen, for a given 20° F evaporator control range requirement, the larger the variation in reservoir temperature, the larger the required  $V_R/V_C$  ratio.

ORIGINAL PAGE IS  
OF POOR QUALITY

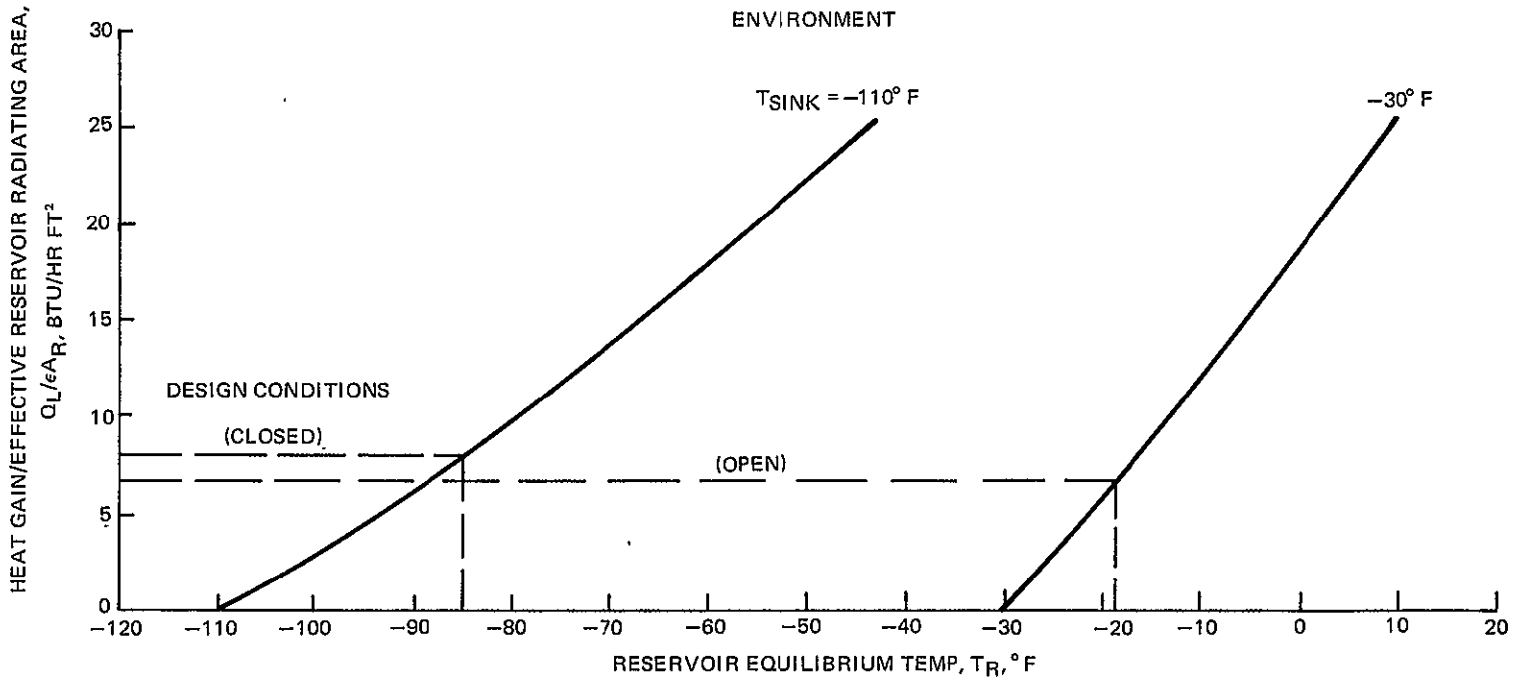
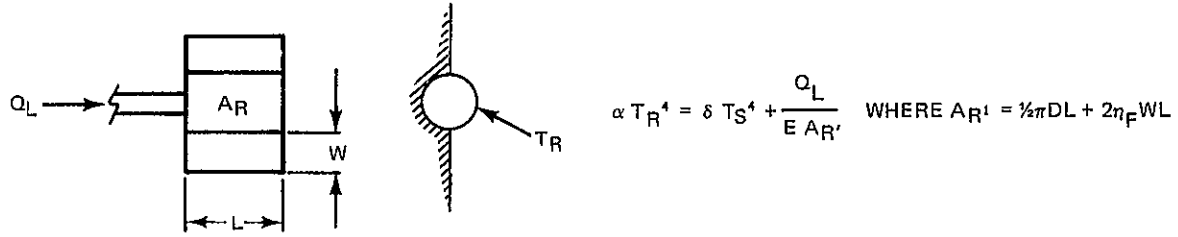


Fig. B-4 Reservoir Equilibrium Temperature vs Heat Gain

ORIGINAL PAGE IS  
OF POOR QUALITY

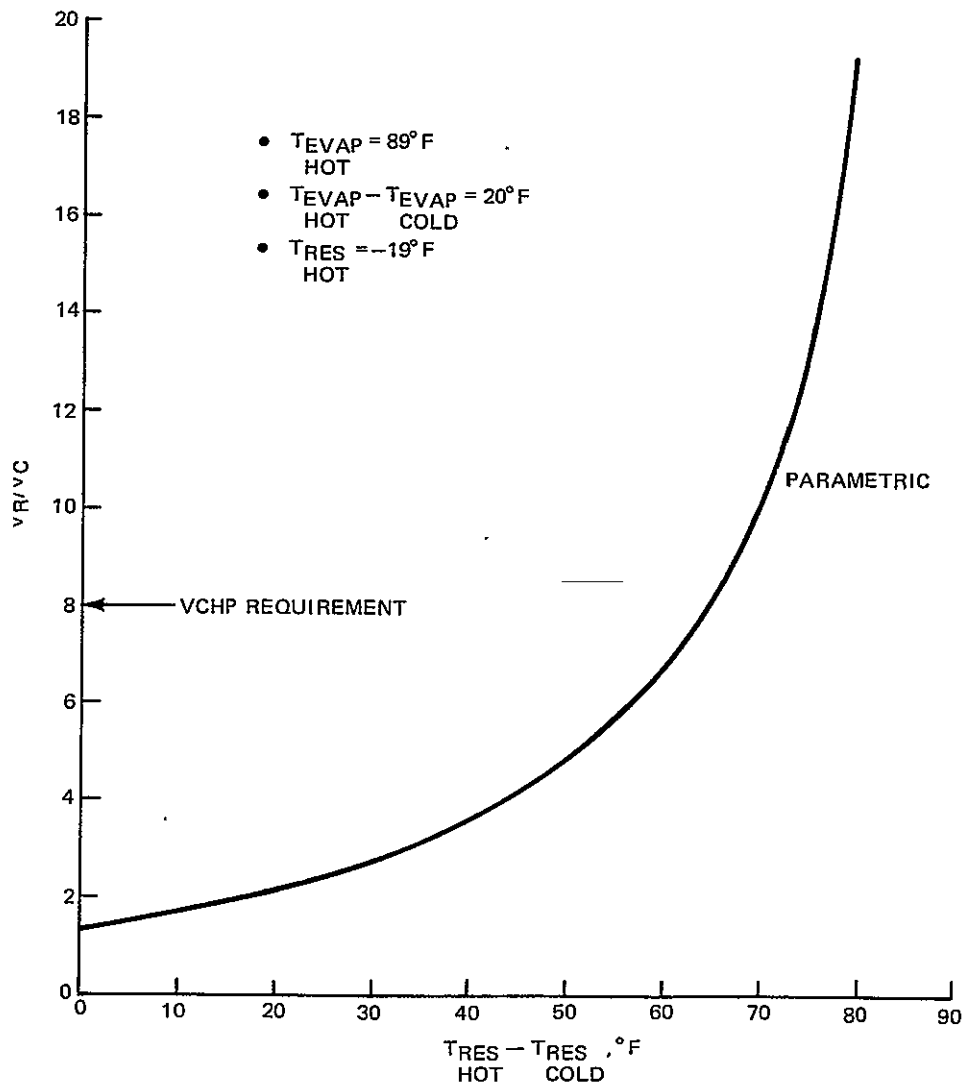


Fig. B-5  $V_R/V_C$  vs Reservoir Temperature Variation (Ammonia and Nitrogen)

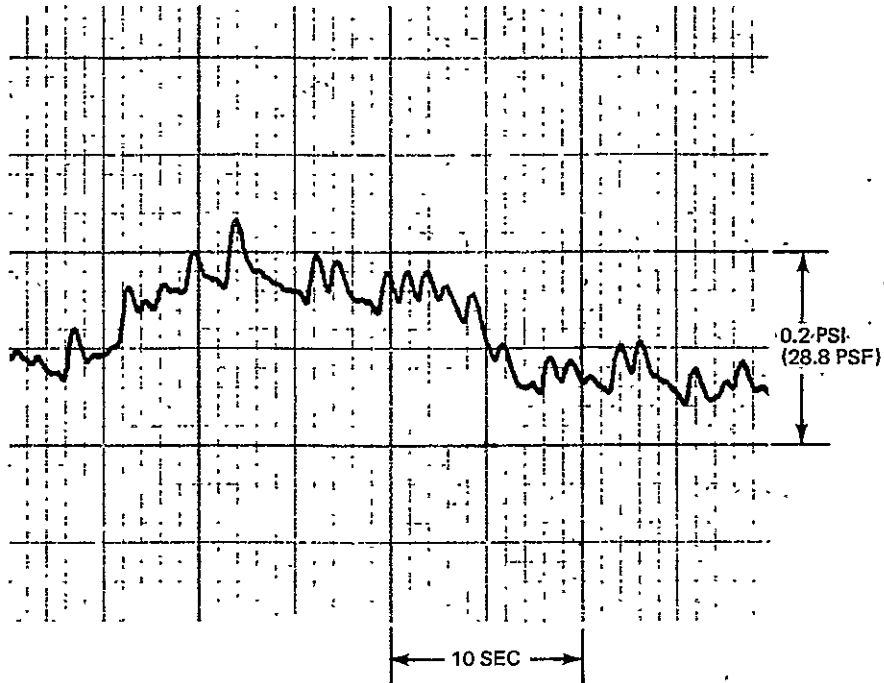
## APPENDIX C - HEADER HEAT PIPE PRESSURE TESTS

When tested as a single fluid device (ammonia) the flexible deployable heat pipe header achieved a capacity of 950 watts in a level orientation. However, upon subsequent addition of nitrogen control gas, the maximum load achieved was only about 200 to 300 watts (see Deployable Heat Pipe Progress Report No. 11, DHPR-11, 12-9-74). To gain insight into this problem, a pressure transducer was installed to record pressure oscillations with and without the presence of nitrogen control gas. These tests were performed with in-house IR&D funds.

The first pressure oscillation test was performed November 14, 1974, with the pipe in a VCHP mode level, and with the vapor bypass section installed. Results of this test showed that at 50 watts, pulses ranged from 3 to 4psf (Fig. C-1) and that at 100 watts, pulses ranged from 10 to 17psf with approximately a three second period. These values are high considering that the total available head in the capillary system is about 12psf. In the reflux mode (approximately 1 in.) the observed oscillations were lower, (1-2 psf at 50 watts and 6 psf at 200 watts).

It is conjectured that these oscillations are initiated by flow instabilities in the diffusion zone separating the blocked and unblocked portions of the condenser. The oscillations may be enhanced by movement of free liquid if present in the region of the diffusion zone. In the reflux mode, any free liquid would run to the evaporator end and reduce the puddle height in the vicinity of the diffusion zone. This may account for the lower pressure oscillations.

On 27 March 1975, pressure oscillations were taken with the pipe charged only with ammonia. Results of this test are presented in Table C-1 along side the VCHP data. It is seen that at higher loads, the amplitude of the oscillations are significantly lower in the single fluid mode compared to the VCHP mode. It is also noticed that above 500 watts there was a marked increase (step change) in oscillation amplitude. Figures C-2 and C-3 show pressure oscillations at 500w and 600w respectively. A possible explanation offered is that the increase in power level causes the condenser grooves to flood creating a liquid wave motion as the condensate runs down the wall. The liquid wave would temporarily reduce the local condensation rate.



- CHART SPEED: 0.1 IN./SEC
- Q = 50W
- VCHP HDR (11/14/74)

Fig. C-1

Table C-1 Single Fluid and VCHP Pressure Oscillation Tests

LOAD (WATTS)	VCHP		SINGLE FLUID	
	$\Delta P$ PSF	PERIOD, SECONDS	$\Delta P$ PSF	PERIOD, SECONDS
50	3 TO 4	1 TO 2		
100	10 TO 17	3		
200			< 1	0.5
300			{ 0.5 1.5	{ 0.5 10
400			0.3	0.25
500			0.3	0.25
600			4	1
700			4.5	0.7
700*			4.5	0.7

\*PIPE BENT 78° ABOUT FLEX SECTION; ALL OTHER DATA WITH PIPE STRAIGHT. PIPE ORIENTATION: LEVEL.

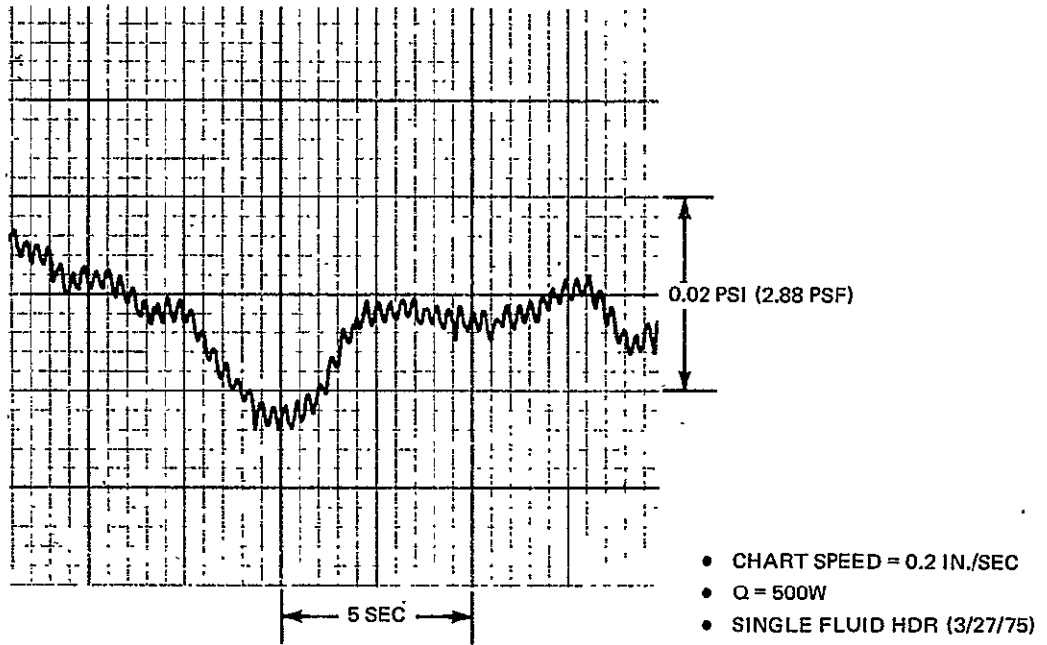


Fig. C-2

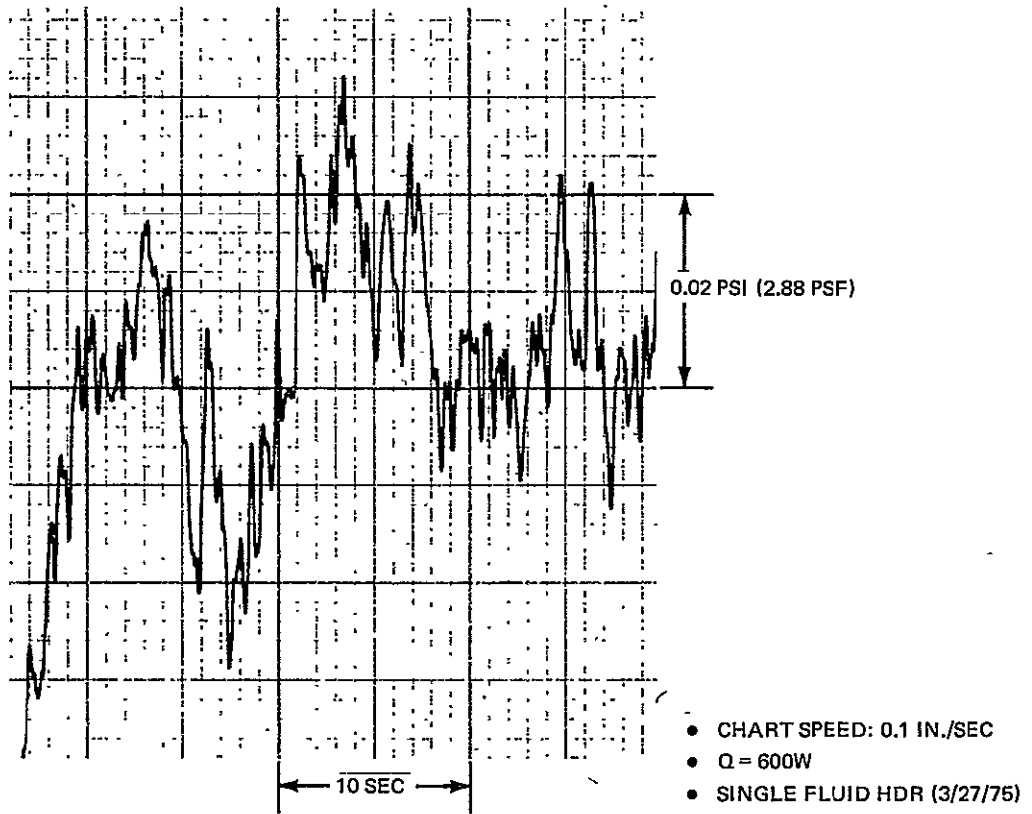
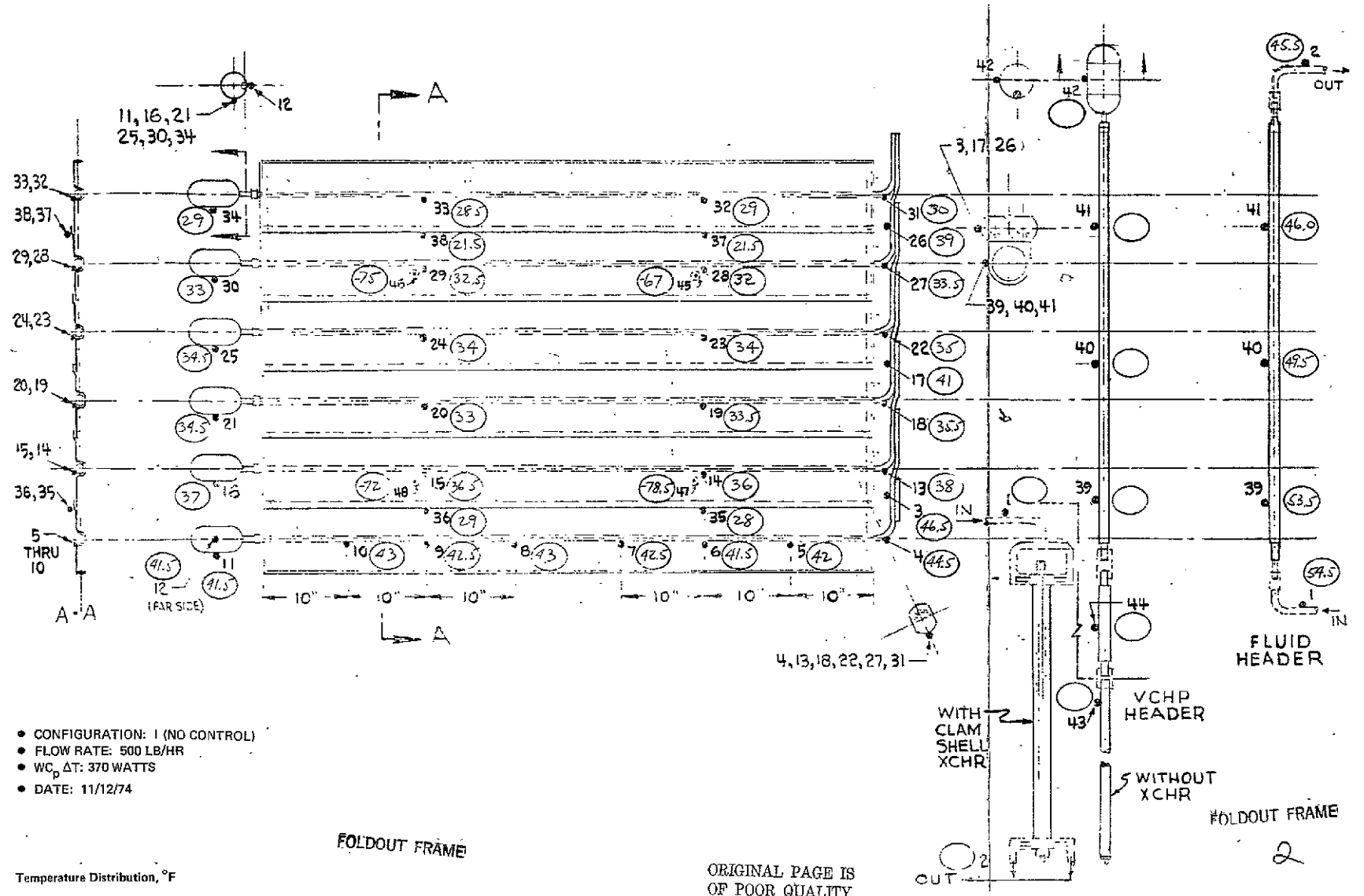


Fig. C-3

ORIGINAL PAGE IS  
OF POOR QUALITY

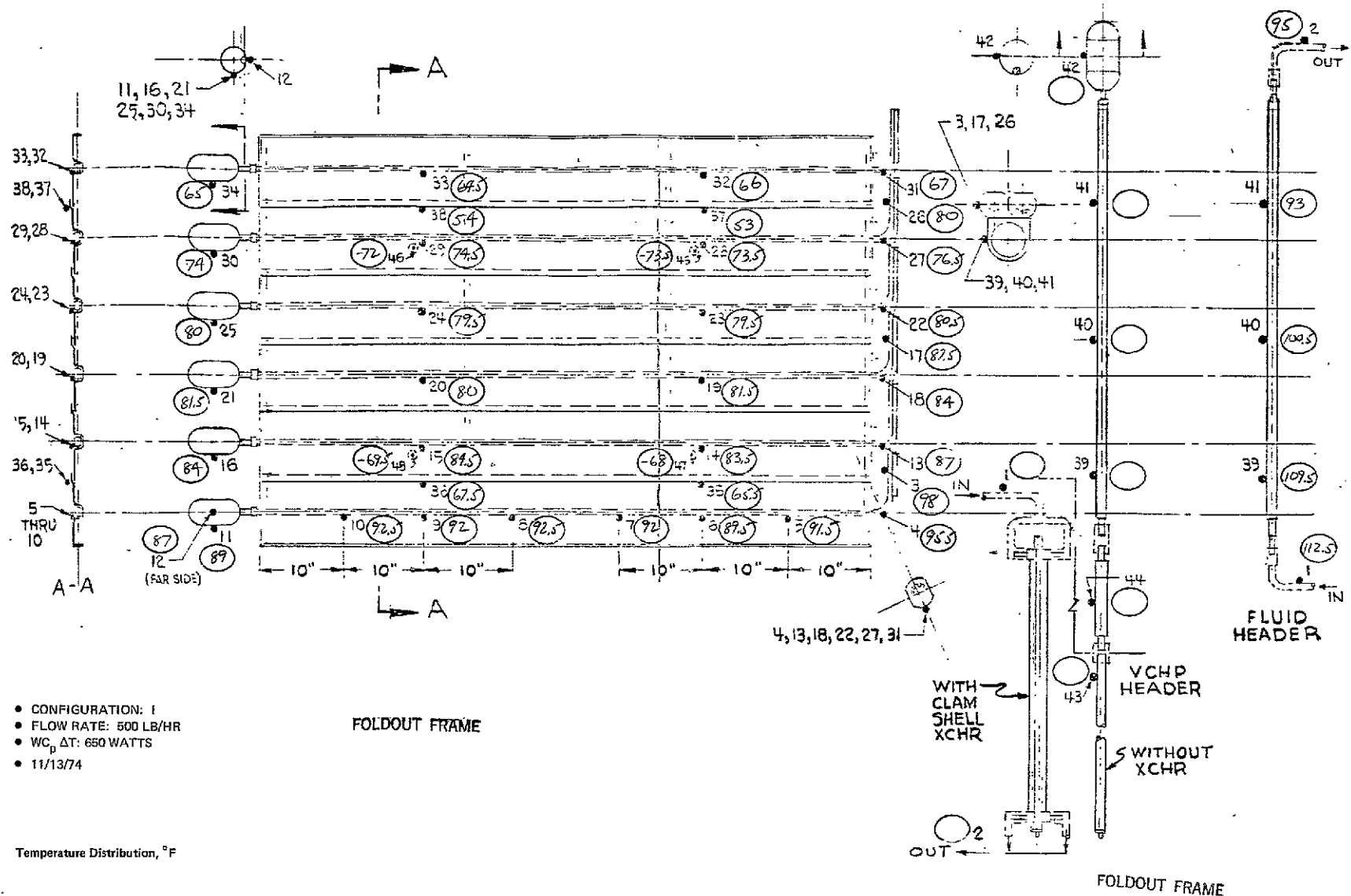
The conclusions, regarding the comparison of VCHP and single fluid test data are:

- (a) The amplitude of the oscillations are significantly larger when nitrogen control gas is present in the pipe. Their magnitude is of the same order as the capillary head, i. e. , 12 psf.
- (b) In the absence of nitrogen gas smaller but still relatively large oscillations, e. g. , 4 psf, were observed at high power levels ( $\sim 700\text{w}$ ). These apparently do not impair pipe performance.
- (c) It is felt that oscillations, in themselves, may not cause artery/tunnel de-priming but instead aggravate the growth of bubbles that already exist within the artery, or cause the growth of bubbles at active nucleation sites within the artery. The bubble growth would occur as the pressure drops, with liquid being expelled from the artery and draining to the bottom of the pipe. The liquid might then not be available during the pressure rise part of the oscillation, resulting in a depressed meniscus, and initiation of dry-out in the evaporator.
- (d) No further pressure testing of the pipe is planned, and it will therefore be prepared for shipment to Marshall Space Flight Center as a single fluid heat pipe.



C2

Figure D-1

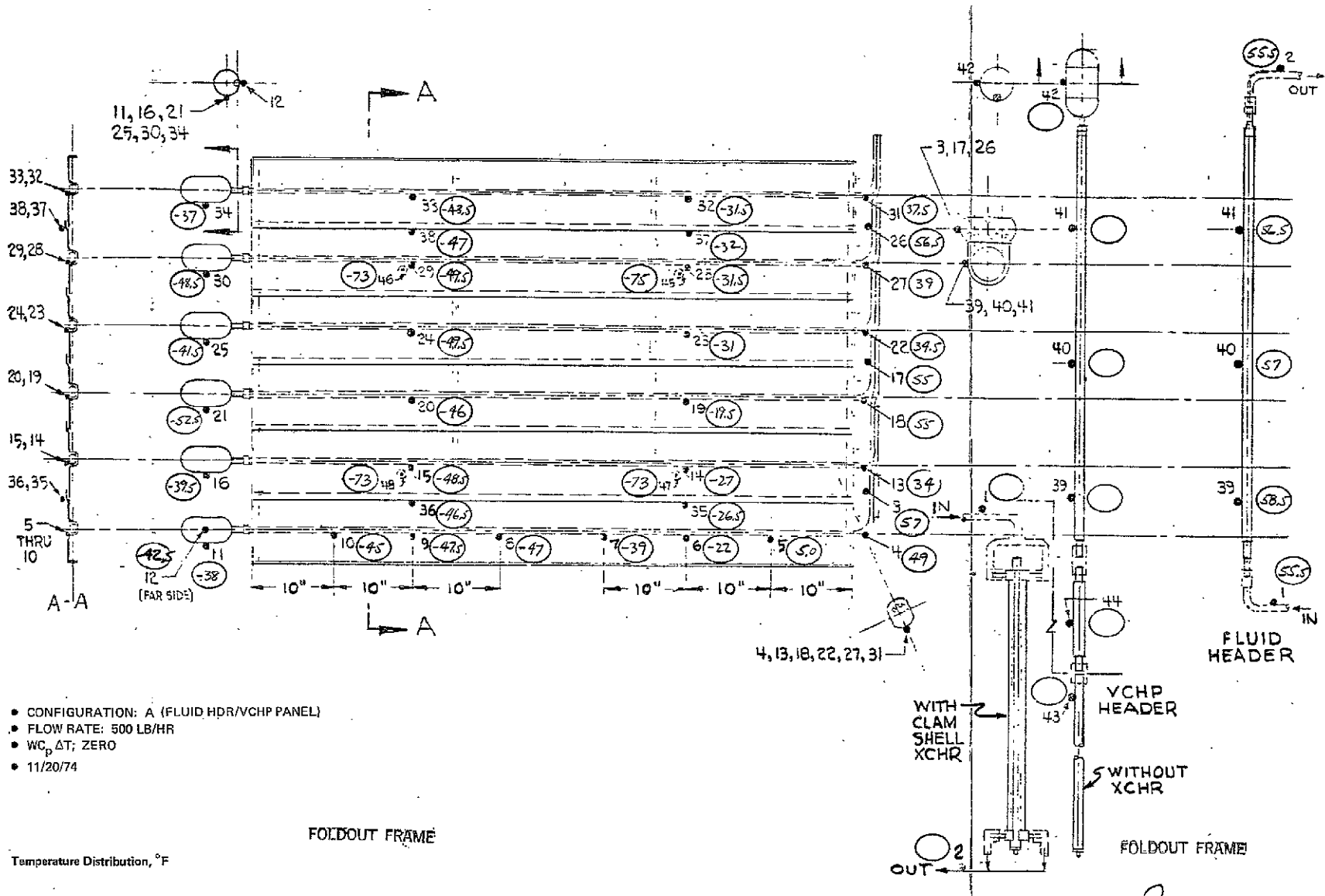


- CONFIGURATION: I
- FLOW RATE: 500 LB/HR
- $WC_p \Delta T$ : 650 WATTS
- 11/13/74

Temperature Distribution, °F

Figure D-2

2



- CONFIGURATION: A (FLUID HDR/VCHP PANEL)
- FLOW RATE: 500 LB/HR
- WCP ΔT; ZERO
- 11/20/74

FOLDOUT FRAME

Temperature Distribution, °F

Figure D-3

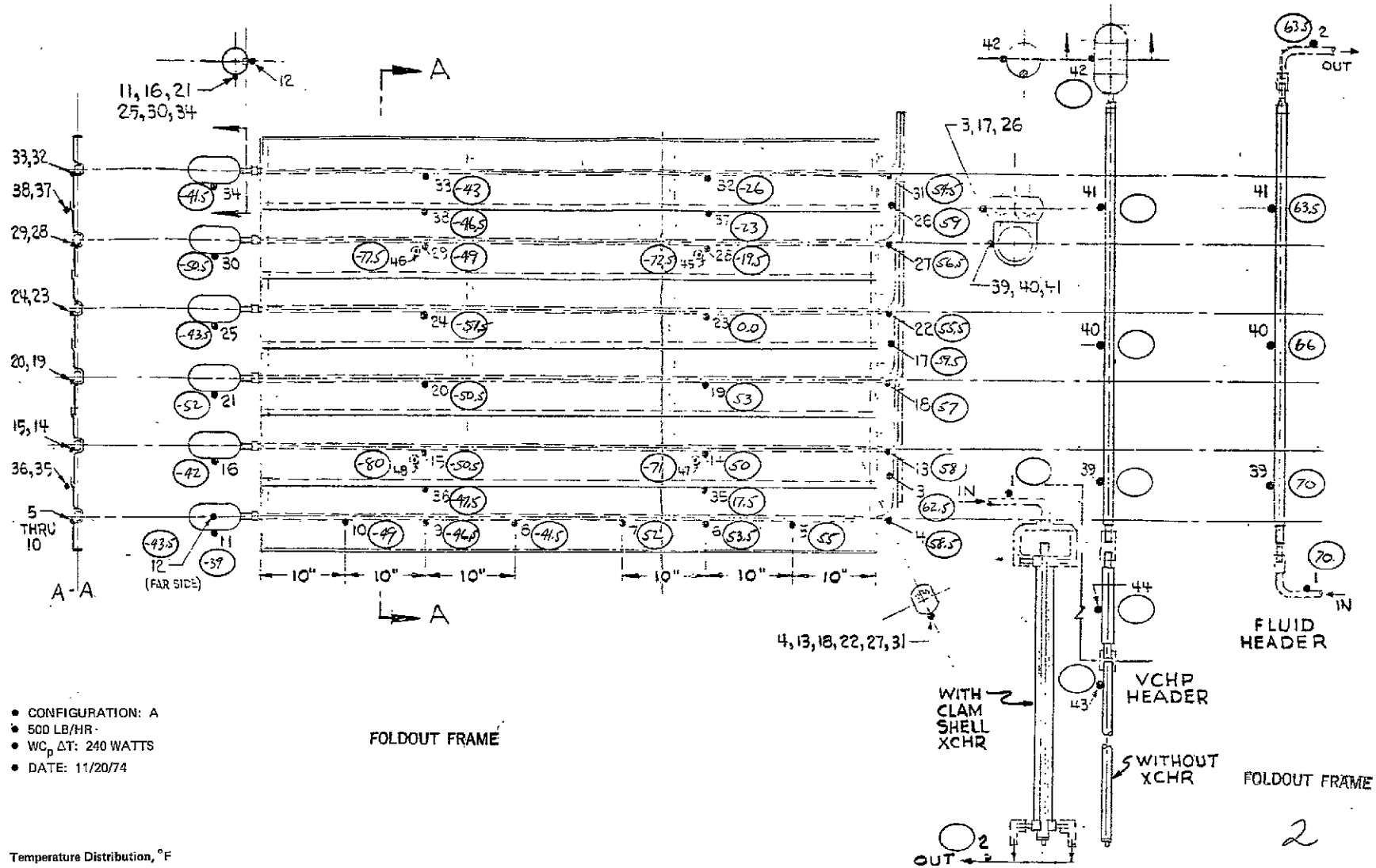


Figure D-4

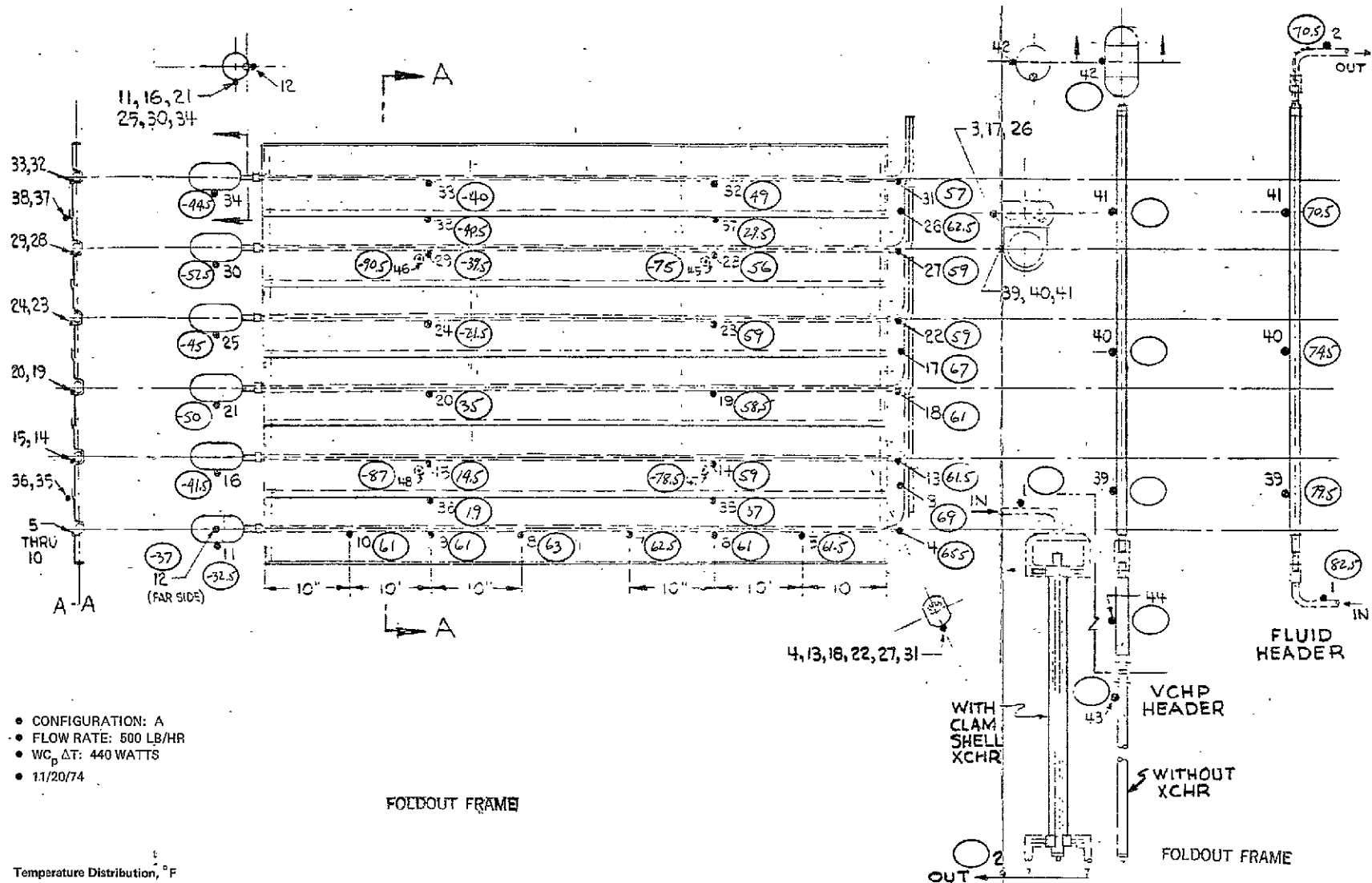


Figure D-5



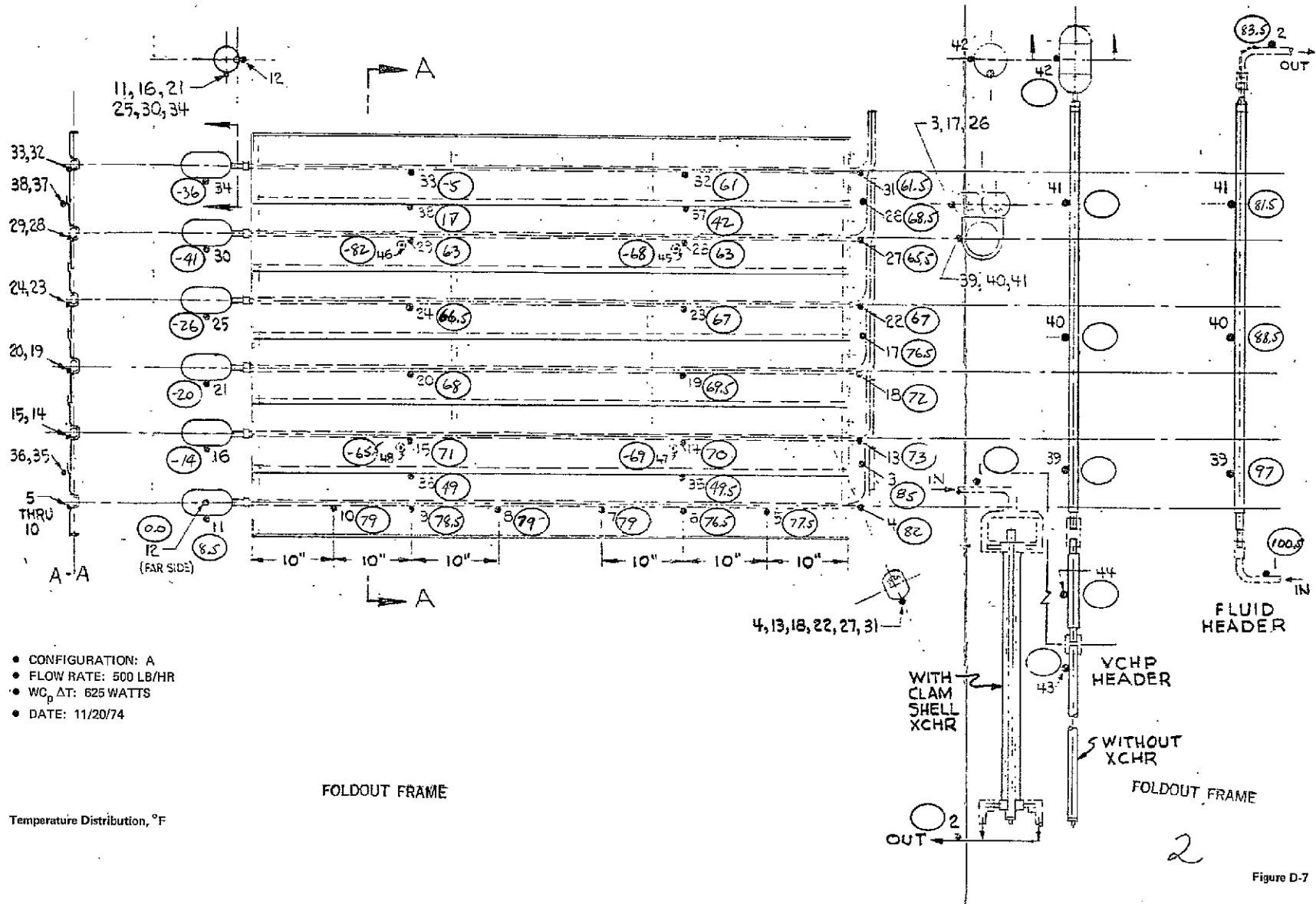
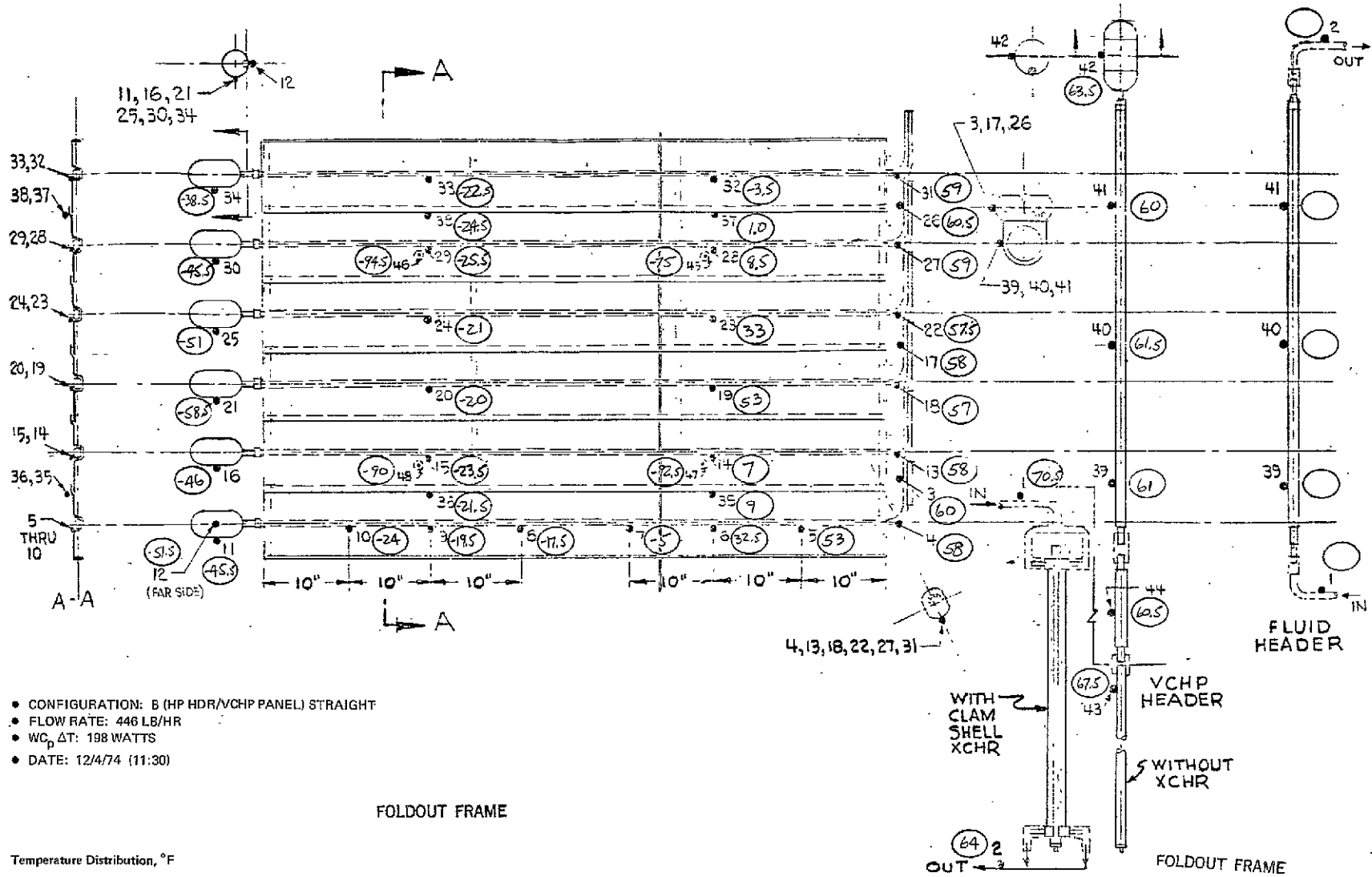


Figure D-7



- CONFIGURATION: B (HP HDR/VCHP PANEL) STRAIGHT
- FLOW RATE: 446 LB/HR
- $WC_p \Delta T$ : 198 WATTS
- DATE: 12/4/74 (11:30)

FOLDOUT FRAME

Temperature Distribution, °F

Figure D-8

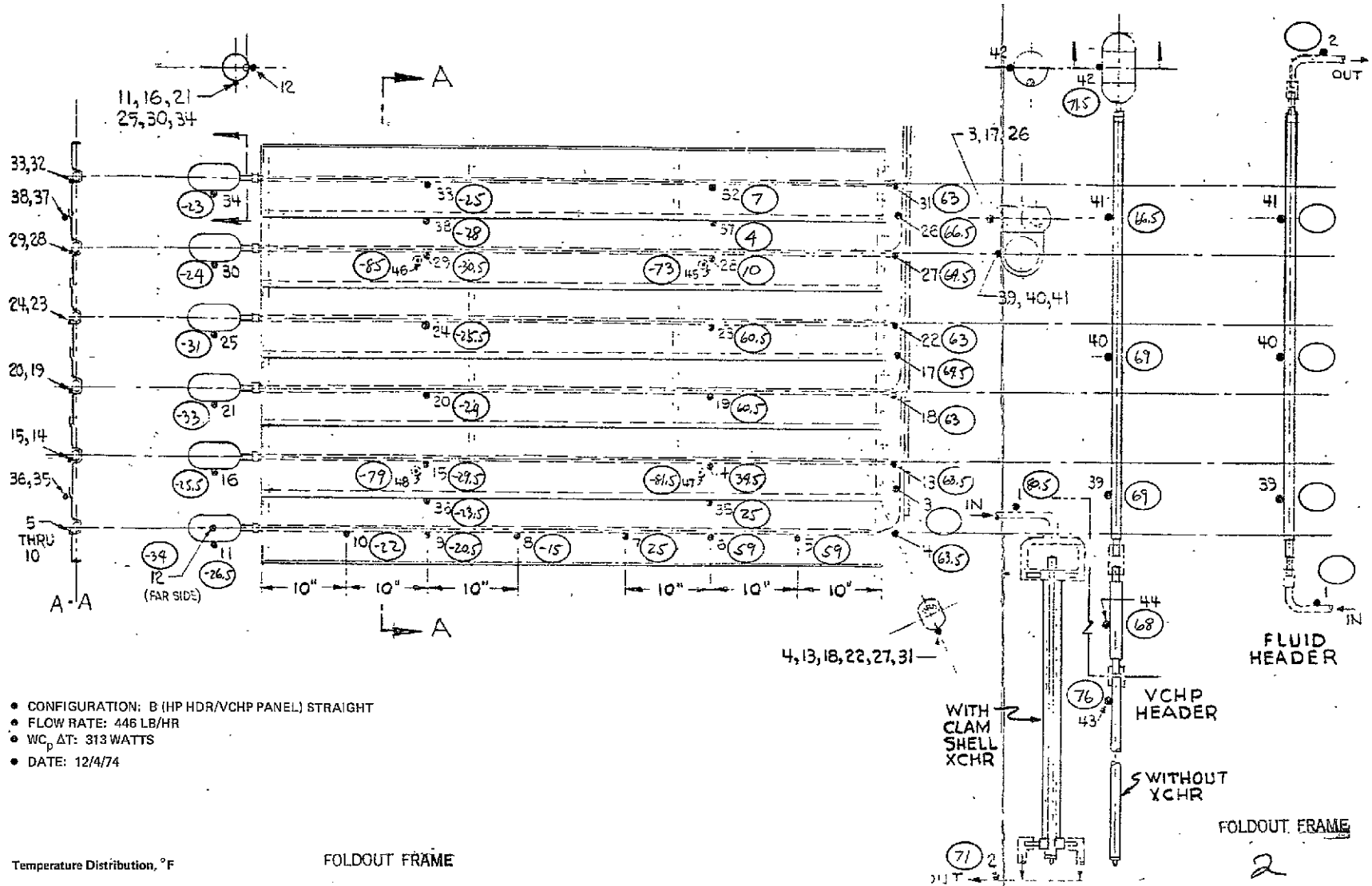


Figure D-9



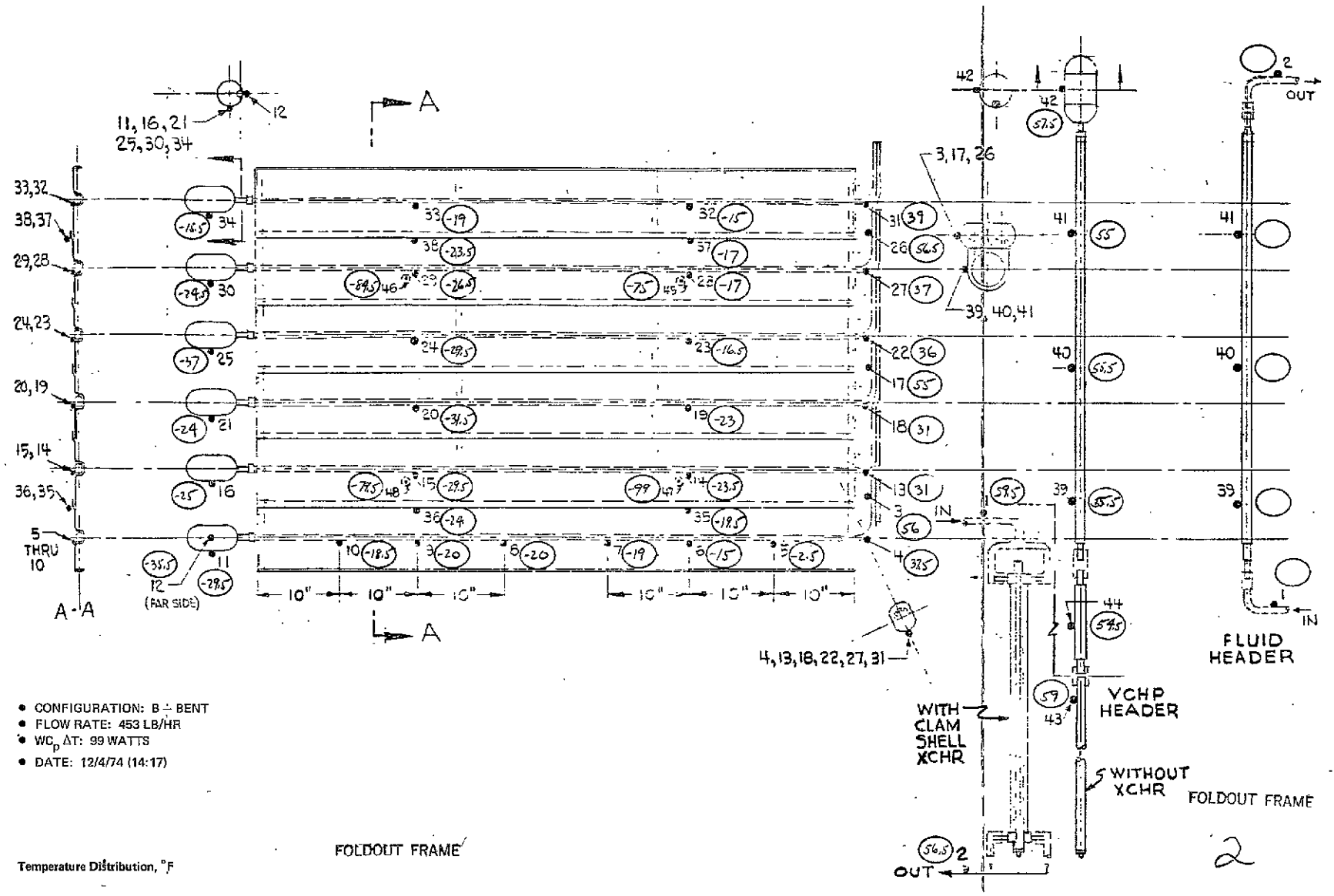
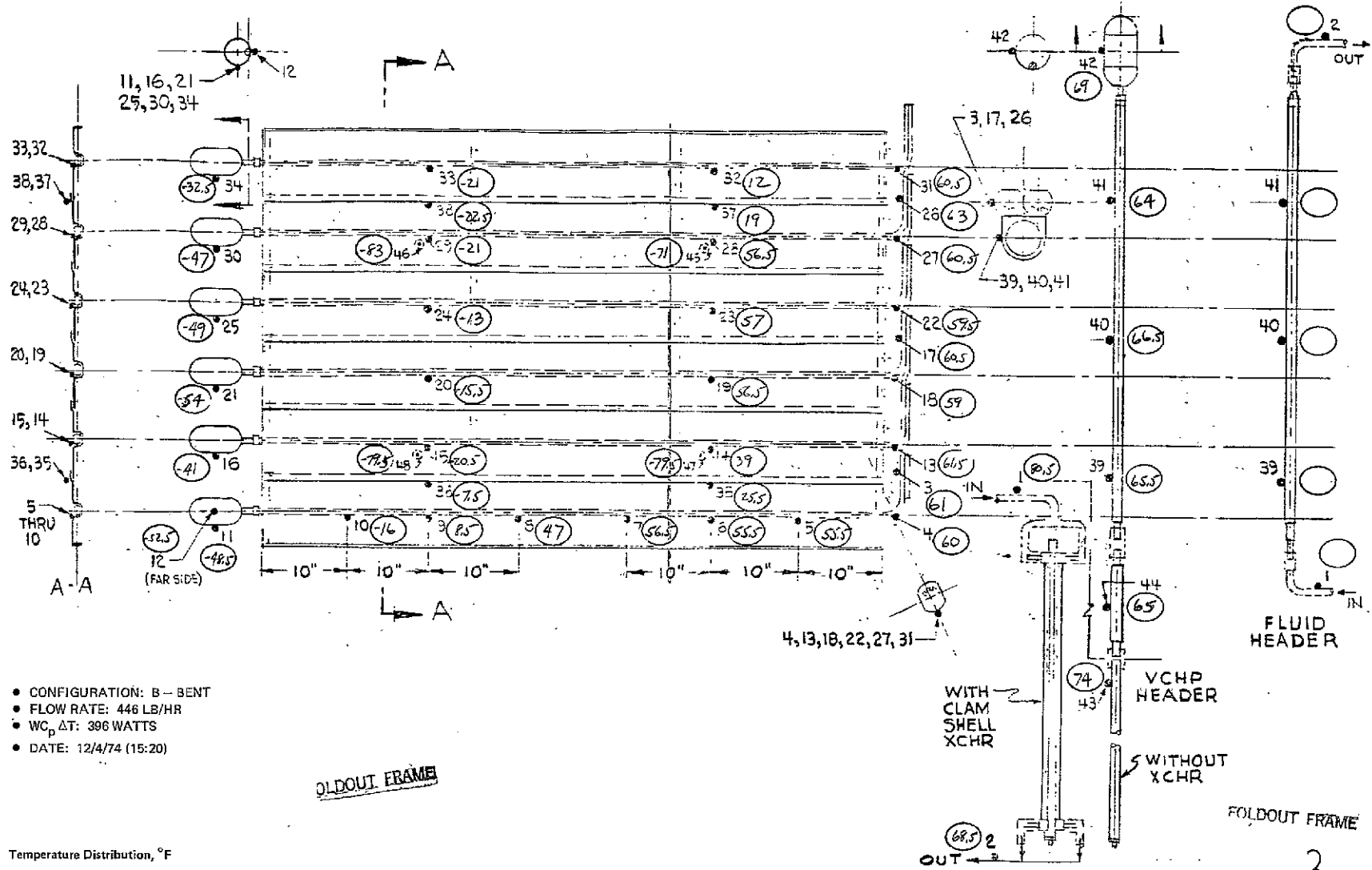


Figure D-11



- CONFIGURATION: B - BENT
- FLOW RATE: 446 LB/HR
- $WC_p \Delta T$ : 396 WATTS
- DATE: 12/4/74 (15:20)

Figure D-12

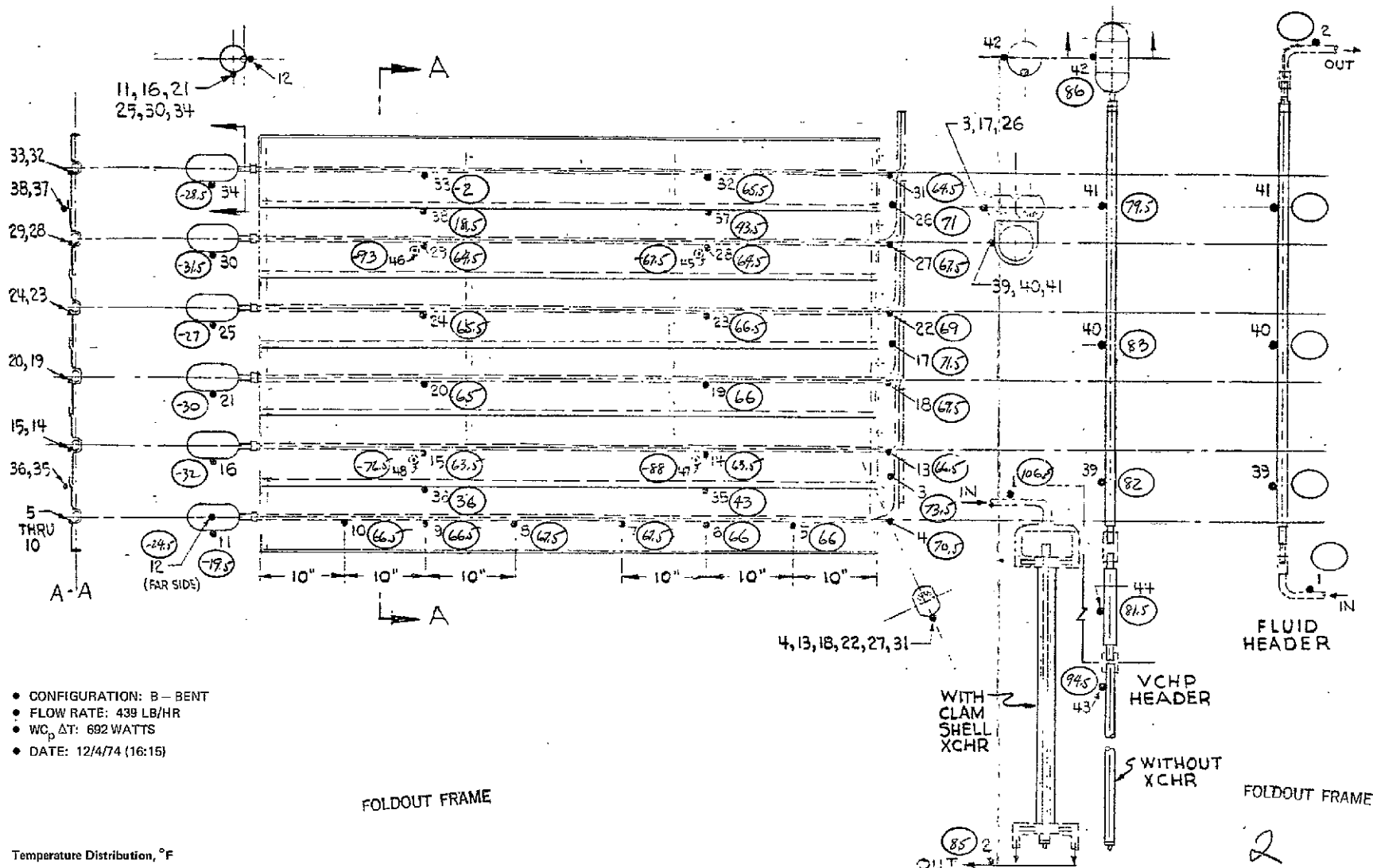


Figure D-13

